Princeton Plasma Physics Laboratory

PPPL-5232 REV

Fusion Energy Systems Studies (FESS) FNSF Study Year-End Report for 2015

C. E. Kessel[1], J. Blanchard[2], A. Davis[2], L. El-guebaly[2], L. Garrison[3], N. Ghoniem[4], Y. Huang[4], P. Humrickhouse[5], Y. Katoh[3], A. Khodak[1], S. Malang[6], E. Marriott[2], N. Morley[4], M. Rensink[7], T. Rognlien[7], A. Rowcliffe[3], S. Smolentsev[4], P. Snyder[8], M. Tillack[9], P. Titus[1], L. Waganer[6], A. Ying[4], and Y. Zhai[1]

1 Princeton Plasma Physics Laboratory, 2 University of Wisconsin, Madison, 3 Oak Ridge National Laboratory, 4 University of California, Los Angeles, 5 Idaho National Laboratory, 6 Consultant, 7 Lawrence Livermore National Laboratory, 8 General Atomics, 9 University of California, San Diego

February 2016

Prepared for the U.S. Department of Energy under Contract DE-AC02-09CH11466.

Princeton Plasma Physics Laboratory
Report Disclaimers

Full Legal Disclaimer

Trademark Disclaimer

PPPL Report Availability

Princeton Plasma Physics Laboratory:

http://www.pppl.gov/techreports.cfm

Office of Scientific and Technical Information (OSTI):

http://www.osti.gov/scitech/

Related Links:

U.S. Department of Energy

U.S. Department of Energy Office of Science

U.S. Department of Energy Office of Fusion Energy Sciences

Fusion Energy Systems Studies (FESS) FNSF Study Year-End Report for 2015

C. E. Kessel[1], J. Blanchard[2], A. Davis[2], L. El-guebaly[2], L. Garrison[3], N. Ghoniem[4], Y. Huang[4], P. Humrickhouse[5], Y. Katoh[3], A. Khodak[1], S. Malang[6], E. Marriott[2], N. Morley[4], M. Rensink[7], T. Rognlien[7], A. Rowcliffe[3], S. Smolentsev[4], P. Snyder[8], M. Tillack[9], P. Titus[1], L. Waganer[6], A. Ying[4], and Y. Zhai[1]

[1]Princeton Plasma Physics Laboratory, [2]University of Wisconsin, Madison, [3]Oak Ridge National Laboratory, [4]University of California, Los Angeles, [5]Idaho National Laboratory, [6]Consultant, [7]Lawrence Livermore National Laboratory, [8]General Atomics, [9]University of California, San Diego

1. Introduction

The Fusion Nuclear Science Facility (FNSF) is the next step confinement facility beyond ITER, that significantly extends fusion development into the fusion nuclear regime and plasma science into ultra-long pulse at high performance [1]. An example of the fusion pathway, with the critical FNSF step, is shown in Fig. 1, with several important parameter/metrics describing the advance toward a commercial fusion power plant.

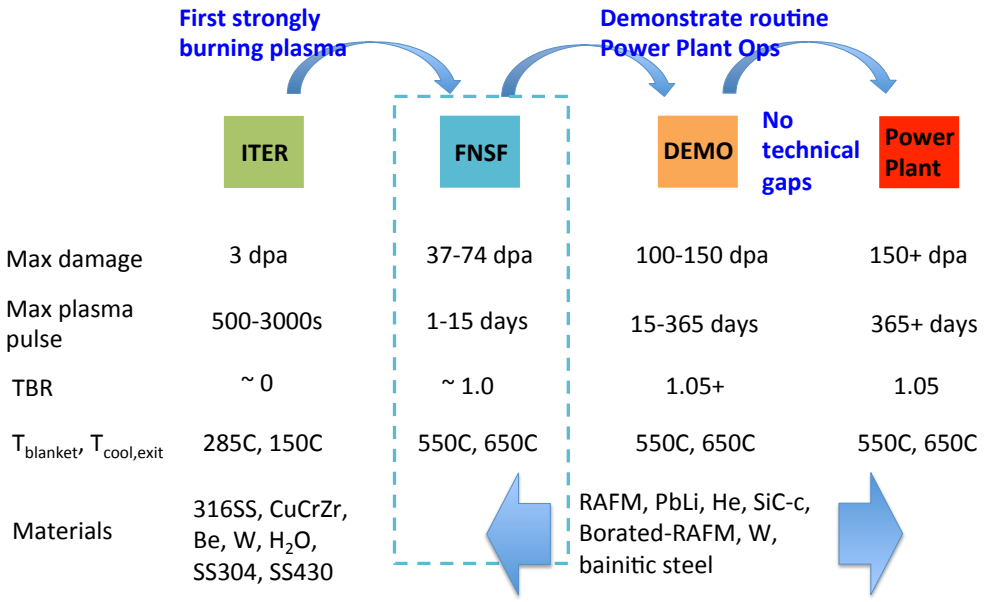

Figure 1. Fusion development pathway from ITER to commercial power plants, with the FNSF and the demonstration power plant (DEMO) bridging the tremendous gap from ITER burning plasma operations.

The material's maximum neutron damage, maximum plasma pulse length, tritium breeding ratio, blanket and divertor operating temperatures, and fusion relevant materials

are strongly advanced in the FNSF, to establish the database for the construction and operation of the DEMO, which will produce electricity and demonstrate routine power plant operations. ITER provides the burning plasma demonstration, but with limited relevance to the fusion nuclear regime. However, the simultaneous controlled plasma operation on ITER with burning plasma, plasma materials interactions, high divertor heat loads, and numerous technology advances (e.g. plasma exhaust pumping and fueling, heating and current drive, super-conducting coils, cryo-distribution, tritium handling, and plasma diagnostics) provides a critical springboard for all next step facilities. The FNSF establishes a strong fusion nuclear environment for the entire device from the fusion core components (breeding blanket, shield/structure, and divertor) to the vacuum vessel and the superconducting magnets. In the fusion core the environment is complex, combining the high energy fusion neutrons (their material damage and transmutation production), intense plasma loading on plasma facing components, surface and volumetric heating, high temperatures, strong magnetic fields with conducting liquid metal breeder, strong hydrogen environment with tritium and transmutation hydrogen, chemical interactions of liquid metal breeder and solid materials under high temperature and flow conditions, and gradients in all these features through the various components in the fusion core. The FNSF is a necessary scientific platform for understanding and developing a database upon which fusion plasma and fusion nuclear science is projected to fusion power production.

An important technical philosophy is adopted for the FNSF based on the experience in the fast breeder and pressurized water fission reactor development. This is that a strong pre-qualification program is required before any material or component is installed and operated in the FNSF. This includes the 1) fusion relevant and fission neutron testing of individual materials up to the anticipated damage levels, 2) fission testing of subassemblies (e.g. breeder and structural material) where possible, and 3) non-nuclear fully integrated testing of prototype FW/blanket, structural ring, divertor, H/CD launcher, etc. This is motivated by the incompatibility of plasma-vacuum operation with constant failures in fusion core hardware, and the significant timescales needed for remote maintenance in the nuclear environment. Several material behaviors led to major disturbances in the development program for the liquid metal fast breeder program, described in detail in refs [2,3]. A wide range of material behaviors in the actual service environment of these fission facilities were observed, and new phenomena can be expected in the fusion operating regime as well, since it can not be accessed in testing before. On the FNSF the plasma durations and duty cycles, neutron fluence, operating temperatures, and materials are advanced through a series of 1 DD and 5 DT phases. Inspections and autopsy of components during any phase, and at the end of a phase, is used to monitor the evolution of materials. This requires highly efficient hot cell turnaround and radiation hardened equipment. Test blanket modules can be used to look ahead to the next phase's material and operating temperature regimes. All in all, the FNSF requires a high level of pre-qualification of materials and components, a progressive program toward maximum parameters, and a rigorous inspection and examination capability for all fusion core and ex-core components. This is needed for the FNSF to provide an efficient and effective platform for developing a database for fusion energy systems.

The FESS group is studying the conventional aspect ratio tokamak configuration. There have been a number of proposals for a pilot plant, FNSF, or component test facility (CTF), or volumetric neutron source (VNS) [4-7]. The FNSF step can take many forms, and here we will separate them into minimal, moderate and maximal mission scopes. The moderate mission scope is being pursued in the present FESS activity in detail, and the other mission scopes will be examined at a systems analysis level. The advances in many parameter/metrics in the FNSF determine what is left for the DEMO to further advance toward power plant levels. A minimal FNSF will advance metrics the least and a maximal FNSF would advance metrics the most, subsequently leaving a large amount of advancing or a small amount of advancing for the DEMO to compensate, respectively. Roughly speaking the minimal scope FNSF would defer as much power plant relevant features as possible, with the potential to begin construction and operation of a facility earlier, and focus on the lower level neutron exposure (< 20 dpa), with a plant DT lifetime of ~ 15 years. The fusion core components such as the blanket or divertor would likely be made of fusion relevant materials, but other components (structural ring, vacuum vessel, manifolding, shielding materials) would not. A water coolant might be considered for the divertor or blanket in spite of its irrelevance to the power plant regime, in order to access an available database of PWR operation. Such a facility would be kept small and have low fusion power in order to minimize tritium consumption, since it is unlikely that a TBR approaching 1.0 could be reachable. The plasma would operate in a heavily driven mode and would require significant first wall area for heating and current drive. The toroidal and poloidal field magnets might be copper rather than superconducting. On the other end of the spectrum would be a maximal FNSF mission scope, where virtually all power plant relevant features would be included and significantly approach the power plant regime. In particular, net electricity production would be a target, and excess tritium production (TBR > 1.0) would be planned, high neutron exposure and damage levels, with a neutron wall load that could be the same as a power plant, and all relevant materials for the entire plant. The facility would require ~ 35 years of DT operation to reach its goals. The moderate FNSF falls in between these two limiting cases, with possible shortfalls to power plant relevance that can include tritium breeding falling slightly below 1.0, no net electricity production although electricity can be produced, about half of the required neutron exposure (e.g. 74 vs 150 dpa), and would likely have a lower neutron wall load (1.5 vs 2.25 MW/m^2). However, power plant relevance still weighs heavily on the moderate case with superconducting magnets, all fusion relevant materials, with an intermediate plant DT lifetime of ~ 25 years. Table 1 provides a number of features for these possible FNSF mission scopes, and are highlighted in terms of low (red), medium (orange), and high (green) power plant relevance. The neutron wall loading has not been highlighted in spite of the differences since no impact from this parameter has been identified, but the irradiation rate may influence damage or transmutation phenomena.

Table 1. Approximate parameters characterizing the possible FNSF mission scopes. Red denotes strong departure, orange some departure, and green indicates small departure from power plant parameters or relevance.

	minimal	**moderate**	maximal	Power plant
Plant DT operations	~ 15 yr	~ 25 yr	~ 35 yr	47 yr (40 FPY)
Peak neutron wall load, MW/m^2	1.0	1.5	2.25	2.25
Plasma on-time per year	10-35%	10-35%	10-45%	85%
Max dpa on first wall (or max dpa to replace)	5 -18,36	7 - 37,74	10 - 70,140	150-200
Q_{engr}	<< 1	< 1	> 1	4
Tritium breeding ratio	< 1	~ 1	> 1	1.05
Plant life, peak dpa	32, 50	88, 126	202, 274	765
TF/PF magnet	Cu	LTSC or HTSC	LTSC or HTSC	LTSC or HTSC
Vacuum vessel material	SS	Baintic steel	Bainitic steel	Bainitic steel
Divertor	W/CuCrZr/H_2O	W/W/He	W/W/He	W/W/He

2. FNSF Operating Point Identification and Examination of the Operating Space

The systems analysis was used to identify an operating point for further detailed analysis. This mainly establishes the plasma geometry around which the device can be built. Recent improvements to the systems code include a new buildout algorithm for layering the fusion core components and magnets around the plasma. The systems analysis includes a zero-dimensional plasma description for power and particle balance, along with plasma radiation, external heating and current drive, bootstrap current, using parabolic with finite edge profiles for density and temperature, and up to 3 impurities. The systems code uses a database approach where large numbers of viable operating points are identified, and filtered by constraints to produce a range of desirable configurations or "operating space". One particular operating point is used for specifying the device for use with detailed physics and engineering analyses. This is described in more detail in Section 6-a and 6-b.

Preliminary 1D nuclear analysis (further reported in Section 6-c) was generated in order to construct the inboard radial build of first wall, breeding blanket, structural/shield ring, vacuum vessel, and low temperature shield. The inboard radial build is critical to the device's size. The neutron damage to the superconducting TF coils, dose to the insulator in the TF coils, heating in the winding pack and coil case, and damage to the copper stabilizer were examined to set the requirements for overall shielding (reduction in neutron flux and high energy component of the neutron energy spectrum). Since there is a desire to keep the device smaller at the intermediate stage of an FNSF, tungsten carbide

(WC) was used for the shielding filler in the structural ring, vacuum vessel and low temperature shield. Only helium cooling is allowed inside and in the vacuum vessel, and water cooling is only allowed outside the vacuum vessel. The lead-lithium breeder also cools the blanket. These cooling choices have strongly impacted the nuclear aspects of the device. The resulting inboard build is composed of 50 cm of first wall and breeding blanket, 20 cm for the structural ring, 10 cm for the vacuum vessel, and 23 cm for the low temperature shield, giving a total material build to the TF coil of 103 cm. The systems code has assumed 20 additional cm's of undefined gaps, and a 10 cm plasma scrape-off width on the inboard, leading to the inboard build distance from the plasma to the TF coil of 133 cm.

Systems scans were performed over toroidal magnetic field, plasma beta, edge safety factor, plasma density, plasma fusion gain, plasma major radius, and impurity content. Constraints imposed on these operating points are low temperature superconducting limits, described by < 16 T at the TF coil and < 15 MA/m^2 current density in the TF coil. Ninety percent of the power reaching the divertor is assumed to be radiated, with a power scrape-off width determined from Fundamenski [8], and a peak divertor heat flux < 10 MW/m^2. Finally a minimum peak neutron wall load on the outboard first wall is imposed of 1.5 MW/m^2. In addition, these scans were done at plasma aspect ratios of 3.0, 4.0 and 5.0. When examining different aspect ratios the scalings used for β_N and plasma elongation as a function of aspect ratio are critical to arriving at proper conclusions. The no wall beta limit β_N was taken to be 2.6 at the low end for all configurations, and was 3.75 at A = 3.0, 3.55 at A = 4.0, and 3.35 at A = 5.0, at the high end, based on analysis in ref [9]. The elongation was scaled from a combination of detailed vertical stability analysis in ref [10] and ideal MHD calculations reported in ref [11], giving a maximum x-point elongation of 2.3 at A = 3.0, 2.2 at A = 4.0, and 2.15 at A = 5.0. These elongations are based on conducting structures in the blanket and feedback control coils located behind the blanket/shield. Over the aspect ratio range examined, the plasma size did not decrease with decreasing aspect ratio, and the plasma current significantly increased with decreasing aspect ratio. Higher plasma current is unattractive due to larger external current drive requirements, larger disruption forces, and stronger drive for runaway electron production in disruptions. There was no incentive to move to lower aspect ratio based on any parameters, and so it was chosen to be 4.0. Although the highest aspect ratio was attractive, there is little experimental database in this region. The plasma operating point major radius is 4.8 m, minor radius is 1.2 m, and elongation is 2.2 and triangularity is 0.63 at the x-point. Other parameters are listed in Table 1. The FNSF is shown in Fig. 2 with other next step and DEMO proposals [12-16], fusion power versus plasma major radius space. The devices are not all derived with the same "design" criteria or assumptions. For example, the FNSF is not required to produce net electricity, while the K-DEMO, JA DEMO and EU DEMO are required to produce net electricity, and among other things, contributes to the larger device size.

Table 1. Parameters for FNSF operating point.

A = 4	
R, m	4.8
κ_x, δ_x	2.2, 0.63

Ip, MA	7.87
B_T, B_T^{coil}	7.5, 15.85
$\langle j_{TF} \rangle$, MA/m^2	15.0
β_N^{th}, β_N^{fast}	2.2, 0.23
q_{95}	6.0
H_{98}	1.0
f_{BS}	0.52
Z_{eff}	2.43
n/n_{Gr}	0.9
$n(0)/\langle n \rangle$, $T(0)/\langle T \rangle$	1.4, 2.6
P_{fusion}, P_{aux}, MW $P_{rad,core}$, $P_{rad,div}$, MW	517, 130 60, 160
Q, Q_{engr}	4.0, 0.86
η_{CD}, A/m^2-W	0.2 (assumed)
$\langle N_w \rangle_{plas}$, $N_W^{peak, FW}$, MW/m^2	1.18, 1.78
q_{div}^{peak} (OB,IB), MW/m^2	10.7, 3.9

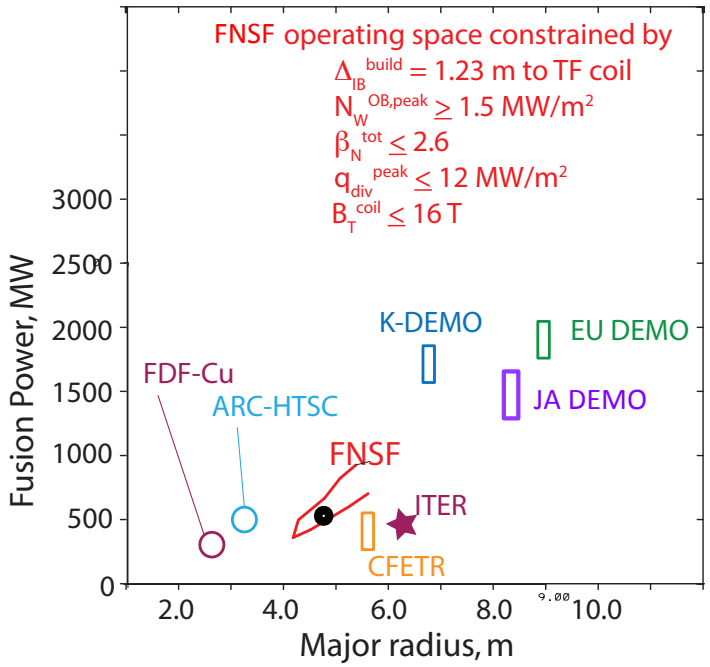

Figure 2. Fusion power versus plasma major radius for the FNSF operating point at R = 4.8 m, and several DEMO and next step proposals, and ITER.

Although an operating point is needed to pursue more detailed analysis of the FNSF plasma and engineering, based on the uncertainty of achieving these plasma and engineering parameters, the operating space, around the operating point, is needed to establish the robustness of the device's operation. Once the plasma geometry is chosen further scans with the systems code can be done to examine robustness to uncertain

parameters with the geometry fixed (e.g. R, a, κ, δ). The systems code then scans over a more limited range in some parameters, while expanding others, while imposing the same filters of peak neutron wall load > 1.5 MW/m^2, maximum peak heat flux in the divertor of 10 MW/m^2, and maximum total β_N of 2.6. Here the toroidal field is scanned from 6.5 to 7.5 T, β_N from 1.8 to 3.4, q_{95} from 5.0-8.0, n/n_{Gr} = 0.7-1.1, $n_o/\langle n\rangle$ from 1.25 to 1.5, $T_o/\langle T\rangle$ from 1.9 to 2.9, and fusion gain from 2.0-10.0. Other parameters are the same as in previous scans. Examples of uncertainties include the impact of not reaching the desired B_T, the impact of a lower allowable q_{div}^{peak}, the impact of a lower radiated power fraction in the divertor, or the impact of accessing higher β_N values. It is found that the operating point is robust to many variations, however, some variations require a reduction in the fusion power to maintain operating space, or an increase in the plasma beta to recover operating space. This type of exploration of the operating point and space is important for assessing the criticality of given parameters to the facility's accomplishing its mission, and provide some guidance on critical R&D areas in physics and engineering. This is described in more detail in Section 6-a.

In the coming year systems examinations of the minimal and maximal FNSF configurations will be done for comparison to the reference moderate design. In addition, the robustness examination will continue, and a high B-field (>16 T) exploration will be done to identify benefits of this technology.

3. FNSF Technical Assumptions for Detailed Analysis

The FNSF overall facility is based on the ARIES-ACT2 design [17], however, it is being adjusted for the significant difference in size. The reference breeding blanket is the Dual Coolant Lead Lithium (DCLL) concept. This utilizes RAFM (or variant) steel for the structural material, liquid lithium lead ($Li_{17}Pb_{83}$) for the breeder, and silicon-carbide composite for the insulator material in the conduits with lithium lead. The divertor is tentatively defined as a tungsten structure, where the precise tungsten material is undefined. The structural ring, which lies outside the blanket and divertor and serves as the rigid component that they are attached to, is also made of RAFM steel. The vacuum vessel, which lies outside the structural ring, is made of a 3Cr-3WV(Ta) bainitic steel due to the lower neutron damage levels in this location and stable microstructure that does not require post-weld-heat-treatment (PWHT), which RAFM steels do. The structural ring and vacuum vessel are double-walled with ribs, and contain a shielding filler material, which is WC on the inboard side and borated ferritic steel (B-FS) on the outboard side. The bainitic steel is also the preferred structural material for the low temperature shield, which lies outside the vacuum vessel. This shield is water cooled (water cooling is allowed because it lies outside the fusion core and vacuum vessel), and contains WC shielding filler on the inboard and B-FS on the outboard. On the outboard side the very large vacuum vessel ports have the low temperature shield on the inner port door and are helium cooled (which increases its thickness there). Fig. 3 shows a sector of the blanket and structural ring from ARIES-ACT2, and Fig. 4 shows the larger layout with the vacuum vessel, its ports and inner and outer doors. The new CAD representation of the FNSF is being developed as the detailed analysis of magnets, thermo-mechanics and

thermofluids of the blanket, and nuclear analysis proceeds, and this is described in more detail in Section 6-d.

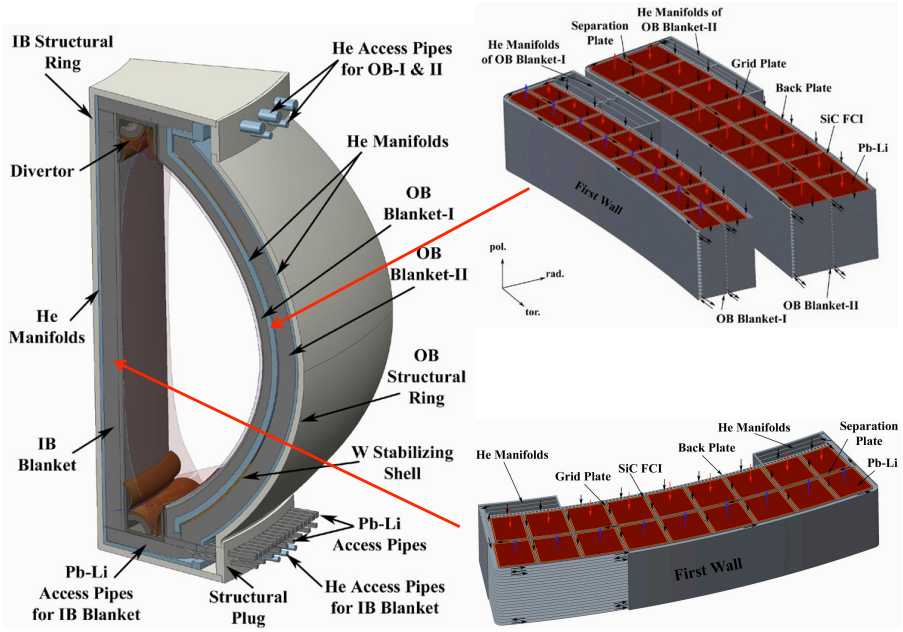

Figure 3. A sector of the fusion power core showing the structural ring on the outside, with inboard and outboard blankets, and divertors mounted to it. The blankets are shown expanded. These are from the ARIES-ACT2 design, ref[ ], and are being resized for FNSF studies.

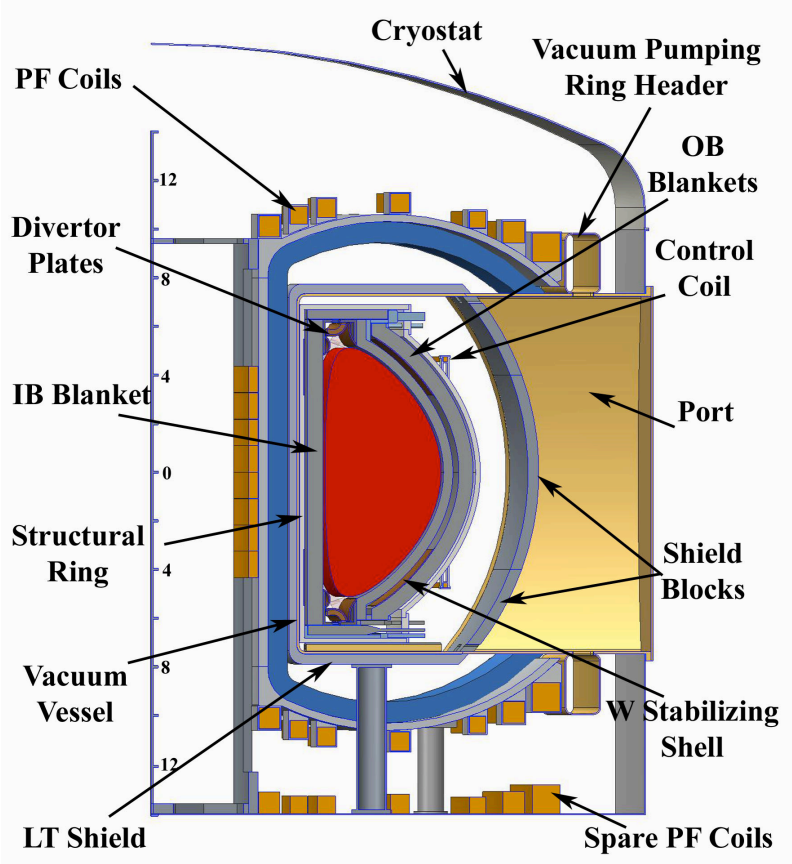

Figure 4. The overall layout of components in the ARIES-ACT2 design, which is being adopted in the FNSF study, showing the large vacuum vessel and outer ports, and the toroidal and poloidal field magnets. A single sector can be removed through the large ports.

The maintenance scheme for the FNSF has been taken to be horizontal with a large port between all TF coils, in which entire sectors (16 sectors for 16 TF coils) can be removed, see Fig. 3 and 4, as opposed to the small module approach through small ports as done in ITER. This is driven by the need for much higher availability both on the FNSF and in future commercial power plants. A series of qualitative measures were established to judge among maintenance schemes to arrive at the choice for the FNSF, including 1) number of power core units, 2) number of coolant connections that must be cut and rewelded, 3) amount of remote handling equipment needed inside the vacuum vessel, 4) number of complex maneuvers and in-vessel equipment, 5) compatibility with heating and current drive, diagnostic, and test blanket module systems, 6) ready access to any failed sector or segment for replacement in the power core, and 7) flexibility to alter/improve downtimes. Competitive schemes include vertical maintenance of more smaller sector parts, dedicated divertor port maintenance for lower single null plasma configurations, and a range of vertical and horizontal approaches with fewer openings for access. This is discussed in Section 6-e, and next steps would be to assess the maintenance options with detailed data on times required for the various functions (e.g. cutting and welding, component movement).

In addition to full sized sectors, it is proposed to have 4 test blanket modules (TBMs) which allow 1) the testing of next phase materials or operating parameters, 2) the testing of DEMO or commercial parameter regimes not accessed directly in the FNSF, and 3) the maintenance of backup blanket concepts. The question of whether to use TBMs or to test in a full sector is being explored, since the reference blanket concept is a full sector approach, and not a modular approach as proposed by EU, JA, KO and CH. These modules are independent of the sector in terms of their coolant feeds and operating parameters, and penetrate the sector from the structural ring all the way to the first wall. However, maintenance examinations indicate that an integrated (with sector) TBM is better than a discrete TBM, and this is discussed further in Section 6-d. Testing of material samples is also proposed with a single specific test module (MTM) or multiple test modules of smaller size. Since the fusion neutron flux and energy spectrum are unique in a fusion device, compared to those produced by fusion relevant accelerator based facilities (e.g. SNS or IFMIF), the opportunity exists to test material samples. This is further discussed in Section 6-c.

Analysis of the tritium extraction using a vacuum permeator, the envisioned concept for the DCLL type blanket with PbLi breeder/coolant, has established a number of important observations. The extraction unit is likely a large apparatus like a heat exchanger, with many tubes. The permeator material is preferably from group 5 (V, Nb, Ta) on the periodic table, however, these must be augmented with coatings to avoid interaction with possible impurities in the liquid metal flow. Fortunately, the industrial development of such permeators exists for general hydrogen application, but is likely to require modifications for the fusion application. The incorporation of the tritium extraction unit, and a wide range of other components, in the tritium plant modeling (TMAP) is critical to understanding the dependences for tritium sources, movement, retention, and leakage, and is discussed in more detail in Section 6-f.

The thermo-mechanics of the breeding blanket are important to understand the operating conditions and design aspects for an FNSF. The standard analysis includes computational fluid dynamics for the coolants, heat transfer in solids, heat transfer in fluids, and thermal and primary stress determinations in solids. Analysis is typically done separately for each of these assessments, but here they have been coupled into a multi-physics calculation using the COMSOL software. Although all parameters and assumptions are not presently self-consistent with the blanket design, it demonstrates that coupled calculations are possible. The computational results were used to compare with the ITER Structural Design Criteria for In-Vessel Components. Loading cases for the blanket have been established and include, 1) nominal, 2) He over-pressure, and 3) plasma disruption, and this work is continuing for the blanket and will be continued for the divertor. This is reported in more detail in Section 6-g.

The toroidal (TF) and poloidal/central solenoid (PF/CS) coils are being examined for the high magnetic fields desired in the FNSF (7.5 T at the plasma and ~ 16 T at the TF coil), as well as, the added structural requirement for the horizontal maintenance scheme. An advanced (more advanced than ITER) low temperature superconductor version of Nb_3Sn

is targeted for the FNSF baseline design along with winding pack design upgrades and conductor grading. Some of the PF or CS coils may also use this conductor type. Winding pack assumptions are being reviewed and chosen based on the latest data for irradiation response, ITER R&D progress, and proposed targets for the Korean magnet program and the high energy physics (HEP) magnet development. The possible use of high temperature superconductor magnets is being maintained as the development and applications for these types of conductors continues. More details can be found in Section 6-h. Global structural analysis has been performed for the TF coil with particular emphasis on the impacts of the horizontal maintenance scheme. This maintenance scheme requires that an entire sector ($1/16^{th}$ of the fusion core for 16 TF coils) can be removed through a single port lying between the TF coils on the outboard side. This requirement forces the TF coil outboard leg to larger major radius. Analysis for the required support structure showed that it is feasible with super-structures to support the coil at top and bottom (caps), on the outboard of the TF coil leg, and with constraining torque cylinder at the outboard top and bottom. Interaction with the PF coils was also examined. Advantage is being taken of the significantly reduced number of cycles expected in the FNSF compared to ITER. Greater detail is provided in Section 6-i.

The breeder and blanket coolant, PbLi, is a conducting fluid, which must move through a magnetic field. Analysis has begun for the MHD thermofluid behavior in the FNSF, which will include 1) evaluation of the pressure drop in the blanket and pressure distribution along the flow path, 2) heat transfer to determine the temperature distribution in the fluid, flow channel inserts (FCI, insulator in the flow channel) and steel conduit walls, and 3) mass transfer to address corrosion from the steel and PbLi interaction. Here the MHD pressure drop for the inboard blanket (B ~ 10 T) was analyzed, examining 4 cases at low temperature with a sandwich FCI at low temperature, and a SiC-composite FCI at low, medium and high temperature. The heating was taken from the 1D nuclear analysis. The sandwich FCI case has an excessively high pressure drop and could only be acceptable with lower fusion power and flow velocity. The low temperature SiC-composite FCI case is also marginal without reduced power and flow velocity, while the medium and high temperature cases were acceptable. The contributions to the pressure drop were dominated by the fluid flow velocity needed, and the inlet/outlet manifolding assumption. These results indicate further examination of the manifolding are required, and also outboard region for comparison where the magnetic field is ~ 5 T. More detail can be found in Section 6-j.

The presence of transients (ELMs) and disruptions can provide serious design driver loading conditions. Transients are examined in the divertor, using prescriptions developed from experimental data on tokamaks. The conditions where melting just begins are sought, since in long pulse plasma operation melting is not tolerable. The energy released per ELM to the divertor is determined as a function of the inter-ELM heating, the latter determines the nominal operating temperature for the divertor structures. This shows clearly that for the FNSF a lower ELM energy is required to avoid melting in the divertor, while the first wall appears to be capable of avoiding melting. The large numbers of ELMs that would be accumulated over long plasma pulses can lead to serious cyclic loading, which will be investigated. Disruptions pose

the most difficult off-normal event, with a thermal quench and subsequent current quench. A model has been constructed for the electromagnetic analysis that includes all conducting structure of the blanket, divertor, structural ring, vacuum vessel, and includes the PF and TF coils. The impact of ferromagnetic material (RAFM) is also being investigated. Analysis continues for these phases, with the assumption that all disruptions are mitigated. More details of the ongoing analysis can be found in Section 6-k.

4. The Program on the FNSF

The FNSF is intended to advance several parameter/metrics toward a fusion power plant, however it is a first of a kind facility with substantial scientific exploration related to ultra-long pulse high performance plasma operation and fusion nuclear science. The program is divided into 7 phases. The first is a He/H shakedown phase for the facility. The second is a DD phase with the primary mission of establishing the very long pulse lengths that will be used in the next 5 DT phases. These subsequent 5 DT phases then ratchet up the fusion neutron damage level reaching approximately 7, 19, 26, 37, and 37 to 74 dpa, respectively. After each DT phase all sectors of the fusion core are removed, de-contaminated, disassembled, cut into samples and examined for a wide range of properties. These sectors, which are integrated multi-material components, have experienced the fully integrated environment of a fusion core, never seen before in any pre-FNSF R&D. Phase 7 has the option of starting over or leaving the sectors (or subset of sectors) in the fusion core to accumulate up to 74 dpa. The examination of the materials that compose these sectors is one of the most critical functions of the FNSF. During the sequence of DT phases it is assumed that the primary structural material can be advanced from a generation I reduced activation ferritic martensitic (RAFM) steel to generation II, and then to oxide dispersion strengthened nano-structured versions of RAFM. Although not developed in detail, the concept of being able to test structural materials within the "family" of RAFM steels is considered viable, and could include the range of low to mid to high chromium level RAFM steels that have been or might be developed for fusion, and also reduced activation versions of alloys developed for fission, or even fossil applications. Since the approach for the FNSF is to qualify materials in advance of using them in the device, any materials used as structural or functional materials would have to have reached the dpa level in a fusion relevant neutron facility (e.g. SNS, IFMIF) and undergone integrated non-nuclear blanket or divertor testing. The capacity to examine different materials on the FNSF making up a component is determined by what can be qualified in the pre and parallel FNSF time frames.

Table 2. The program on the FNSF in phases.

	1-He/H	2-DD	3-DT	4-DT	5-DT	6-DT	7-DT	PP
Years	1.5	2-3	3	5	5	7	7	40 FPY
Peak neutron wall			1.5	1.5	1.5	1.5	1.5	2.25

loading, MW/m^2								
Plasma on-time, % of a year (days per year)		10-50	15 (55 days)	25 (91 days)	35 (128 days)	35 (128 days)	35 (128 days)	85
Plasma duty cycle, %			33	67	91	95	95	100
Inspect/maintenance time, days/year			200	228	212	231	231	55
Peak neutron damage, dpa (for Fe)			6.8	18.8	26.3	36.8	36.8-73.5	100-200
RAFM operating temperature, ^oC			400	450	500	550	550	500-600

The program as shown in Table 2 provides about 8.4 years of total fusion neutron exposure over 27 years of DT operation. The program is being reviewed to compress the time required to reach the desired dpa levels by looking at 1) higher beta operation above the no-wall beta limit, 2) reaching higher plasma on-time and/or higher duty cycles in the first DT phase, 3) critically examining time-frames and activities in the various phases, and 4) distributing the plasma operations and maintenance times to search for efficiencies. In fact, the operating point identified for detailed study has a peak neutron wall loading of 1.78 MW/m^2, higher than assumed in the program, which can reduce the years to 23 for the DT phases, or it can be used to increase the neutron fluence and dpa (damage) levels.

The FNSF has both a material testing and a component (blanket and divertor) testing strategy. The material testing strategy involves removing one, some, or all sectors after a given neutron exposure and moving them to a hot cell, where they are 1) allowed to have short lived isotopes decay (~few weeks maximum), 2) are de-contaminated, 3) inspected, 4) are dismantled, 5) are cut to make samples for a wide array of material tests and examinations, and 6) stored for safe isolation and ultimate disposal. The basic program plan calls for all sectors, such as that shown in Fig. 3, to be removed, and each subsequent phase begin with a new set of sectors. This is because each phase is advancing the operating temperature, structural material, and neutron exposure in one form or another, and a full exposure trajectory is desired. It is conceivable that in some instance a sector could be inspected and returned to service, and it is also possible to replace the blanket and divertor components and reuse the structural ring, as anticipated in power plants, assuming an inspection or autopsy indicates it is acceptable. The materials that compose the components of a sector are exposed to the fully integrated fusion environment including both nuclear and non-nuclear features. This includes the

many environmental features noted earlier and the significant spatial variations (gradients) in these features. This makes the retrieval and diagnosis of the materials extremely important to establishing a database for future fusion devices, and constitutes one of the most critical scientific and developmental activities on the facility. The demands on the hot cell to provide this inspection and material assessment are tremendous, and include the need for a wide range of high radiation resistant and remotely controlled apparatus for handling, inspecting, cutting, transferring, testing and examining. All this must be done on site, and the turnaround for assessments cannot be long if they are to inform the next phases, material production, component manufacturing or other aspects of facility operation.

Material testing can also be done with dedicated modules (MTM's) that penetrate a sector like TBM's where samples are exposed to the unique fusion neutron flux and energy spectrum. These samples do not see the full service environment that functioning sectors do and so provide material testing similar to accelerator based testing. The unique features provided by this testing is 1) the actual fusion neutron spectrum, 2) materials do not need to be qualified to be tested since they are not functioning as a component, 3) they can potentially reach higher damage levels than the materials in the components by exposing the same samples in multiple phases, and 4) can potentially allow larger volume for large sample arrays or for larger sample pieces.

The other aspect of the FNSF program that is being examined is the distribution of plasma operations and maintenance activities, that is *"what is actually done in specific parts of a phase in the program?"* It is desirable, in principle, to move all the plasma operations, which is where neutrons are produced, into one part of the phase, and move all the maintenance into the remaining part. This provides the most continuous neutron exposure. For example, in Phase 3 lasting 3 years, the total plasma operations occupy 495 days, of which the plasma is on making neutrons 165 days. This leaves a total maintenance time of 600 days. Maintenance here applies to any activity including inspections, minor maintenance, or major maintenance that can require no vacuum break, an inert gas, or a vacuum break. Additional time may be required to remove all the sectors at the end of the phase. It must also be understood that when the plasma is on making neutrons, the components that make up the fusion core are being cooled, while when the plasma is off, the coolants must provide heating to keep the material/component temperatures as constant as possible. This is due to the strong correlation of irradiation damage and other physical phenomena on temperature. This motivates trying to reach long plasma pulse lengths as early as possible, rather than slowly progressing toward the longest pulses during the program, and this is being examined. These and other issues are being explored. More detail in the plasma operations have been developed to better understand activities and timeframes required, and an example is given in Section 6-l.

5. Plasma Strategy for the FNSF

The strategy for choosing plasma operating parameters is strongly influenced by the requirement in the FNSF for ultra long plasma discharges, reaching ~ 10 days. Present

higher performing tokamaks typically reach 2-10 s plasma pulse lengths, while JT-60U reached about 25-30 second discharges. Lower performing plasmas have reached about 400 s on Tore Supra and HT-7 and more than 3-5 hours on TRIAM-1M, which all have superconducting coils. The demonstration on JT-60U of recovering and sustaining shorter pulse (few seconds) operating modes for 15-30 s pulses after upgrading the device for extended heating and power handling is encouraging, and indicates that the limitations from hardware in virtually all tokamak experiments should not be considered a fundamental limit to the pulse duration and sustainment. The most recent achievements in long pulse tokamak operation have come from EAST, reaching 410 s pulse length in diverted L-mode plasma, and > 30 s in H-modes with ELMs, using ICRF and LHCD. These plasmas are 100% non-inductive. Fig. 5 shows the normalized plasma beta as a function of the plasma pulse duration, including present tokamaks, and proposed goals of long pulse devices like EAST, KSTAR, JT-60SA, and ITER.

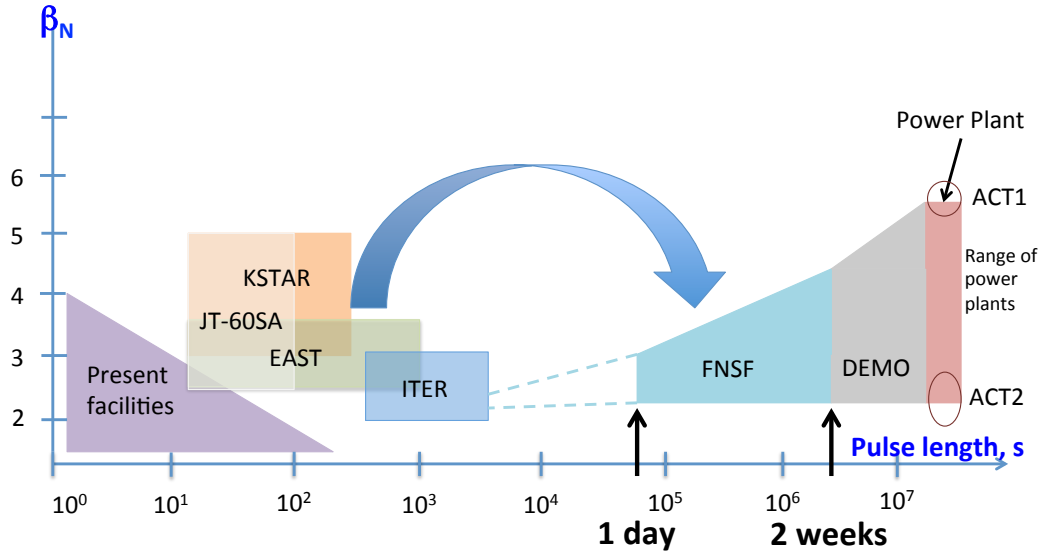

Figure 5. The plasma normalized beta versus plasma pulse duration for several present tokamak experiments, the proposed long pulse tokamaks (EAST, KSTAR, and JT-60U), and ITER. A large gap exists between the longest ITER or EAST discharge and FNSF pulse length requirements.

The significant gap in plasma pulse length between the planned tokamak devices and the desired range of pulse lengths required for the FNSF indicates that the FNSF itself will have to establish the long pulse lengths, primarily in the deuterium phase. A preliminary examination of how to build up these pulse lengths is given in Section 6-l. However, in advance of the FNSF, R&D is required on existing shorter pulse tokamaks, linear plasma facilities with very long durations, high heat flux facilities, and numerical simulations covering SOL and divertor physics, plasma materials interactions, and particle control, to provide the needed design basis for the FNSF. It should be noted that both the plasma pulse length and the duty cycle (fraction of plasma operations when plasma is on) must be increased to ~ 1 year and 100%, respectively, for a commercial power plant. Present tokamak experiments in the US have pulse lengths of 2-10 s, duty cycles of 0.2-1.0%

(assuming 15-20 minutes between shots), and the total plasma on-time in a year is typically 0.2-0.6% (assuming 15 run weeks and 9 hour rundays). ITER targets are 5% plasma on-time in a year, with 25% duty cycle during plasma operations.

The plasma performance, often measured by the normalized beta or parameter combinations such as $\beta_N H_{98}/q_{95}^2$, must be balanced against the plasma duration over which it was sustained. JT-60U and DIII-D [18-23] have demonstrated the most promising plasma discharges and some of these are listed in Table 3. With the FNSF operating point β_N of 2.6, bootstrap fraction of 52%, confinement scaling multiplier (H_{98}) of 1.0, q_{95} of 6 the second JT-60U and the 4th and 6th columns for DIII-D are supportive demonstrations. However, several other parameters, which are not known for these experimental discharges, are likely different. For the FNSF these include 1) high density operation at $n/n_{Gr} = 0.9$, 2) very low plasma rotation, 3) highly radiating divertor operation, 4) $T_i \sim T_e$, 5) active suppression of NTMs, and 6) metallic plasma facing components. Discharges have been produced in various tokamaks addressing these issues in subsets, but not in their entirety. The plasma operating point in the FNSF study is clearly a projection to a plasma operating space that has not been obtained experimentally, and can benefit from experimental activities to combine these properties. In addition to simulated plasmas, identification of existing experimental scenarios [23,24] in the $\beta_N \sim 2.5$-3.5 range is desirable to further improve the basis for projecting plasma configurations.

Table 3. Experimentally achieved plasmas targeting long durations at high performance on the JT-60U and DIII-D tokamaks.

	JT-60U	JT-60U	JT-60U	DIII-D	DIII-D	DIII-D
β_N	2.3	2.4	1.7	3.5	2.0	3.1-3.4
$\tau_{flattop}/\tau_{CR}$	13.1	2.8	2.7	2.0	> 2	~ 0.4-1.0
q_{95}	3.2	4.5	~ 8	6.7	4.7	5.0-5.5
$f_{bootstrap}$	35-40%	45%	80%	40-50%		~ 60%
$f_{non\text{-}inductive}$		90%	100%	75%		80-100%
H_{98}		1.0	1.7	1.0	1.3	>1.2-1.3
$q_{minimum}$	~ 1	~1.5		1.5		1.4
	hybrid	steady state	steady state	Steady state, off-axis NB	QH-mode, no ELMs	steady state

The FNSF studies here have focused on a set of basic plasma assumptions of its operating point, many of which will be varied to assess their impact in future work. These are

Steady state current (100% non-inductive plasma current)

Operation in the vicinity of the no-wall beta limit (defined here to be $\beta_N \sim 2.6$)

Operation below, but near the Greenwald density limit

Maintaining the peak divertor heat flux below 10 MW/m^2, with highly radiating divertor solutions

Pursue strong plasma shaping (κ_x = 2.2, δ_x = 0.63) in the DN configuration

Pursue high toroidal field

The no wall beta limit $\beta_N \sim 2.6$ is based on analysis of power plant plasmas in the ARIES-ACT2 study, where the current profile and pressure profile come from time-dependent simulations. The current is composed of a bootstrap and externally driven sources (including NB, ICRF, and LH) which will dictate the shape of the profile. When pressure is changed to find the beta limit, the bootstrap current is self-consistently re-calculated and the external current drive sources are modified to keep the total plasma current fixed. Fig. 6 shows the data in β_N vs l_i, with the red points indicating the no wall beta limit, and the green points showing the increased beta limit with a conducting wall located at a distance from the plasma boundary of 0.55 times the minor radius. The basis for the FNSF is to design the device to succeed with beta limits near the no wall limit, but include the benefits of operating slightly above the no wall limits using feedback control, plasma rotation, and kinetic fast particle stabilization in some combination, as demonstrated on DIII-D. So determining what the required systems are for operating in this regime is an important research direction. Additional ideal MHD stability studies are on-going for the FNSF and these are reported in Section 6-m.

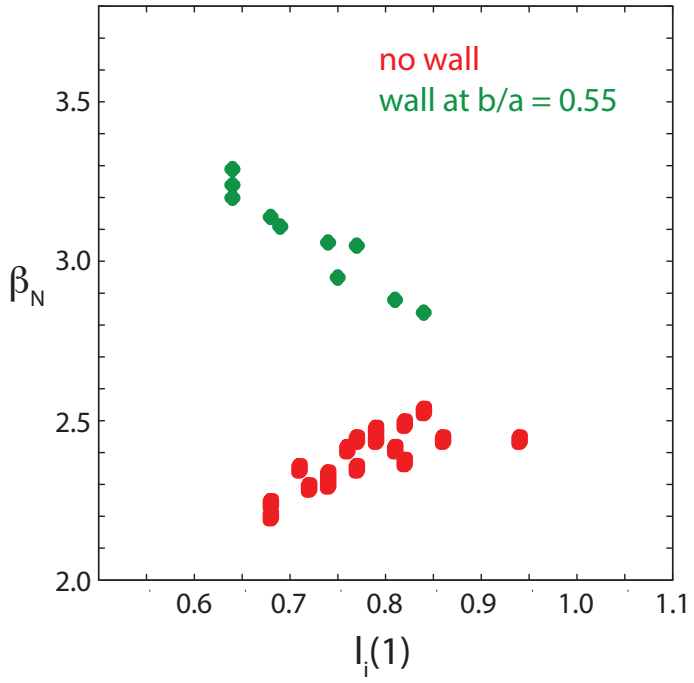

Figure 6. Maximum stable β_N as a function of the plasma internal self-inductance (current profile peakedness) assuming no conducting wall near the plasma and assuming a conducting wall located 0.55 times the minor radius from the plasma boundary. These

plasma profiles were generated from time-dependent 1.5D simulations for the ARIES-ACT2 power plant study, with heating and current drive profiles from neutral beams, lower hybrid, and ion-cyclotron sources.

Highly radiative divertors are the basis for the power handling in the FNSF, with recent analysis for the ARIES-ACT1 study [25] identifying candidates for divertor operation of an ITER-like vertical target with ~ 75% of the plasma power radiated and a peak divertor heat flux of < 12 MW/m^2, or a wide slot detached mode with ~ 100% of the power radiated and a peak divertor heat flux of 3 MW/m^2. Research on the compatibility of such operating regimes with attractive core plasma operation is continuing, albeit with the extreme difficulty of modifying divertor geometries to assess their impact. Some success has been obtained with special divertor magnetic geometries, although in general these are simply flux expansions, and do not necessarily show the detailed divertor configuration or the self-consistent particle control. Systems analysis to determine the divertor power handling have assumed a simple formulation for the peak heat flux,

$$q_{div}^{peak} = P_{SOL} f_{vert} f_{IB/OB} \left\{ \frac{f_{div,rad}}{A_{div,rad}} + \frac{1 - f_{div,rad}}{A_{div,cond}} \right\}$$

where the $A_{div,rad}$ is the divertor area available for absorbing radiation which is large, and $A_{div,cond}$ is the area available for the absorption of conducted power, which is small, $2\pi R f_{tilt}\, f\psi\, \lambda_{pow}$. The power scrape-off width, λ_{pow}, is taken from a formula from Fundamenski [8]. The radiated power fraction ($f_{div,rad}$) is assumed to be 90% in the systems analysis, but is ultimately subject to detailed analysis with 2D SOL/divertor simulations, and these detailed calculations for the FNSF are summarized in Section 6-n.

The FNSF fusion core structures and vacuum vessel must be designed to maintain their integrity during a mitigated disruption. A mitigated disruption here means that action has been taken based on the signal of an imminent disruption, which involves the injection of particles (as a pellet or jet or gas) into the plasma which ultimately also creates a disruption. However, rather than have the majority of the plasma stored energy go to the divertor, it is radiated to the first wall due to the large influx of particles. In addition, the introduction of a large particle inventory must eliminate the production of runaway electrons. The mitigation should not significantly alter the current quench phase of the disruption. Since the plasmas being examined for the FNSF are nearly up-down symmetric DN, the most likely and worst event is the midplane disruption (as opposed to the VDE for SN plasmas). Here the plasma releases ~ 100% of its stored energy in the thermal quench, and disrupts in place with little vertical motion. The thermal quench delivers a large radiative surface heat flux to the first wall and divertor domes, providing a large transient heat load. The current quench, whose duration is taken from the tokamak database developed for ITER, occurs over ~ 30 ms, and provides the drive for electromagnetic simulations. Halo currents can still be generated, with poloidal current paths through the closest poloidally continuous structures to the plasma, however experimental mitigation results indicate that the halo current can be reduced. Thermomechanical and electromagnetic simulations for the FNSF are reported in Section 6-k. Overall, the disruption philosophy for the tokamak applied here, and for commercial tokamak power plants, has the following elements. Disruptions must become extremely

rare events, with a utility tolerating only a few over the full 40 full power year plant lifetime, which would be based on the economics of replacing all the blanket sectors after such an event. The event may lead to some damage of the fusion core components, but cannot lead to a potential accident sequence (e.g. loss of coolant, loss of coolant flow), as this would make it intolerable for the utility. The event cannot lead to damage or compromise of the vacuum vessel since this is the primary radiological barrier. Based on this perspective, the FNSF, which could have a higher disruption frequency than targeted for a commercial power plant, must demonstrate the severe reduction of disruptions over the course of its operation, the lack of accident potential, and the recovery operations required following such an event. The FNSF would rely strongly on the development of disruption avoidance and mitigation research prior to its operation.

References

1. C. E. Kessel, et al, Fus Sci Technol, **68**, 225, (2015).
2. G. S. WAS, *J. Nucl. Mater.*, **367-370**, 11**,** (2007).
3. E. E. BLOOM, et al, *J. Nucl. Mater.*, **367-370**, 1**,** (2007).
4. M. Abdou et al Fusion Technology **29** (1996) 1.
5. R. Stambaugh et al Fusion Science and Technology **59** (2011) 279.
6. Y-K. M. Peng et al Fusion Science and Technology **56** (2009) 957.
7. J. Menard et al Nuclear Fusion **51** (2011) 103014.
8. W. Fundamenski et al, Nucl Fus, **45**, 950, (2005).
9. J. E. Menard et al, Phys Plasmas, **11**, 639, (2004).
10. C. E. Kessel et al, Fus Eng Des, **80**, 63, (2006).
11. R. D. Stambaugh et al, Nucl Fus, **32**, 1642, (1992).
12. G. FEDERICI, et al, Fusion Eng. Des., 89, 882, (2014).
13. K. KIM, et al, "A Preliminary Conceptual Design Study for Korean Fusion DEMO Reactor Magnet", Symp. On Fusion Engineering, San Franciscso, June 10-14, 2013.
14. Y. T. SONG, et al, "Concept Design of CFETR Tokamak Machine", Symp. On Fusion Engineering, San Franciscso, June 10-14, 2013.
15. B. N. SORBOM, et al, "ARC: A compact high field fusion nuclear science facility and demonstration power plant with demoutable magnets", submitted to Fusion Eng. Des; http://arxiv.org/pdf/1409.3540v1.pdf
16. V. S. CHAN, et al, *Nucl. Fus.*, 51, 083019, (2011).
17. X. Wang et al, Fus Sci Technol, **67**, 193, (2015).
18. S. IDE, et al, *Nucl. Fusion*, 45, S48, (2004).
19. N. OYAMA, et al, *Nucl. Fusion*, 49, 104007, (2009).
20. N. ASAKURA, et al, *Nucl. Fusion*, 49, 115010, (2009).
21. M. MURAKAMI, et al, *Phys. Plasmas*, 13, 056106, (2006).
22. D. N. HILL, et al, *Nucl. Fusion*, 53, 104001, (2013).
23. C. T. HOLCOMB, et al, *Nucl. Fusion*, 54, 093009, (2014).
24. F. Turco et al, Phys Plasmas, **22**, 056113, (2015).
25. M. E. Rensink and T D. Rognlien, Fus Sci Technol, **67**, 125, (2015).

6-a. Systems Analysis to Determine the FNSF Operating Point *(C. Kessel, PPPL)*

The systems code is used to scan large numbers of possible operating points for the plasma by scanning through a series of parameters, which include toroidal field, q_{95}, normalized beta, temperature and density profiles, plasma shape, plasma density, fusion gain, major radius, and impurity fraction. Parameters that are typically fixed include the plasma triangularity, plasma internal inductance, current drive efficiency, and ratio of global particle to energy confinement times. Every point that satisfies the power and particle balance is accepted. These points are passed through an engineering module to examine the peak heat flux to the first and divertor, the plant power balance, the inboard radial build (usually supplied), the TF coil build, bucking cylinder build, and the CS coil build. Filters are applied to obtain solutions of interest; here they are $\beta_N^{total} \leq 2.6$, $q_{div}^{peak} \leq 10$ MW/m^2, $N_w^{peak} \geq 1.5$ MW/m^2, and $B_T^{coil} \leq 16$ T. A database was established for aspect ratio values of 3.0, 4.0, and 5.0. One of the most important parameter scalings is the dependence of β_N on aspect ratio and maximum plasma elongation on aspect ratio. These two parameters have a significant influence on the operating space.

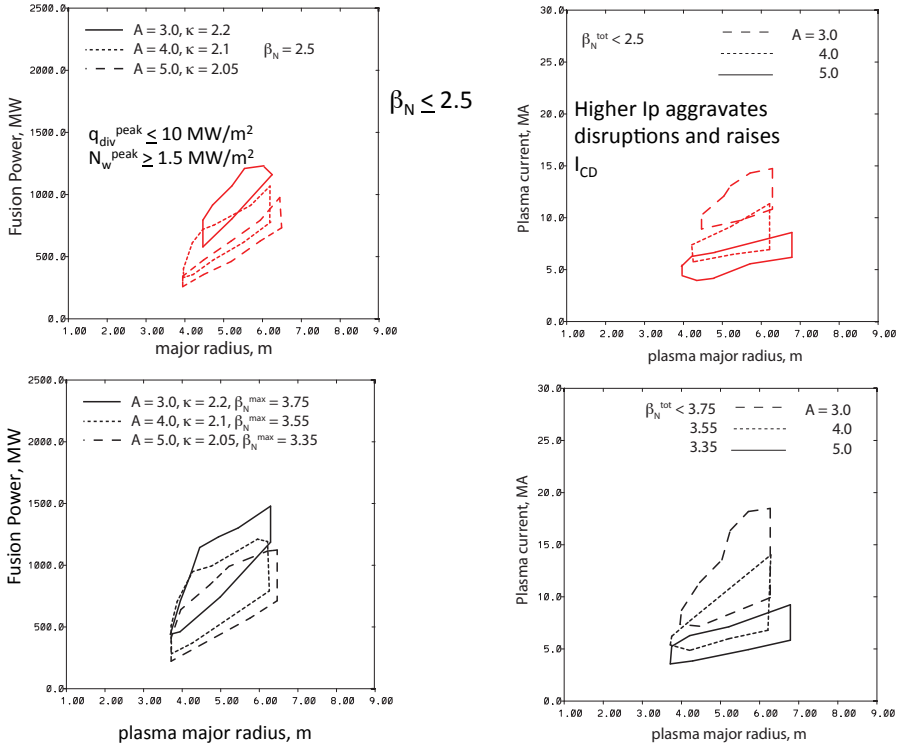

Figure 1. Plasma operating points from the systems code, in fusion power versus plasma major radius, that satisfy physics, engineering and filter criteria, in the no-wall low beta regime and no-wall maximum beta regime, showing the strong increase in plasma current with decreasing aspect ratio.

The no wall beta limit β_N was taken to be 2.6 at the low end for all configurations, and was 3.75 at A = 3.0, 3.55 at A = 4.0, and 3.35 at A = 5.0, at the high end, based on analysis in ref [2]. The elongation was scaled from a combination of detailed analysis in

ref [3] and ideal MHD calculations reported in ref [4], giving a maximum x-point elongation of 2.3 at A = 3.0, 2.2 at A = 4.0, and 2.15 at A = 5.0. These elongations are based on conducting structures in the blanket and feedback control coils located behind the blanket/shield. Over the aspect ratio range examined, the plasma size did not decrease with decreasing aspect ratio, and the plasma current significantly increased with decreasing aspect ratio. This is shown in Fig. 1. Higher plasma current is unattractive due to larger external current drive requirements, larger disruption forces, and stronger drive for runaway electron production in disruptions. There was no incentive to move to lower aspect ratio based on any parameters, and so it was chosen to be 4.0. Although the highest aspect ratio was attractive, there is little experimental database in this region. The plasma operating point major radius is 4.8 m, minor radius is 1.2 m, and elongation is 2.2 and triangularity is 0.63 at the x-point.

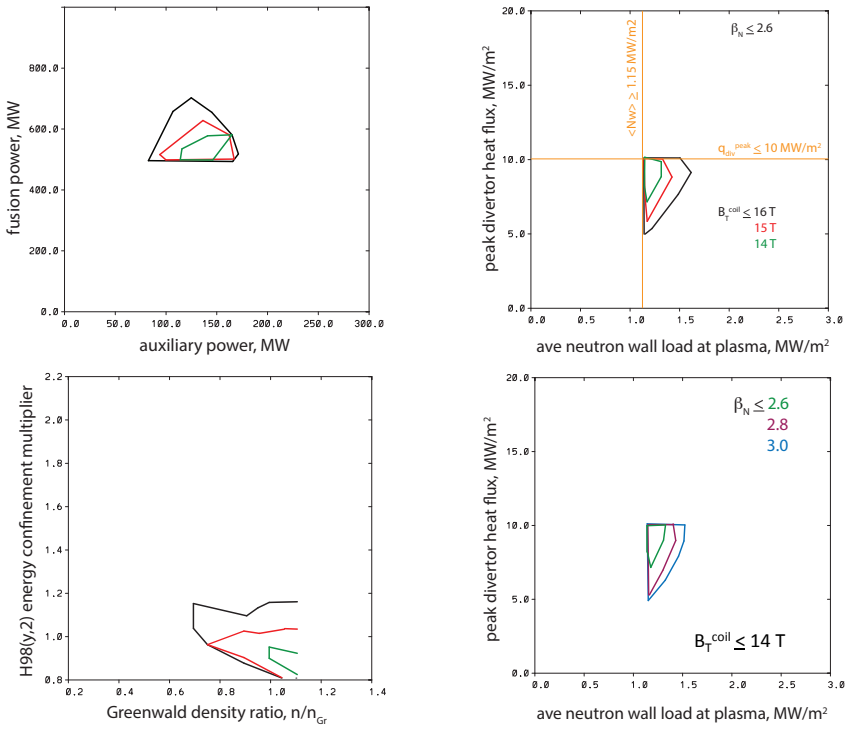

Figure 2. The variation of the FNSF operating space with decreasing maximum field at the TF coil, from 16 T (reference) to 14 T, showing a shrinking operating space of viable solutions (upper left, upper right, and lower left), and utilizing a higher beta to recover the operating space (lower right) for the 14 T case.

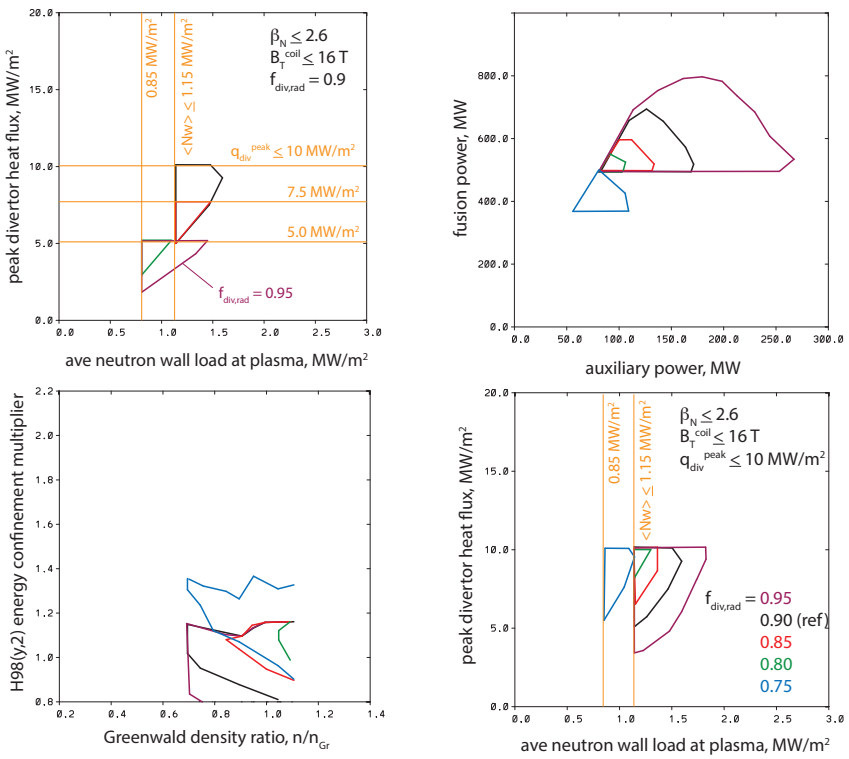

Figure 3. The FSNF operating space under a reduction in the allowed peak heat flux in the divertor (upper left), including a reduction in neutron wall loading to recover operating space. The variation in assumed radiated power fraction in the divertor (upper right, lower left and lower right) showing loss of operating space when $f_{div,rad}$ drops below 80%, and recovery with a reduced neutron wall loading.

Although an operating point is needed to pursue more detailed analysis of the FNSF plasma and engineering, based on the uncertainty of achieving these plasma and engineering parameters, the operating space, around the operating point, is needed to establish the robustness of the device's operation. Once the plasma geometry is chosen further scans with the systems code can be done to examine robustness to uncertain parameters with the geometry fixed (e.g. R, a, κ, δ). The systems code then scans over a more limited range in some parameters, while expanding others, while imposing the same filters of peak neutron wall load > 1.5 MW/m^2, maximum peak heat flux in the divertor of 10 MW/m^2, and maximum total β_N of 2.6. Here the toroidal field is scanned from 6.5 to 7.5 T, β_N from 1.8 to 3.4, q_{95} from 5.0-8.0, n/n_{Gr} = 0.7-1.1, $n_o/\langle n\rangle$ from 1.25 to 1.5, $T_o/\langle T\rangle$ from 1.9 to 2.9, and fusion gain from 2.0-10.0. Other parameters are the same as in previous scans. Examples of uncertainties include the impact of not reaching the desired B_T, the impact of a lower allowable q_{div}^{peak}, the impact of a lower radiated power fraction in the divertor, or the impact of accessing higher β_N values.
It is found that if the maximum toroidal field at the TF coil is less than the target 16 T (15 and 14 T) operating space shrinks but remains finite within all targets, although 14 T

would require operating at the Greenwald density. It is found that raising β_N from 2.6 to 2.8 and 3.0 can recover the original operating space at the lower field of 14 T. These variations are shown in Fig. 2. In addition, if the maximum tolerable peak heat flux in the divertor was lowered to 7.5 MW/m^2 from 10.0, the operating space shrinks but remains finite, while dropping it to 5.0 loses all operating space. If the peak neutron wall loading is allowed to be lower, such as 1.1 MW/m^2, then operating space is recovered, and can be expanded further by increasing the radiated power fraction from 0.9 to 0.95. The radiated power fraction was also examined over the range from 0.95 down to 0.75 (the reference is 0.9), and it is found that the operating space is lost at or below 0.8, but can be recovered by operating with a reduced neutron wall load (reduced fusion power). This is shown in Fig. 3. This type of exploration of the operating point and space is important for assessing the criticality of given parameters to the facility's accomplishing its mission, and provide some guidance on critical R&D areas in physics.

6-b. Design Options, Systems, and Transient Heating Prescriptions for FNSF *(M. Tillack, UCSD)*

1. Evaluation of design options

Starting in 2014, design options for FNSF were evaluated. Most notably, at UC San Diego we published a journal article on the use of water in the fusion power core and a technical report on the use of helium as a power core coolant. In 2015 we continued this activity by reviewing divertor design options and DCLL blanket design options.

The most attractive and credible divertor option for high-temperature operation in a high-fluence neutron environment is the He-cooled W-alloy concept. That concept has remaining uncertainties, but the database is growing with worldwide R&D efforts, especially at KIT. If we restrict water from the power core, then the only alternative under scrutiny is liquid metal cooling. That option has much greater uncertainty, especially the free surface option with its strong interactivity with the plasma. We contributed to the 2015 DOE PMI workshop, with results published in two white papers and in the final report, "Fusion Energy Sciences Workshop on Plasma Material Interactions: Report on Science Challenges and Research Opportunities in Plasma Materials Interactions," May 4-7, 2015. We also presented a review of divertor design options at an FNSF project meeting.

The DCLL blanket was chosen as the top candidate base blanket for FNSF due to its attractive features, compatibility with FNSF design parameters, and long history of R&D in the US and worldwide. The DCLL blanket can operate in different temperature regimes, which is one of its attractive features. We provided input to the evaluation of operating parameters, and also helped to coordinate analysis tasks performed at other institutions, most notably UCLA.

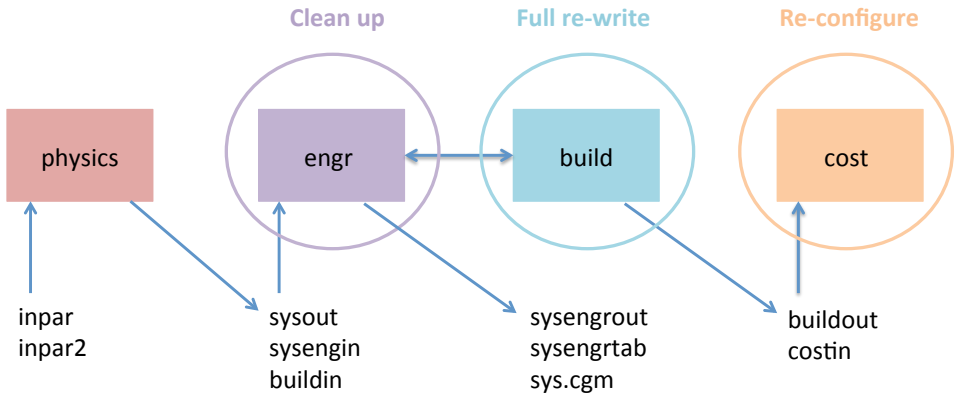

Figure 1. Schematic of the system code flow from physics analysis, to engineering analysis to build and costing.

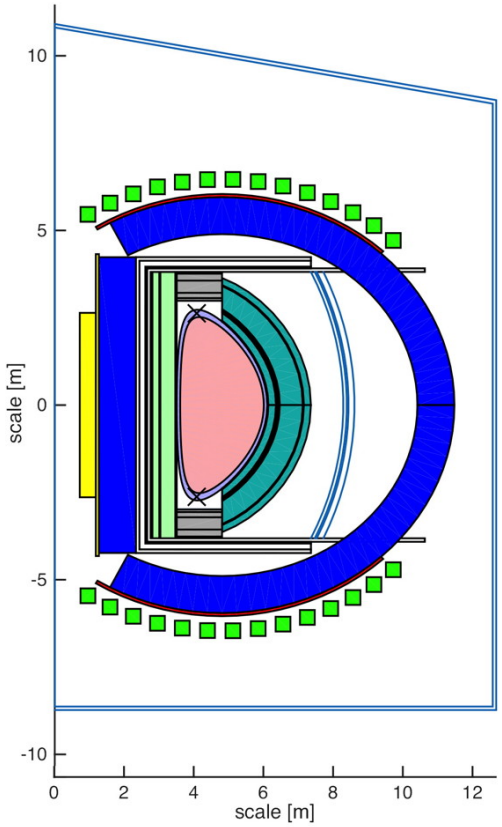

Figure 2. Cross section of latest FNSF reference design as defined by the new build algorithm

2. System code efforts

In 2015, the system code, shown in Figure 1, which is used to impose self-consistency and explore design variations, was extensively rewritten. The engineering, tokamak build and costing routines were recreated "from scratch". In 2015, we continued debugging activities, performed benchmarking against results obtained using the previous code, and implemented several improvements. Most notable among these improvements were: (1) changes to costing for concepts that do not generate and sell electricity, and (2) fixes to the build, espcially in the placement of the outboard TF coils. (Figure 2 shows a current cross section of the tokamak as produced by the build section of the code).

Many of the costing algorithms used in the old ARIES systems code were based on net electric power. For FNSF, electricity to operate the plant may be purchased rather than generated. Even using net electric power as a "placeholder" would be inappropriate, because these devices tend to use large amounts of recirculating power for sustainment. For example, Figure 3 shows a scan of design points comparing the gross electric power vs. net electric power (assuming electricity is generated using high grade heat from the power core). Net electric can be much less than gross electric, or even negative in some cases. Costing algorithms were changed to use thermal power, electricity consumption, or other parameters that more accurately represent system size and cost in this regime.

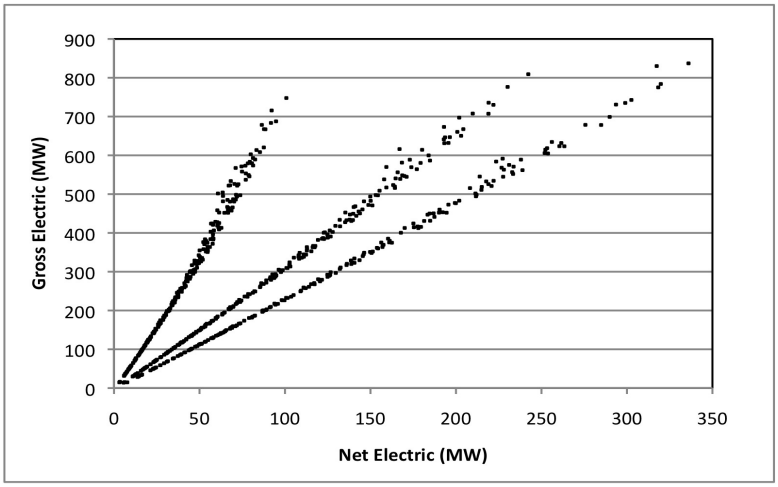

Figure 3. Comparison of gross electric and net electric power for a range of FNSF design points

Several scans of parameter space were generated as part of the debugging and testing of the code. These were also used in the selection of a reference design point for more detailed analysis. For example, Figure 4 shows a scan of the facility total capital cost as a function of the fusion power for three different major radii (4, 5 and 6 m). The chosen reference design point has a major radius of 4.8 m and fusion power of 517 MW.

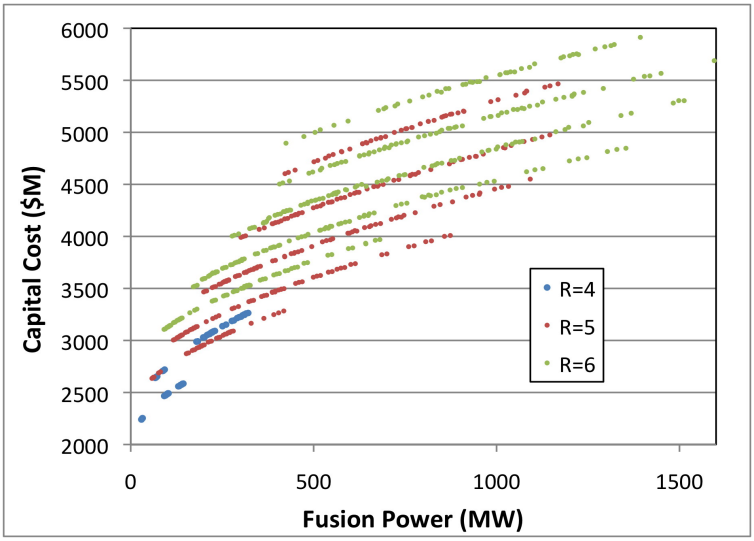

Figure 4. Capital cost of the facility vs. fusion power

3. Transient specifications

In order to perform analysis of the transient behavior of in-vessel components, transient loading conditions must be defined. In ARIES-ACT, a methodology was established to approximate the thermal and electromagnetic loading on in-vessel components using scaling laws calibrated against real experimental data [1]. Using that methodology, we

estimated FNSF loading conditions from ELMs and disruptions using baseline FNSF design parameters (see Table 1).

The general methodology is to determine the total energy released, E, (sometimes as a fraction of the total available energy), the time over which the energy is released, t, and the deposition area, A. A temporal profile of heat flux, q, can be obtained from q=E/(At). In most cases, a triangular waveform is assumed, such as that shown in Figure 5, with the possibility of different rise and fall times. Results for ELM's and disruptions are presented in Tables 2 and 3.

Table 1. Baseline parameters for transient analysis

Parameter	**Value**	**Explanation**
P_f, MW	517	fusion power
R, m	4.8	major radius
P_{SOL}, MW	173	particle transport power through the scrape off layer
$f_{rad,divertor}$	0.9	Fraction of SOL power radiated in the divertor
λ_q, mm	5.05	λ_q (m) = $7.25 \times 10^{-2} q_{95}^{0.75} n_L^{0.15} / (P_{SOL}^{0.4} B_T)$
$q_{div,OB}^{peak}$, MW/m^2	10.8	peak outboard divertor heat flux averaged over the conduction footprint
$q_{div,IB}^{peak}$, MW/m^2	3.9	peak inboard divertor heat flux averaged over the conduction footprint
$A_{FW,OB}$, m^2	183	total outboard first wall area
$A_{FW,IB}$, m^2	97	total outboard first wall area
$A_{div,cond}$, OB, m^2	1.33	steady state (inter-ELM) conduction footprint on the outboard divertor
$A_{div,cond}$, IB, m^2	1.14	steady state (inter-ELM) conduction footprint on the inboard divertor
$A_{div,rad}$, OB, m^2	31.7	steady state (inter-ELM) radiation footprint on the outboard divertor
$A_{div,rad}$, IB, m^2	13.6	steady state (inter-ELM) radiation footprint on the inboard divertor

Table 2. ELM loading conditions

Parameter	**Value**	**Explanation**
V_{plasma}, m^3	263	
W_{ped}, MJ	39	
T_{ped}, keV	3.0	
n_{ped}, 10^{20}/m^3	1.25	
DW_{ELM}/DW_{ped}	0.2	
DW_{ELM}^{large}, MJ	7.8	total ELM energy
$DW_{ELM}^{large,divertor}$, MJ	3.9	half goes to the divertor, half to FW
area expansion factor in divertor	4	observed experimentally
$A_{ELM,div}^{OB}$, m^2	5.32	footprint area in **each** divertor top/bottom
$A_{ELM,FW}^{OB}$, m^2	45.75	1/4 of the OB FW area (IB FW not exposed)
$A_{disrupt,FW}^{OB}$, m^2	91.5	1/2 of the OB FW area for disruptions

$t_{\|\|}$, ms	0.38	$\tau_{\|\|} = 2\pi R\, q_{95}/c_{s,ped}$
$Dt_{ELM,rise}$, ms	0.76	$2 * t_{\|\|}$
$Dt_{ELM,fall}$, ms	1.52	$4 * t_{\|\|}$
f_{ELM}, Hz	6.65	$f_{ELM}*W_{ELM}$ = 20-40% of P_{SOL}
f_{ELM} x DW_{ELM}^{large}, MW	52	transport power into ELM's
$q_{div,OB}^{peak}$ (ELM), MW/m^2	418	peak heat flux in divertor from ELM (actual)
inter-ELM transport power, MW	121	
inter-ELM fraction	0.70	
$q_{div,OB}^{peak}$ (inter-ELM), MW/m^2	7.56	
$q_{div,IB}^{peak}$ (inter-ELM), MW/m^2	2.73	
$q_{FW,OB}^{peak}$ (ELM), MW/m^2	74.8	actual peak

Table 3. Disruption loading conditions

Parameter	**Value**	**Explanation**
W_{th}, MJ	169	plasma stored energy
mitigation factor	0.1	10% W_{th} to divertor in mid-plane disruption
$W_{th,div}$, MJ	16.9	
$W_{th,FW}$, MJ	152.1	90% W_{th} to first wall
$W_{th,FW,OB}$, MJ	121.7	80/20 split OB/IB
$W_{th,FW,IB}$, MJ	30.4	
$A_{dis,div}^{OB}$, m^2	13.3	per divertor, 10x expansion *vs.* SS
$A_{dis,div}^{IB}$, m^2	11.4	"
$A_{dis,FW}^{OB}$, m^2	91.5	half of the OB FW
$A_{dis,FW}^{IB}$, m^2	48.5	half of the IB FW
Dt_{TQ}, ms	1.9	(average of 1.2-2.5 ms)
thermal quench rise time, ms	1.9	
thermal quench fall time, ms	5.7	2-4 times the rise time (we use 3)
$q_{th,div}$, MW/m^2	217	peak, 10% to 2 OB divertors, 65% imbalance
$q_{th,FW,OB}$, MW/m^2	350	peak, 90% to FW, 80%OB
$q_{th,FW,IB}$, MW/m^2	165	peak, 90% to FW, 20%IB
W_{mag}, MJ	124.6	$W_{mag,int} + 0.2W_{mag,ext}$
$W_{mag,int}$, MJ	70	plasma internal energy
$W_{mag,ext}$, MJ	273	external inductance with structures
Dt_{CQ}, ms	18	(correlation from ITER database)
$f_{rad,FW}$	0.8	fraction of W_{mag} radiated to FW
$f_{rad,FW,OB}$	0.8	fraction of FW radiation to OB
$f_{rad,FW,IB}$	0.2	fraction of FW radiation to IB
$q_{mag,FW,OB}$ MW/m^2	48.4	
$q_{mag,FW,IB}$ MW/m^2	22.8	

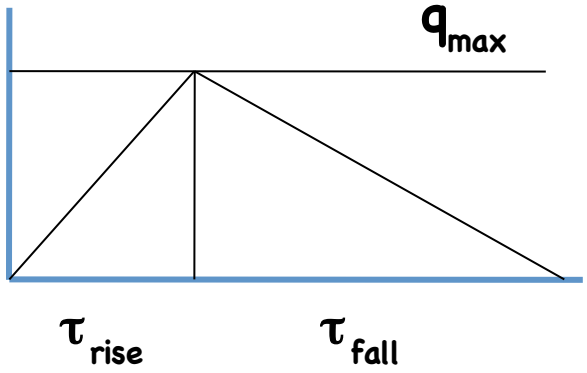

Figure 5. Generic description of heat flux vs. time due to transients.

1. C. E. Kessel, M. S. Tillack and J. P. Blanchard, "The Evaluation of the Heat Loading from Steady, Transient, and Off-Normal Conditions in ARIES Power Plants," *Fusion Science and Technology* **64** (3) 440-448 (2013).

6-c. Nuclear Analysis and Blanket/Materials Testing Strategies *(L. El-Guebaly, M. Harb, B. Madani, M. Elias, A. Davis, Univ of Wisconsin, A. Rowcliffe, S. Malang. L. Wagner)*

Radial/Vertical Build Definition

UW issued the radial/vertical builds that include the size and optimal composition of all components. These builds are a precursor to the physics code, systems code, and CAD drawings. In 2015, the builds involve preliminary 1-D estimates of radiation damage to structural components and magnets in absence of penetrations. Such estimates will be confirmed in 2016 with detailed 3-D analyses that consider the effect of neutron streaming through several large penetrations needed for plasma heating and current drive (H/CD). The radial/vertical builds are shown in Fig. 1.

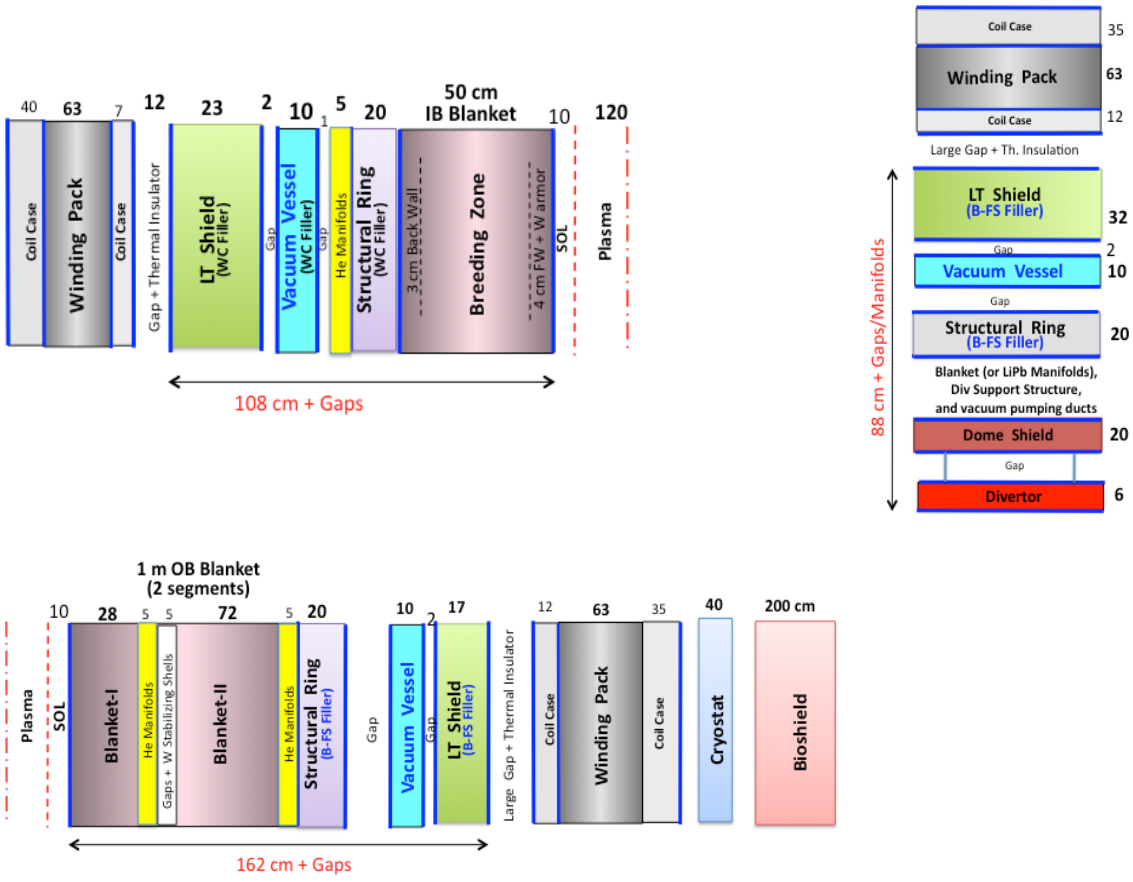

Fig. 1. FNSF radial and vertical builds, upper left is the inboard, lower left is the outboard, and upper right is the vertical build above the divertor.

It is assumed that 50 cm inboard (IB) blanket and 1 m outboard (OB) blanket with 90% Li-6 enrichment could provide an overall TBR around unity. Lower breeding level than predicted requires purchasing T from outside sources that may represent an economic burden for FNSF. The He-cooled RAFM structural ring (SR) supports the blanket and divertor. As in ARIES-ACT, the thin VV (10 cm) is made of 3Cr-3WV bainitic steel,

cooled with helium, and runs hot at ~300°C. The primary shielding component (LT shield) is located outside the thin VV. This shield operates at room temperature to help dissipate the decay heat during loss of coolant/flow accidents. The highly efficient WC filler is included only in the three IB components (SR, VV, and LT shield) to help reduce the IB standoff. On the negative side, WC generates higher decay heat than RAFM alloys and mandates design solutions to avoid melting the IB side during severe LOCA accidents. The design requirements of Table 1 determined the dimensions of FNSF components. A common goal for all specialized components (blanket, SR, and VV) is to provide a shielding function to collectively satisfy the radiation protection requirements for the LTS magnets. This helps define the most compact operational space of the machine with minimum radial standoff in order to free some ex-vessel space for structural connections, cooling pipes, coil leads, etc. Using the PARTISN radiation transport code and FENDL data library, 1-D tradeoff analyses of water and fillers defined the optimal composition of the IB and OB LT shields [1,2] as shown in Fig. 2.

Table 1. FNSF TBR goal and radiation limits

Overall TBR (to be calculated using 3-D analysis) (Goal for T self-sufficiency)	~ 1
Damage to steel alloys	20 < 50 > 65
Damage to W alloys	?
Helium Production (for reweldability of RAFM alloys)	1 ?
LTS Magnet (@ 4 K):	
Peak fast n fluence to Ternary Nb_3Sn (E_n > 0.1 MeV)	3×10^{18}
Peak nuclear heating @ winding pack	1
Peak nuclear heating @ coil case	2
Peak dose to electrical insulator	5×10^{10}
Total nuclear heating in 16 TF coils	15
Peak dpa to Cu stabilizer	10^{-4} ?

The radial/vertical builds defined so far has been assumed to be free of penetrations. As anticipated, several penetrations for plasma H/CD exist around the OB midplane, protruding through all OB components. Such penetrations along with the TBM and MTM ports, and surrounding assembly gaps allow neutrons to stream through, putting the shield efficiency in jeopardy. For these reasons, the peak damage to the SR and VV occurs around these penetrations/ports, not behind the bulk shield. Selected streaming issues will be addressed with 3-D analysis in 2016.

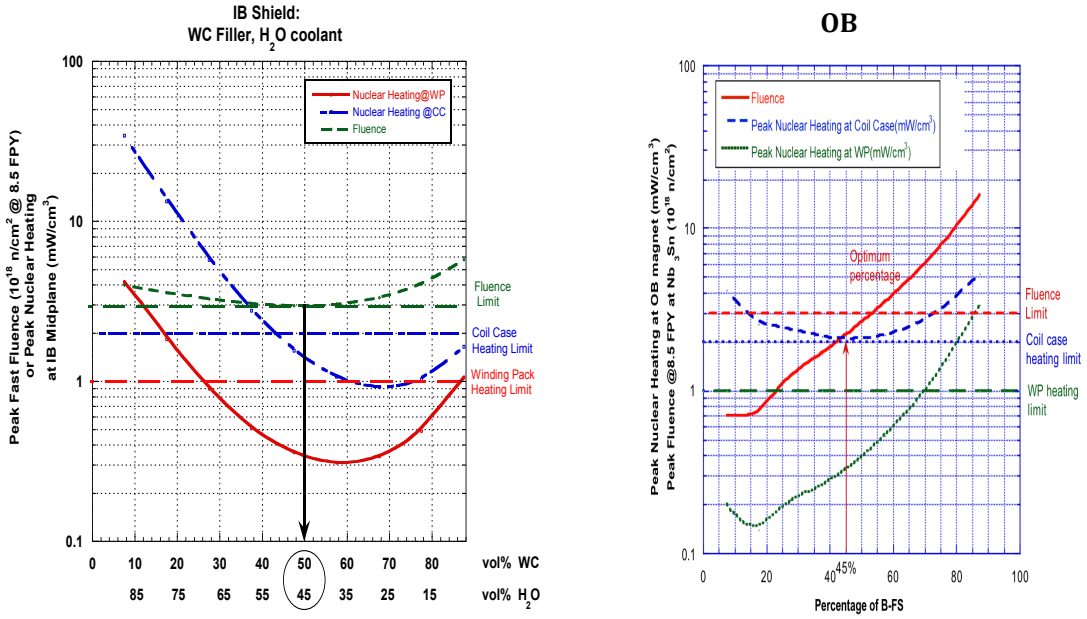

Fig. 2. IB and OB shielding optimization, trading filler for water coolant .

Nuclear Heating

Table 2 provides the breakdown of nuclear heating in FNSF components needed to obtain details on the thermal hydraulic analysis and eventually the thermo-mechanical stresses the device is subjected to during operation. Dividing the total heating by the neutron power (526 MW x 0.8), an overall energy multiplication of 1.2 is obtained. About 50:50 split between He and PbLi thermal power loads is expected.

Table 2. Total nuclear heating to FNSF components

Nuclear Heating (MW)	**Inboard**	**Outboard**
FW/Blanket	101	317
Divertor plates, support structure, and dome shield	---	---
Stabilizing shells	3	24
Structural ring	9	4
Total	**113**	**345**
	(22%)	(68%)

An essential input to the IB thermostructural analysis is the radial distribution of nuclear heating deposited in individual elements of the DCLL blanket: LiPb, RAFM steel, and SiC FCI. This distribution is shown in Fig. 3. The 2 mm thick W armor on the first wall (not shown) generates relatively high nuclear heating (~30 W/cm^3).

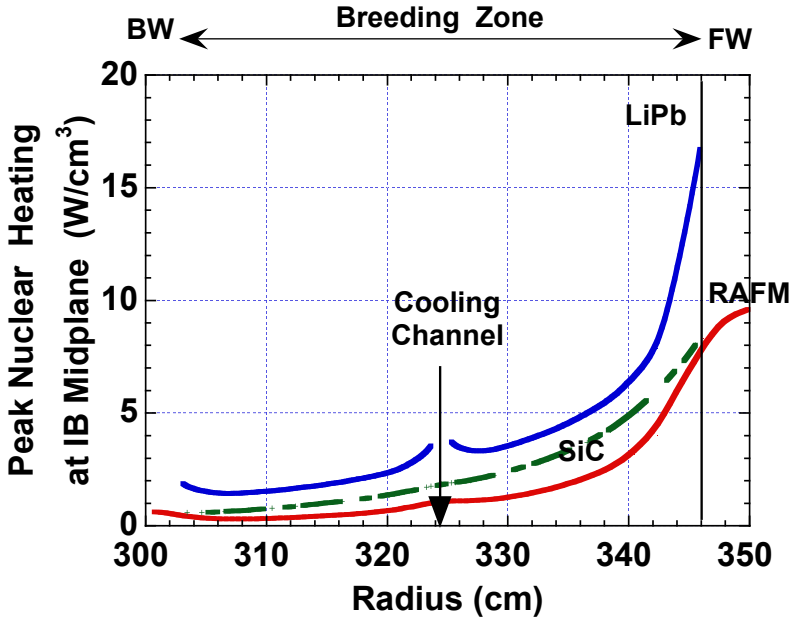

Fig. 3. Radial distribution of the nuclear heating in individual elements of the DCLL blanket at the inboard midplane.

Activation Analysis

UW examined the radioactive inventory, decay heat, and radwaste classification and management options for the IB and OB regions [1,2]. The high decay heat of the WC filler in IB components raises safety concerns and requires a specific analysis to check the temperature response during LOCA accidents. All FNSF components are recyclable shortly after shutdown. Most components qualify as Class A low-level waste – the least hazardous type of waste based on the NRC classification.

In recent years, ORNL researchers have been investigating advanced alloy systems that offer potential solutions for the corrosion problem facing the DCLL blanket by adding 5 wt% Al (and other Zr and Hf additives) to the 12Cr ODS alloys. We assessed the activation implications of these alloys of and compared their activation characteristics to that of F82H – the first generation of RAFM steel that limits the blanket operating temperature to less than 550°C. Our results confirmed that all candidate corrosion-resistant ODS alloys qualify as low-level waste at the end of FNSF operation [3].

Blanket and Materials Testing Strategies

An essential mission for FNSF is to test, understand, and enhance the blanket and materials performances with the end goal of qualifying the most advanced, highest performing DCLL blanket for DEMO. Such strategies are tailored to meet the FNSF timeline and reach beyond the traditional testing mission of ITER. Up to four generations of the DCLL blanket concept could be tested first in the volume-limited test blanket modules (TBM), and then converted (assuming positive results) into full sectors for qualification before use in DEMO [4]. The main goal of the TBMs is to test more

advanced variants of the DCLL blanket that could operate with progressively higher temperatures and new generations of structural materials. Other He-cooled blanket concepts could be tested in the TBMs as well: the backup concept of He-cooled PbLi blanket, a variety of ceramic breeder blankets, and other more attractive blanket concepts than presently known. Geometrically, the TBMs will be located on the outboard midplane, embedded in the GEN-I DCLL blanket that could breed the T fuel needed for plasma operation. This base blanket must be robust, highly reliable, operate at a lower temperature, and cover the entire space surrounding the TBMs and other ports.

Since material testing is equally important as blanket testing, we developed a comprehensive multi-materials database for new materials for blankets, divertors, magnets, insulators, etc. The most important attribute would be the much larger specimen volumes compared to the 10-500 ml range available in other proposed neutron sources, such as IFMIF, DONES, and HINEG. To take advantage of the unique fusion neutron environment produced in the FNSF, a materials testing module (MTM) will be embedded in the outboard base blanket of the FNSF to contribute to the comprehensive multi-materials database with the potential to reach cumulative neutron exposures up to 126 dpa during all phases of operation. A wide variety of materials and test specimens could be accommodated simultaneously, as illustrated in Fig. 4. For example:

- New generations of structural steels, if not tested before the FNSF, including:
  - GEN-II RAFMs designed for operation up to 650ºC,
  - RAFM variants with reduced susceptibility to radiation-induced DBTT shifts for operating temperatures < 385ºC,
  - Nanostructured ODS steels (12-14% Cr) with enhanced radiation damage tolerance and high temperature capability
- Multi-material PbLi corrosion capsules
- SiC/SiC composites for advanced blanket designs
- W alloys for divertor and stabilizing shells (W-TiC, WL10, W-K, W/W composites, VMW, etc.)
- Low-temperature and high-temperature magnet materials: superconductors, jackets, insulators, etc.
- New materials variants arising from:
  - Continuing development of improved compositions/microstructures
  - Application of advances in fabrication technologies (additive manufacturing, precision casting, joining technologies, etc.).

The results from both blanket and materials testings are essential to build high confidence and lower risk for successful operation of advanced blankets with advanced materials in DEMO and power plants.

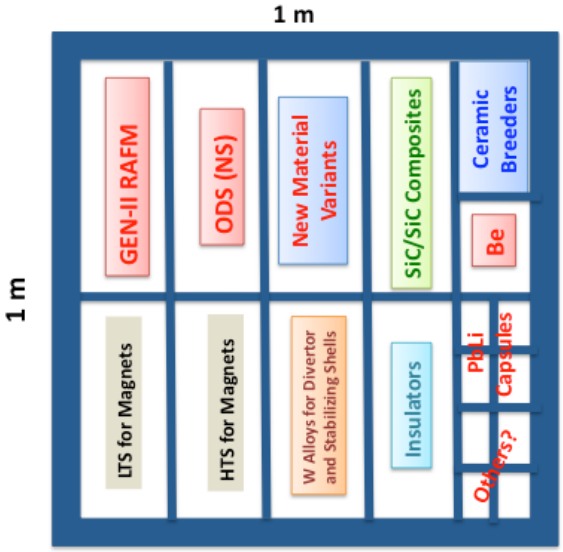

Fig. 4. Layout of material samples within 1x1 m MTM.

References:

1. B. Madani and L. El-Guebaly, "Shielding and Activation Analyses for Inboard Region of FESS-FNSF Design," University of Wisconsin Fusion Technology Institute Report, UWFDM-1423 (November 2015). Available at: http://fti.neep.wisc.edu/pdf/fdm1423.pdf.
2. M.T. Elias and L. El-Guebaly, "Shielding and Activation Analyses for Outboard Region of FESS-FNSF Design," University of Wisconsin Fusion Technology Institute Report, UWFDM-1424 (November 2015). Available at: http://fti.neep.wisc.edu/pdf/fdm1424.pdf.
3. L. El-Guebaly, S. Malang, A. Rowcliffe, and L. Waganer, "FNSF Nuclear Analysis and Blanket and Materials Testing Strategy," presented at US/JA Workshop, Oct. 28-30, 2015, Denver, CO. Available at: https://sites.google.com/a/pppl.gov/fusion-energy-system-studies-fess/u-s-ja-workshop-october-2015.
4. L. El-Guebaly, S. Malang, A. Rowcliffe, and L. Waganer, "Blanket/Materials Testing Strategy for FNSF and its Breeding Potential," Fusion Science and Technology, Vol. 68, No. 2 (2015) 251-258.

6-d. CAD Layout of the FNSF *(E. Marriott, Univ of Wisconsin)*

UW has begun work on creating a 3D Computer-Aided Design (CAD) model of the FNSF geometry. This work is being performed with SpaceClaim [1], which is a direct-modeling CAD software. Design parameters are obtained from the radial and vertical builds. Further parameters are obtained from physics and systems code outputs. The magnet designers provided the magnet configuration and dimensions.

CAD data are extremely useful as it could be exported for subsequent analyses to correctly model the complex geometry of tokamaks. For example, CAD data will be incorporated into the 3-D neutronics code DAGMC to estimate the overall TBR and other nuclear parameters. ANSYS and SpaceClaim now share a common data interface. UW has been using ANSYS in thermomechanical and electromagnetic analyses and also to estimate the temperature response during severe accidents.

The initial CAD work focused on the general layout of all the components as defined by the radial and vertical builds. The initial version of the model was scaled down from the ARIES ACT 2 model. Upon scaling the ACT 2 the inboard and outboard builds were created. The outboard build is the more complicated geometrically as it follows the curvature of the plasma. Figure 1 shows a size comparison between ARIES ACT 2 and FNSF.

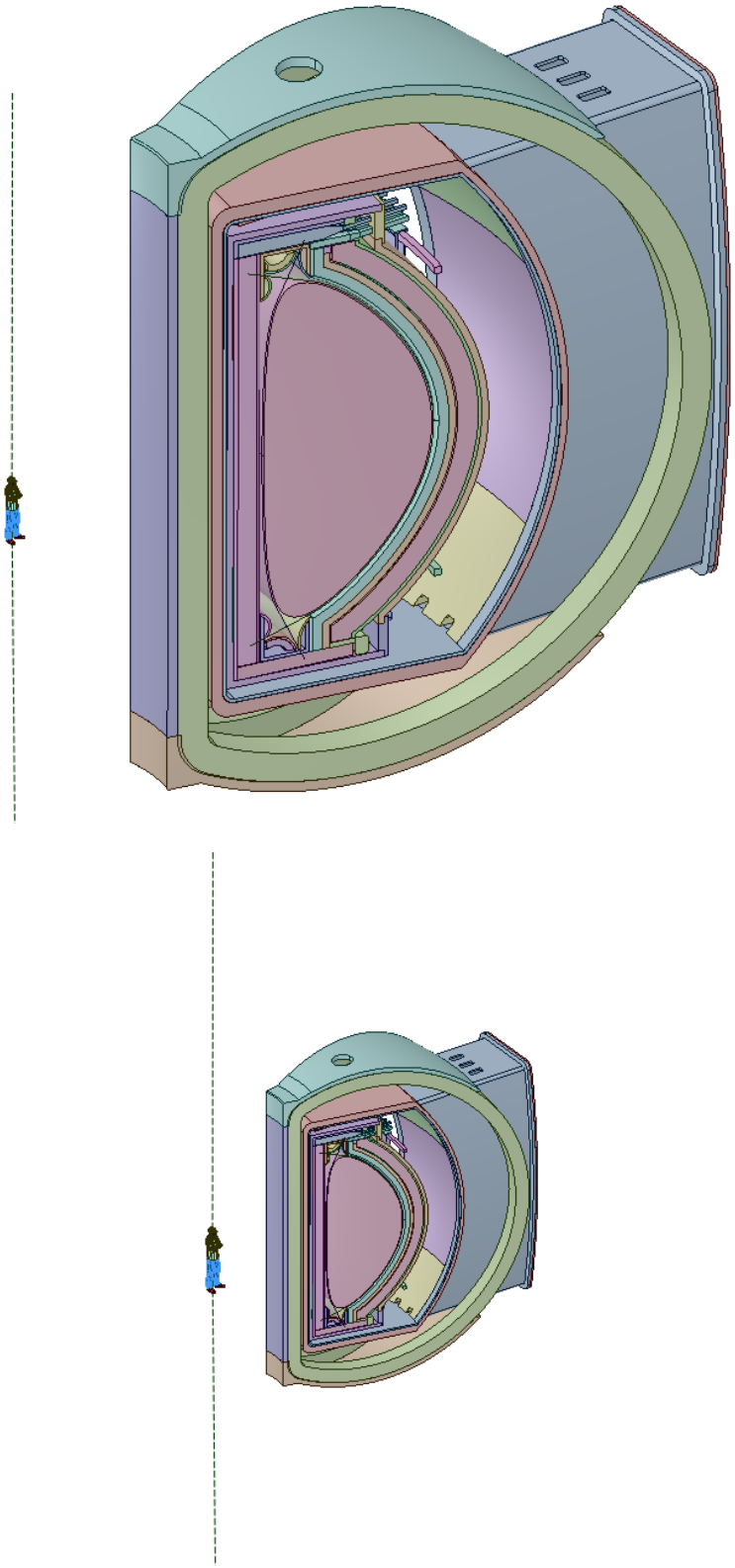

Figure 1. CAD Size Comparison of ARIES ACT 2 (left) and ACT 2 scaled to FNSF size (right).

Once the ACT 2 geometry was scaled then the inboard and outboard radial builds were modified. Figure 2 illustrates the initial FNSF CAD model as built from the scaled ACT 2 geometry.

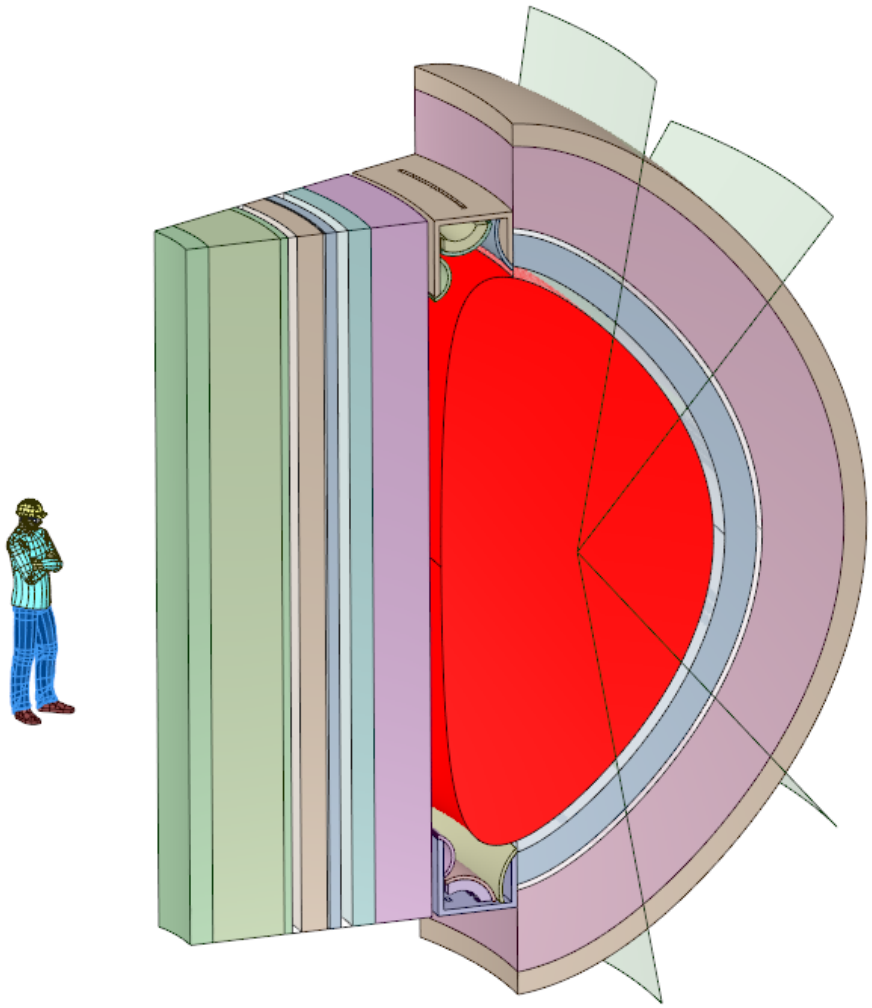

Figure 2. The initial CAD drawing of the FESS-FNSF design.

With the initial design in place work began on the TF coils. Data were received from Mark Tillack and imported into SpaceClaim to create the TF coils. At that point an investigation was made regarding the required radius for the placement of the TF coil outboard legs. This requirement is based on the horizontal maintenance scheme and the clearances for a gap, the vacuum vessel, and the thermal insulation around the TF coil. Figure 3 illustrates the TF coil placement based on the radial build and required clearance.

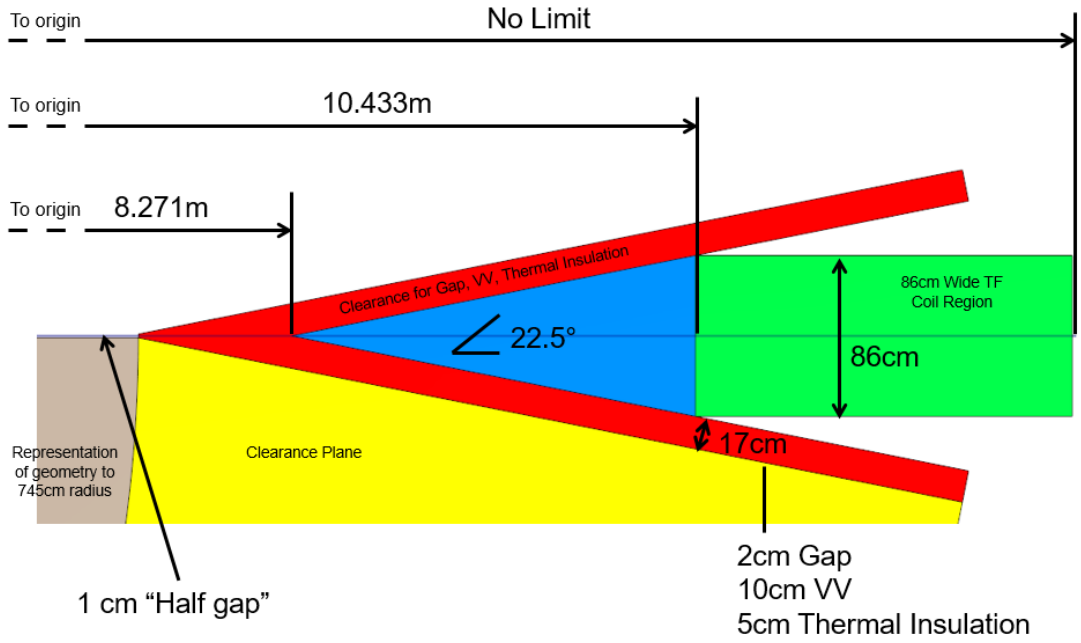

Figure 3. TF Coil Placement investigation

The result of the TF coil placement investigation was that the current TF coils would be required to be moved outward from an inner radius of 9.9m to a minimum radius of 10.433m.

Work on the upper region, including the divertor has also begun. The scaled ACT-2 divertor plates were not thick enough, so these were adjusted. Subsequent changes to the divertor followed to accommodate the thicker plates. The scaled ACT 2 geometry and modified geometry can be seen in Figure 4.

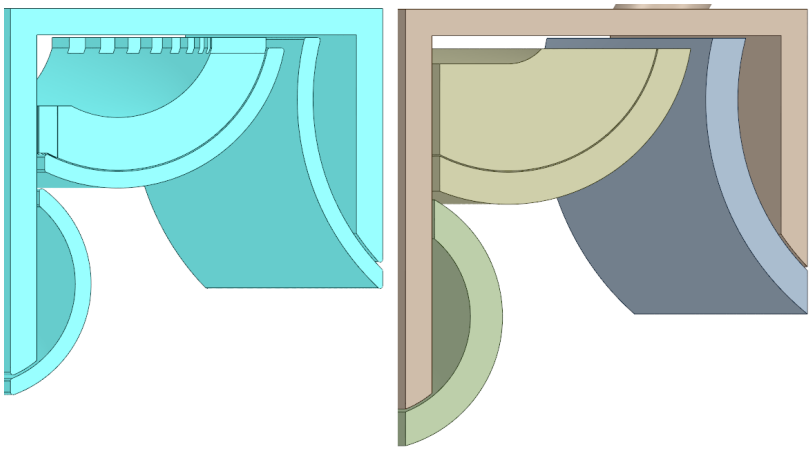

Figure 4. The scaled ACT 2 divertor in blue and the revised FNSF divertor with thicker plates.

While progress has been made on the FNSF CAD model there is still much work to be completed. The TF coils will need to be redone. The internal blanket details will be completed. The outboard blankets will be revised based on a new plasma volume. Pumping ducts and flow manifolds will be incorporated. The sector removal port will be

completed. Once all these are done then a full FNSF CAD model will be completed. Figure 5 shows the current state of the FNSF CAD model.

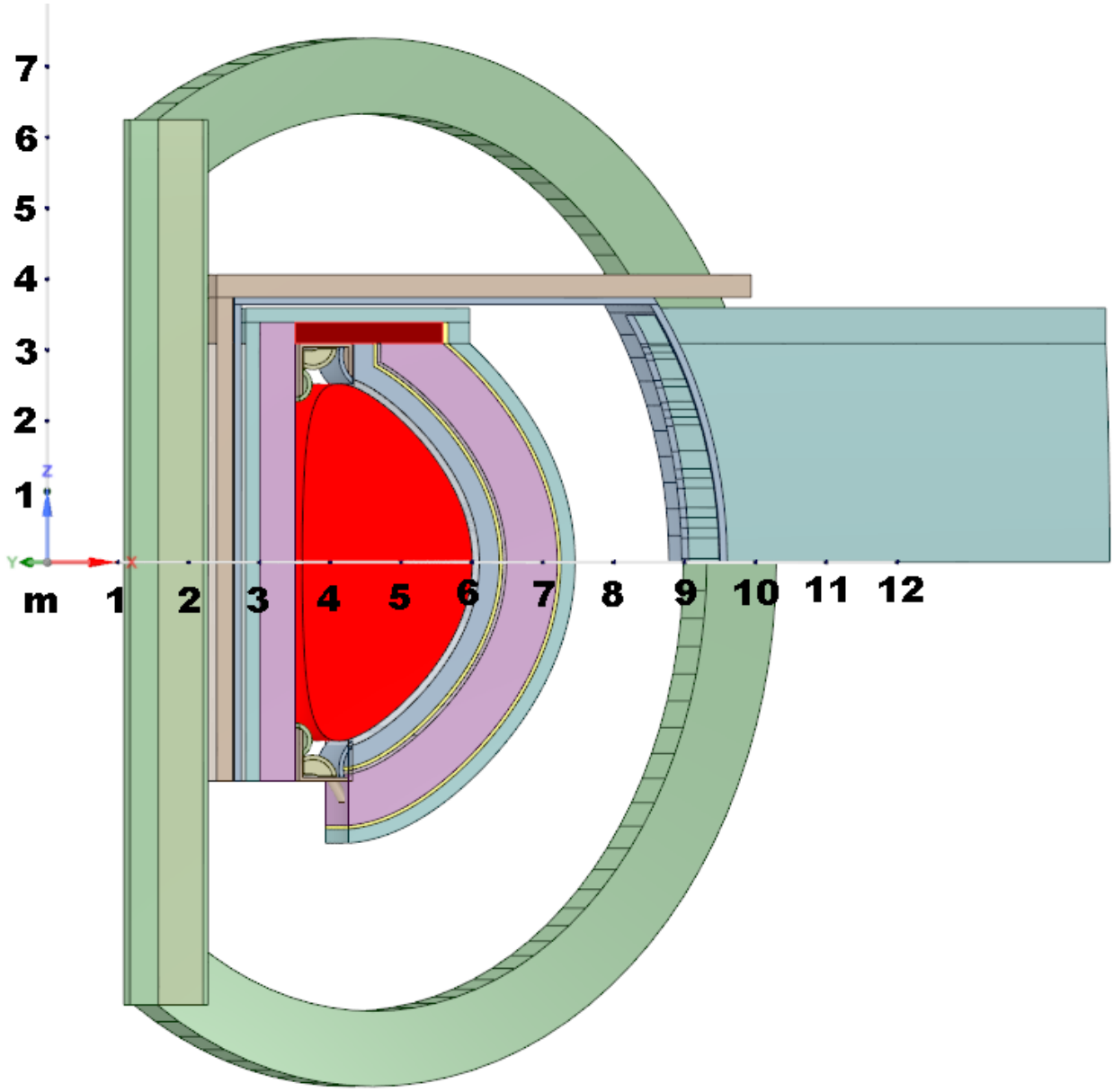

Figure 5. The current FNSF CAD model.

Reference:

SpaceClaim: http://www.spaceclaim.com/en/default.aspx.

6-e. Maintenance, Remote Handling *(L. Waganer, consultant)*

1. Affirming Autonomous Remote Handling for FNSF Power Core

Ref: Waganer Presentation at Feb 16-17, 2015 FNSF Systems Study Meeting, ORNL
The FNSF is envisioned to be a very large, high-energy, high flux neutron power core that will be well-shielded for long-term operation. The generated high energy neutrons will convert the internal power core materials into radioactive isotopes that are harmful to humans. Therefore, the environment within the power core and extending out to the bioshield cannot be accessed by humans either during operation or between operations for years. Thus the maintenance of all subsystems inside the bio-shield cannot be accomplished hands-on and must be achieved with complete remote handling. To be assured the power core and all its subsystems inside the bio-shield can be maintained, disassembled, reassembled and tested, it is assumed that the FNSF (and other similar machines) must be assembled remotely to completely validate the maintenance and disassembly processes.

The remote handling can be done with varying levels of human involvement, ranging from remote manipulators controlled with skilled human operators, remote manipulators controlled with a combination of computers and skilled human operators and semi-autonomous robots with human oversight. All of these approaches may function as envisioned, but they may be limited in use. Maintenance of the fusion power core requires high precision to assure extremely reliable operations, very repeatable execution and expedient maintenance actions to achieve high plant availability. These demanding requirements suggest it would be advisable and highly recommended to include more automated equipment and processes, starting with the construction of the FNSF (approximately 15-20 years from now).

The evolution of autonomous robotic equipment and controls has significantly advanced over the past several decades to the point it is well demonstrated and in use in many industries. It has the advantages of lower labor cost and predictable and precise geometric control with repeatable movements. The most important attribute is that it can be used without any humans being exposed to dangerous environments inside the bio-shield or hot cell. During the initial FNSF phases, there would likely be robotic assembly and operation with human oversight, but in the latter operational phases, the maintenance actions would transition to be completely autonomous operations, thus preparing the way for DEMO.

These maintenance actions would include removal of the sectors from the power core and transport of the sectors from the power core through the access corridors to and from the Hot Cell (faster, more reliable, less likelihood of damage). Inside the Hot Cell, there would be other specialized automated robots to disassemble, inspect and reassemble the refurbished sectors, segments or modules.

Conclusions

- The need to safeguard the health of the plant workers mandates the use of robotic assembly, maintenance and disassembly of all fusion power core elements inside the bio-shield.
- The use of highly automated, autonomous robotic assembly and maintenance operations will be commonplace when the FNSF (or the next large developmental fusion facility) is designed and built.
- This capability will enable faster, higher precision and more reliable assembly and maintenance of the power core that will result in a project cost savings and ensure the highest plant availability possible.
- These qualities are essential to the project success not only of FNSF, but also to all following facilities leading to the first fusion power plant.
- The development of autonomous robotic operations must be a keystone element of the FNSF design.

2. Comparison of Horizontal and Vertical Power Core Access

Ref: Waganer Presentation at Feb 16-17, 2015 FNSF Systems Study Meeting, ORNL
The levels of radiation within and around any high flux/fluence fusion power core is too onerous to permit human involvement – thus all access and handling inside the biological shield must be accomplished remotely. To assure the capability of the power core remote handling will be adequate, it is presumed the power core and all elements inside the bio-shield must be completely assembled and disassembled remotely. However, there are several proposed concepts to achieve the remote handling (RH) of the power core - either horizontally removing large sectors or vertically removing more, smaller segments (sub-sectors). Historically, all pre-conceptual tokamak power plant studies conducted in the U.S. have proposed the use of horizontal removal of large power core sectors (one per TF coil). L. Waganer did an intensive investigation and comparison of the several proposed design approaches for tokamak power core remote handling. The EU-Demo, K-DEMO, PPPL ST and one option for JA-DEMO designs have proposed vertical access to the power core through smaller upper maintenance ports with extensive internal operations required. The U.S. and JA have proposed horizontally removing full sectors through large ports between the TF coils with few or no operations are required inside the vacuum vessel (VV).
At this time, all the RH concepts are in the pre-conceptual stages with no credible design or operational experience. In the near future, ITER may have demonstrated some RH of less-capable power core, but this experience will not be relevant to the level of complexity and capability of reaching commercial levels of power plant availability and safety. So new RH approaches are required that will significantly impact the power core design as well as the RH equipment, power core building and hot cell.

Effectively comparing the attributes and benefits of the disparate RH approaches requires quantifiable data that is not available until actual power plant-level power cores are

operated and maintained. Therefore, an alternate set of proposed physical attributes will be used to compare the envisioned RH approaches. These attributes include: 1) number of replaceable units including divertors, 2) number of hydraulic connections to be severed and reconnected, 3) number of in-vessel RH equipment required, 4) complexity of maneuvers and in-vessel equipment, 5) compatibility with H/CD systems, diagnostic systems and test blanket modules, 6) easy and quick access to any sector or segment to replace a prematurely failed internal PC element, and 7) flexibility to alter downtimes. This set of attributes can be quantified and are related to how well the proposed RH concepts can function in the power core.

The conclusions of this assessment were that the horizontal access maintenance approach with one full sector and a port per TF coil offers the easiest, most expedient, most reliable and most flexible approach to achieve the required plant availability for future facilities. The other approaches do offer the desired maintenance of the power core, but their solutions entail a higher level of technical risk, longer maintenance period durations and do not offer flexibility to accommodate access for special systems and an approach for higher levels of availability. Based on this assessment, it is concluded that the horizontal maintenance option with one port per TF coil offers the most favorable power plant maintenance approach for any high power, high flux, and high fluence fusion power core.

3. Initial Assessment of the FNSF Test Blanket Design and Maintenance Approach

Ref: Waganer Presentation at Oct 27-30, 2015 FNSF Systems Study Meeting, Denver CO

An effort was undertaken to understand the key aspects for accommodating FNSF Test Blanket and Material Test Modules to facilitate easy and prompt replacement while not compromising the availability of the primary facility.

There is a consensus that the FNSF must accommodate several Test Blanket Modules and a Material Test Module to help develop and validate advanced blanket concepts and materials in an intense, high flux, high fluence and extended-operation (> 20 y) environment. ITER has TBM test ports that are being built, however they are not amenable to the FNSF design, fast removal and increased plant availability goals.

At present, there is no FNSF design basis for the TBM/MTM test ports, therefore the following analysis is solely based on a set of "tentative" design assumptions, as follows

- Several TBMs and one MTM will be located on OB mid-plane, , ≈ 0.5 - 1 m wide and ≈ 1 - 2 m high
- Each TBMs will have all first wall, blanket and shielding functions of the base subsystems, plus structure to attach to the base Structural Ring (SR) for support and alignment, while the MTM is a module holding material samples and does not function like the blanket.
- The essence of how the TBM/MTMs will be removed, maintained and replaced depends on the attachment design and how the connections will be routed through the maintenance ports.

Based on these design assumptions and not adversely affecting the plant design and availability, two potential design approaches were considered:

1. TBMs/MTMs are Functionally Separate from the Base Blankets and SR - The TBMs/MTMs have their own support structure and are inserted through dedicated doors in the basic blanket, SR, stabilizing shells, shield and VV structure. The TBMs/MTMs will be attached to the back of the SR. All cooling and diagnostic lines are separate from the basic blanket/shield and extend outward through the common barriers of the inner and outer doors of the main VV maintenance ports.

    a. Multiple TBM/MTM doors are used for the Shield and VV functions with all coolant/diagnostic lines passing through these doors. Each door is removed separately and sequentially.

    Conclusion: Functionally separating the TBM/MTM from the base blanket and its connections is a complicated process that will havelong maintenance times, difficult operations, high likelihood for contamination and big impact on sector replacement. (Sector cannot be replaced with TBM lines in place). This approach is not recommended.

    b. The TBM/structure and related shielding, vacuum doors and diagnostic/coolant lines are combined into an integrated module and inserted and removed as a unit.

    Conclusion: Simple in theory, but significant mass and multiple simultaneous interfaces probably cannot work. This approach is not recommended.

2. TBMs/MTMs are Integrated with Sectors -The TBMs/MTMs would physically attach to the back (or front) of the basic common hot structural ring and use the basic large maintenance ports.

    a. The TBM would have its own structure and attach to the back of the SR and would be removed separately from the sector through the main maintenance ports after all doors and barriers are removed.

    b. The TBMs will not include the functionality of their hot structural ring, rather the TBMs would attach to the front (plasma side) of the SR. The TBM/MTM would be integral with, and removed with, the parent sector. All coolant and purge connections and diagnostic leads will be bundled with the sector lines and all will be disconnected and connected at the same time, place and manner.

    Conclusions: Both of these approaches are feasible for a FNSF TBM/MTM design, attachment to the SR and maintenance approach with minimal impact on the power core design and plant availability. There is no clearly superior approach for these two, so for the time being, it is assumed the FNSF design can maintain the TBM using removal of the main port access elements. The remainder is To Be Determined (TBD) pending final design.

4. Objectives and Design Guidance for Hot Cell

Ref: Waganer Presentation at Oct 27-30, 2015 FNSF Systems Study Meeting, Denver CO

Assuming the FNSF fusion fuel is DT, the power plant (this definition also applies to all fusion power plants with long operational lifetimes) will activate the core elements, which reduces its useful lifetime and requires several core replacements over the plant lifetime, due to life limits or failures. Therefore an adjunct facility called a Hot Cell is needed to process the power core sectors and prepare refurbished sectors.

The Hot Cell (HC) will be defined as a radioactively-secure area to receive, inspect, dismantle and separate all sector materials. Moreover it must refurbish and test all sectors before replacement in the power core.

All past conceptual fusion power plant studies have acknowledged the need for a Hot Cell and have included a cost and a sketch of the Hot Cell building. Starfire (1980) identified a list of Hot Cell tasks and provided a more detailed building definition. In general, the role and definition of the Hot Cell has been lacking. ARIES-RS and ARIES-AT examined how the sectors would be removed and transported to the Hot Cell, but the Hot Cell was not defined.

Therefore the FNSF Hot Cell is tentatively defined as:

- The HC is a radioactively-secure area where the activated components are de-contaminated, disassembled, inspected, cut into samples for examination, refurbished and/or fully re-qualified for service
- The removed components are inspected for property degradation and/or cause of failure with sophisticated instrumentation
- The components are dismantled and tritium and other elements are removed and recycled after which the elements or remaining parts are sent to the Fuel Handling and Storage or the Radioactive Waste Processing System
- The HC facility will be completely robotic with a combination of human and computer oversight
- The HC will provide after-heat cooling for all components

6-f. FNSF Tritium systems progress and plans *(P. Humrickhouse and B. Merrill, INL)*

One of the objectives of the FNSF is to demonstrate tritium self-sufficiency, i.e. to successfully operate a full-scale breeding blanket and to achieve a tritium breeding ratio (TBR) greater than one. Given that our present concept of FNSF will operate at >500 MW fusion power, in steady state during the advanced stages of facility operation, it will be necessary to breed ~10 kg of tritium per year with 35% on-time. This represents an increase of 3-4 orders of magnitude in the amount of tritium bred relative to ITER (TBMs). Furthermore, in order to achieve high thermal efficiencies, a high-temperature DCLL blanket operating at ~700 °C is ultimately envisioned. These high temperatures facilitate tritium losses by permeation through blanket structures, pipe walls, heat exchanger tubes, etc., which may ultimately be released to the building and the environment. On the other hand, safety demands that such losses be kept very low. The DOE Fusion Safety Standard stipulates that a maximally exposed member of the public shall receive no more than 10 mrem/yr (0.1 mSv/yr) as a result of normal operation of a fusion facility. While the tritium release rate that ultimately results in such a dose depends on assumptions about atmospheric dispersion and uptake by the individual, typical assumptions lead to a number on the order of 1 g/yr (~27 Ci/d). Thus the fraction of bred tritium that may be lost is only ~3.5e-5.

There are two ways to decrease the loss rate: increasing the efficiency of the tritium extraction system, and/or applying permeation barriers to reduce tritium permeation through structural materials. The objective of this modeling effort is to outline suitable combinations of extraction system and permeation barrier (if needed) designs to achieve a loss rate below the target given above. This depends strongly on the design of FNSF and its in-vessel structures; a model of FNSF is being built with TMAP, a system-scale code that treats hydrogen isotope (H, D, and/or T) permeation through structures and transport by convection between connected volumes.

Because a TMAP model is intended to represent tritium transport through an entire facility, the nodalization of the model must necessarily be relatively coarse; i.e. design details such as the many parallel flow channels and structures in the actual FNSF design must be lumped in some way, while appropriately conserving volume, surface area, flow length, elevation change, hydraulic diameter, etc. The required geometric calculations are a considerable portion of the overall model development, and an effort is being made in this project to streamline this process while facilitating the tracking of design changes and performance of parameter and sensitivity studies. Because input files are text-based, and most of the volume and structure parameter values are based on the aforementioned combining of geometry, tracking even small changes requires re-performing almost all of these calculations. In order to alleviate this difficulty, we have moved to a spreadsheet-based input file development of a type employed for RELAP5 models at INL. All input parameters (primarily related to geometry) are calculated in a spreadsheet; the input file itself is built in a separate worksheet using cell references. Thus, any change to the calculated parameters automatically propagates through the entire input file (as an example, changing the radial build will affect the size of almost all structures and volumes inside the vacuum vessel). This makes evaluating designs, tracking design

changes, and performing parameter studies much simpler and faster, and results in a better-documented, and less error-prone, model.

Development of the model has begun, and the inboard blanket structures (for which there is presently a detailed design) are complete. Some nodalization studies are planned for early next year with the inboard blanket model. The object of these is to determine what accuracy can be gained by increasing the axial nodalization of the in-vessel structures, which historically (e.g. in ARIES models) have been very coarse (e.g. only one node). The advantages conveyed by this increased axial nodalization will be weighed against the disadvantage of the resultant increased model complexity, and an optimal resolution arrived at before proceeding to build the rest of the model.

Once the system model is built, the requirements for the tritium extraction system can be determined. Both the extraction system and other structures will "compete" for tritium; in order to determine the required efficiency of the extraction system, this will be modeled as a "black box" of varying efficiency, the required value corresponding to that which gives losses below the 1 g/year target. Further parameter studies will investigate the impact of permeation barriers, i.e. to what extent they can ease requirements on the extraction system. Informed by the required efficiency to limit losses sufficiently based on the FNSF design, a more detailed extraction system design can be performed.

Concepts for extracting tritium from PbLi have been reviewed in a series of presentations [1-3]. Many of these are based on various gas-liquid contact schemes, i.e. removal by a purge gas or vacuum; these take the form of sprays, bubblers, or "extraction columns" in which mixing of purge gas and PbLi with a large surface area facilitates tritium release. Such systems are being pursued for application to an HCLL-type blanket, in which the PbLi flow is very slow. Previous work has shown that they do not scale well to the higher flow rates of the DCLL blanket.

These higher PbLi flow rates are actually potential advantage; since less tritium is generated per pass, much lower tritium partial pressures (which drive permeation) are potentially achievable. This advantage can only be realized, however, with an efficient tritium extraction system- based on a different concept than the HCLL systems outlined above. For this reason DCLL-based designs have long planned to rely on a *vacuum permeator* for this purpose. The vacuum permeator concept seeks to *exploit* tritium permeation through solids as a means of extraction. By maintaining a high vacuum outside the pipes containing tritium-laden PbLi, a concentration gradient across the pipe wall is established that drives permeation across it.

While past studies (i.e. ARIES-CS) have included a permeator model for extraction, there has been no attempt to optimize the design or otherwise ensure that it met system requirements. Furthermore, there were apparent uncertainties regarding tritium transport in PbLi, and questions regarding whether or not this was a rate-limiting step in the transport. These issues have been resolved by deriving an analytical solution for a simple shell-and-tube type permeator design [4]. The solution gives the efficiency of the permeator in terms of dimensionless numbers that indicate whether tritium transport in

PbLi, or in the solid tube, is rate-limiting. The analytical solution allows for simple numerical optimizations of permeator design (i.e. minimizing its size) subject to system constraints on efficiency (tritium removal fraction), mass flow rate, pressure drop, etc. Once these have been fixed in the FNSF design, a similar optimization will be performed.

One of the important conclusions of this work is that transport is not always limited by the PbLi, and therefore selection of the solid tube material can have a dramatic effect on the required permeator size. To meet the constraints of ARIES-CS, a stainless steel permeator would have to be comparable to a PWR steam generator or much larger- 70-300 m^3 depending on corrosion-related velocity constraints. Using one of the group five metals (V, Nb, Ta), which have among the highest tritium permeabilities, can reduce this to 3-25 m^3. There are some issues that must be resolved for these materials to be viable; in particular, they oxidize, at partial pressures perhaps lower than reasonably achievable on the vacuum side of the permeator. Pd coatings can prevent this, and are used in commercial hydrogen separators. But at temperatures >400 °C, these diffuse into the substrate, irreversibly lowering the permeability. This may be preventable with a suitable interlayer, and a variety of porous ceramics have shown promise. These are issues that would need to be resolved as part of a pre-FNSF R&D program.

The permeator analysis and analytical solution [4] also clarified where the major sources of uncertainty lie. The mass transport coefficient of tritium in PbLi was previously thought to be among these, but a comprehensive literature survey revealed close agreement between mass transport correlations measured over the relevant range of dimensionless parameters. The largest source of uncertainty was the solubility of tritium in PbLi, which has proven notoriously difficult to measure (and reproduce) experimentally; higher solubility implies higher retention in PbLi and less permeation through the tubes. While varying the solubility through the entire measured range has a dramatic effect on the permeator efficiency, it will similarly effect permeation elsewhere in the system. The net effect on a system therefore depends on its design details, and a sensitivity study is planned to investigate this for FNSF.

[1] P. W. Humrickhouse and B. J. Merrill, "Tritium confinement and safety strategy for FNSF- materials impacts and needs," FNSF project meeting presentation, Oak Ridge National Laboratory, February 19, 2015

[2] P. W. Humrickhouse, A. Ying, and D. Rapisarda, "Tritium in DEMO," presentation at the *3rd IAEA DEMO Workshop*, Hefei, China, May 13, 2015.

[3] P. W. Humrickhouse, "Tritium permeation control and extraction- perspectives from fusion systems studies," presentation at the *Workshop on Tritium Control and Capture in Salt-Cooled Fission and Fusion Reactors*, Salt Lake City, October 28, 2015

[4] P. W. Humrickhouse and B. J. Merrill, "Vacuum Permeator Analysis for Extraction of Tritium from DCLL Blankets," *Fusion Science and Technology* **v. 68** pp. 295-302, 2015.

6-g. Multiscale-Multiphysics Modeling of the FW/Blanket of FNSF *(Nasr M. Ghoniem, Yue Huang, UCLA)*

3D solid modeling was achieved with the commercial software: SOLIDWORKS, while 3D finite element multiphysics modeling of the DCLL first wall and blanket (midplane of one sector) has been performed using COMSOL 5.0. The multiphysics aspect of the design is demonstrated via coupling of Computational Fluid Dynamics (CFD), heat transfer in solids, and heat transfer in fluids modules within the COMSOL software. Both normal and off-normal loading conditions have been analyzed. The results of velocity, pressure, and temperature distributions of helium flow, as well as the primary and thermal stress of the structure were obtained. This was followed by determination of the factors of safety along three critical paths based on the ITER Structural Design Criteria for In-vessel Components (ISDC-IC). We show here that the optimized structural design meets the ITER-ISDC design rules under normal operating conditions. However, the design must consider possibilities of plastic damage and fracture under off-normal conditions. This indicated that further plastic and fracture mechanics analyses are necessary in critical regions, and that a multiscale approach is required. Future efforts will consider the effects of radiation on the lifetime and reliability of the design, improvements in the geometric layout of the first wall and blanket structure, improvements in heat transfer and fluid flow models, and integration of multiscale models of plasticity and fracture.

1. Multiphysics-Multiscale Methdology

The first step of the design process is to perform multiphysics elastic analysis, incorporating the CFD, heat transfer, coupled thermal stress and primary stress (due to pressurization) analyses. ITER SDC-IC design criteria, which were developed by international collaboration for ITER in-vessel components on the basis of the French design code (RCC-MR); RCC-MR code "Design and Construction Rules for Mechanical Components of FBR Nuclear Islands and High Temperature Applications," and the U.S. ASME design code for Boilers and Pressure Vessels (ASME-BPV), were applied to calculate design factors-of-safety. The detailed information of definitions of allowable and design rules can be found in this reference [1].
Three major multiphysics modules have been coupled in the current design. These are: Non-isothermal Fluid Flow, Heat Transfer in Solids, and Solid Mechanics. They are coupled in the Conjugate Heat Transfer module. The Non-isothermal Fluid module was used to simulate helium flow inside cooling channels. CFD simulations were based on laminar helium flow conditions, as a result of computational limitations. Turbulent flow simulations are expected to result in higher heat transfer coefficients, thus reducing the structure temperatures, and such simulations will be considered in the future.

2. Simulation results

- Helium flow

The inlet helium operating pressure in the FW, BW, and all cooling channels is assumed to be 8 MPa. As Fig.1 shows, the pressure decreases due to friction losses all the way through the helium flow channel. With the laminar flow assumption, the average velocity

was set to be over 100 m/s to reach the required heat transfer coefficient, and the pressure drop in one pass through a coolant channel is around 140 kPa.

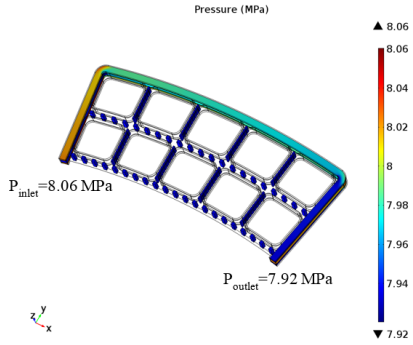

Fig. 1. Pressure distribution of helium flow

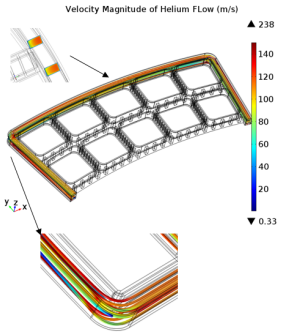

Fig. 2. Streamlines of helium flow

The streamlines of helium flow with velocity information are shown in Fig.2. The entire helium flow stream with an inlet temperature of 400 ℃ (Fig.3) enters the blanket sector. So far, only three channel layers at midplane were studied for the present preliminary design. For the entire FW/Blanket design, there are stacks of helium flow channels in the poloidal direction, and an alternating flow configuration will be applied to create a more uniform temperature thus reducing thermal stresses.

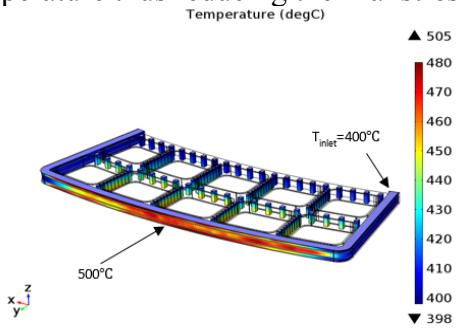

Fig. 3. Temperature distribution of helium flow

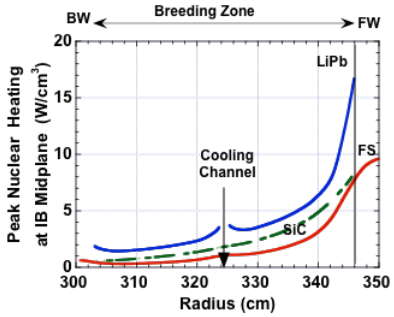

Fig. 4. Radial distribution of nuclear heating

- Temperature distribution of the solid structure

The heat flux from the plasma results in temperature gradients inside the blanket structure, which cause secondary thermal stresses. The peak heat flux is taken as 0.28 MW/m^2 at the inboard blanket midplane. The dependence of the peak volumetric heating on the radial distance at the midplane for different materials is shown in Fig.4 (data provided by Professor El-Guebally at UW).

The surface heat flux and the volumetric heating rates were applied in the Heat Transfer in Solids module in COMSOL. The result of the temperature distribution is shown in Fig.5. The maximum temperature of the LiPb is around 700 ℃, while the steel/LiPb interface temperature is kept at 500 ℃. This result is pretty close to the temperature limitation so it's better to have higher helium heat transfer coefficient to bring the temperature down. Ribs and grooves may need to be manufactured inside the cooling

channels to enhance wall heat transfer. The side effect is that a much higher pressure drop in flow channels will occur.

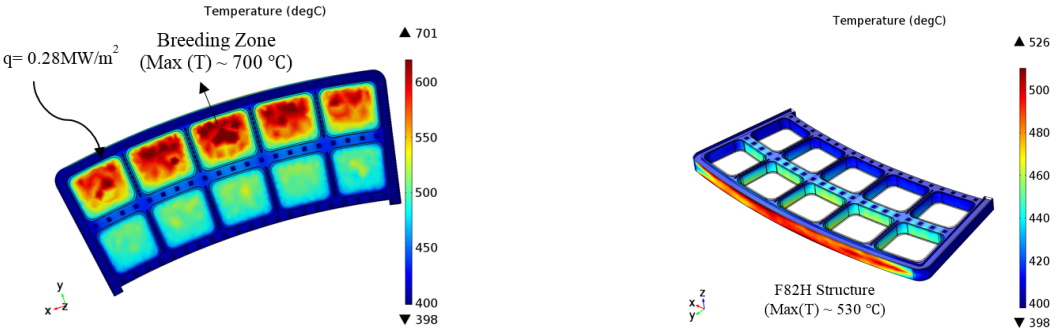

(a) Breeding zone (b) Blanket structure

Fig. 5. Temperature distributions of the global FW/B structure

- Primary stress

The helium and LiPb flow inside the channel generates the pressure against channel walls, which finally leads to the primary stress in the blanket structure. As discussed before, the pressure load under normal operating conditions in helium cooling channels and the LiPb breeding zone is set to be 8 MPa and 1.6 MPa, respectively. The following results shown in in the figures below are based on normal operating conditions. Fig.6 shows the global primary stress distribution of the blanket structure. There are stress concentrations at the junctions and corners. After rounding and adding fillets to junction zones, the stress concentration was reduced below 100 MPa. Deformation of the structure resulting from the primary stress was also obtained, as shown in Fig.7.

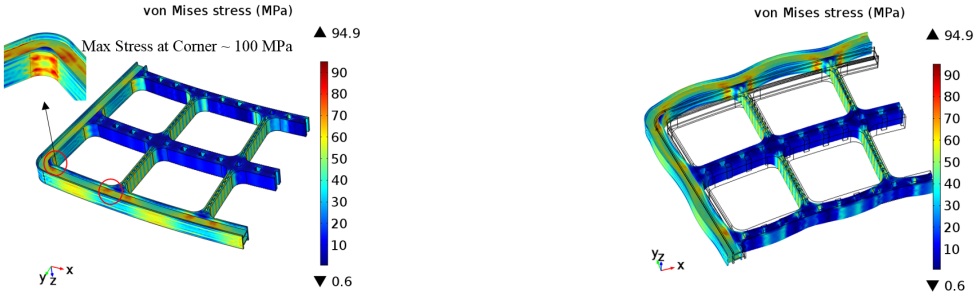

(a) (b)

Fig. 6. Primary stress distribution: (a) Von-Mises stress distribution in the undeformed configuration, (b) Von-Mises stress distribution in the deformed configuration

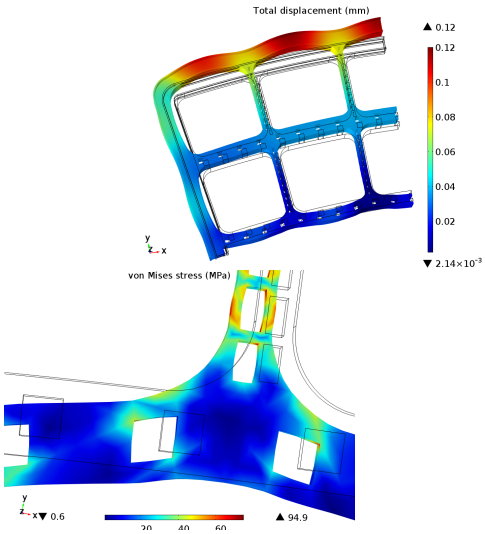

(a) Global deformation (b) Local deformation

Fig. 7. Displacement distribution due to the primary stress

- Thermal stress

Thermal stress was calculated based on the temperature distributions utilizing the Conjugate Heat Transfer module of COMSOL. As illustrated in Fig. 8, the first wall has the largest thermal stress, although a directionally-alternating cooling channel layout has already reduced severe temperature gradients. Also, thermal expansion is shown in Fig 8 (b), illustrating the reason why we need to leave a gap of at least 2 cms between adjacent sectors during assembly to accommodate thermal expansion.

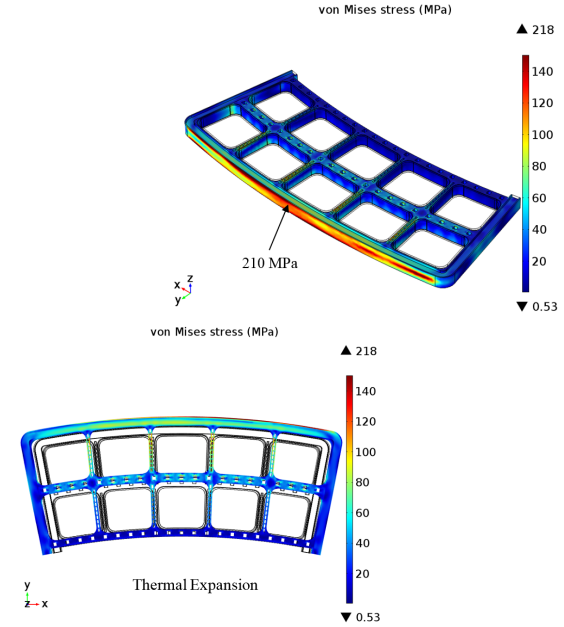

(a) Undeformed configuration (b) Deformed configuration

Fig. 8. Thermal stress distribution

- Design and Margins of Safety

Line integration through the thickness of the structure is used to resolve stresses into membrane, bending and non-linear components. The membrane stress tensor has components that are equal to the mean value of stresses through the thickness. The bending stress tensor has components that vary linearly through the thickness and which, when integrated through the thickness result in equilibrium with the section moment [2]. The line along which this integration is carried out is defined as "a supporting line segment." Three supporting line segments were selected as critical paths to determine the design safety factors, as shown in Fig. 9 (the result in Fig. 9 is under off-normal condition).

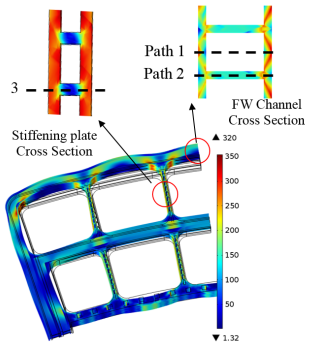

Fig. 9. Critical supporting line segments

With the results of the primary and thermal stresses, factors of safety were determined based on the three different allowable values and the low temperature design criteria. The results are shown in Table 1-3. For reference on the mechanical design procedure, including stress intensity parameters and design criteria, please see reference [2].

Table 1 Factors of safety based on S_m

		$\overline{P_m}$[MPa]		Factor of Safety	
Path	S_m[MPa]	Off-normal	Normal	Off-normal	Normal
1	147.3	86.6	21.5	**1.7**	**6.9**
2	151.2	84.1	28.8	**1.8**	**5.2**
3	148.9	175.2	56.0	**0.85**	**2.7**

Table 2 Factors of safety based on S_e

		$\overline{P_L + Q_L}$[MPa]		Factor of Safety	
Path	S_e[MPa]	Off-normal	Normal	Off-normal	Normal
1	207.9	94.5	37.9	**2.2**	**5.5**
2	213.3	125.5	44.5	**1.7**	**4.8**
3	210.2	225.9	57.4	**0.93**	**3.7**

Table 3 Factors of safety based on S_d

		$\overline{P_L + P_B + Q}$[MPa]		Factor of Safety	
Path	S_d[MPa]	Off-normal	Normal	Off-normal	Normal
1	415.8	259.9	194.7	**1.6**	**2.1**

2	426.6	177.8	65.2	**2.4**	**6.5**
3	420.3	217.1	46.8	**1.9**	**9.0**

The current results indicate that structure, under normal operating conditions, meets all design criteria, while the safety factors under off-normal operating conditions are marginal. Therefore, it is recommended that further plastic and damage analysis be conducted under off-normal operating conditions.

References

[1] Ghoniem, Nasr M., Giacomo Po, and Shahram Sharafat. "Deformation mechanisms in ferritic/martensitic steels and the impact on mechanical design." *Journal of Nuclear Materials* 441.1 (2013): 704-712.

[2] Sharafat, Shahram, Aaron T. Aoyama, and Nasr Ghoniem. "Assessment of the DCLL TBM Thermostructural Response Based on ITER Design Criteria." *Fusion Science and Technology* 60.1 (2011): 264-271.

6-h. FNSF Magnet System *(Y. Zhai and P. Titus, PPPL)*

Fusion power scaling law is known to be $P_F \sim \beta^2 B^4$, where β is the plasma pressure to magnetic pressure ratio and B is the magnetic field at the plasma major radius. The scaling law implies that for any economic fusion power, either improved plasma performance or increased toroidal magnetic field is needed. The design of a large-scale high field fusion magnet system is unique and very different from that of conventional high field solenoid or dipole magnet systems where the longitudinal hoop stress and mid-plane compressive stress (axial clamping force) are the dominant design stress factor. The fusion magnet system has complex geometry (largely as the result of system requirements) and the balancing need of the plasma pressure and magnetic pressure. The toroidal field (TF) coils are designed for plasma confinement, and the central solenoid (CS) coils as the plasma primary transformer are the Ohmic heating (OH) coils to initiate plasma current by the OH current and magnetic flux sweeping. The poloidal field (PF) coils are the equilibrium field coils to generate radially inward force to equilibrate a radially outward force for the plasma pressure equilibrium, and to control plasma shape during operation. Once energized, the D-shaped toroidal field (TF) coils are not only subjected to a large longitudinal hoop stress, but also to a large centering force due to the 1/R TF field decay as shown in Figure 1, and large transverse out-of-plane bending stress as a result of poloidal field interaction from PF and CS coils that requires a large amount of structural support (virial theorem). For large-scale fusion magnets, high current cables (>50-60 kA) are also needed for better protection of the TF coils during the fast discharges. In addition, auxiliary in-vessel coils for vertical stability and plasma ELM mode control and correction coils for refining error field harmonics are needed. The peak magnetic field (>15 T) on the TF inner leg is likely to require the use of high performance advanced Nb_3Sn wires (advanced J_c wires) in the cable-in-conduit conductor (CICC) or even high temperature superconductors as the magnet design options.

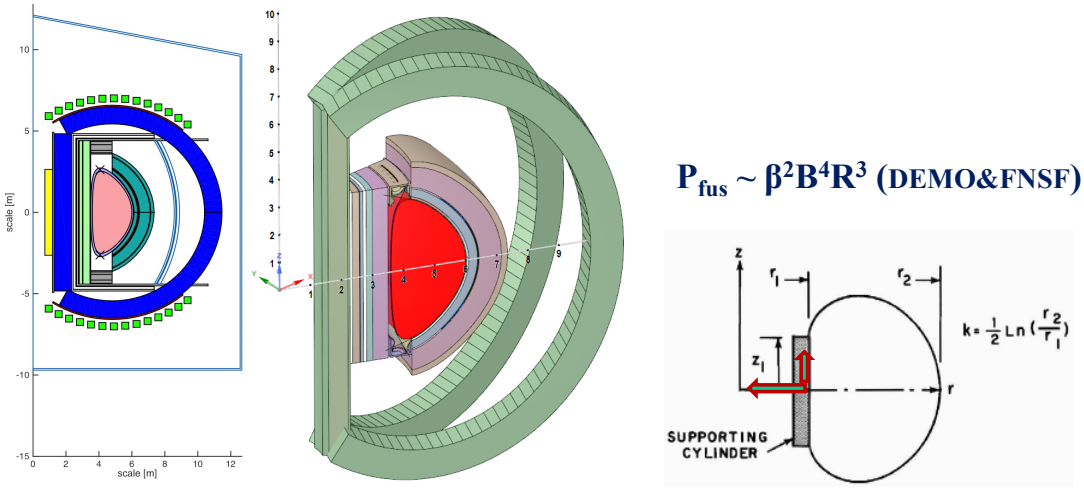

Fig. 1 **CAD model generated based on FNSF radial built**

As the first nuclear fusion device to provide both a fully integrated fusion environment with the fully integrated fusion components, the FNSF magnet design parameters from the system code analysis are listed in Table 1 as compared to ITER and the DEMO

design parameters. The FNSF is smaller than ITER machine while generating higher magnetic field (utilizing high performance Nb_3Sn strands). In comparison, both the K-DEMO – more aggressive in high field (B), and E-DEMO – more aggressive and thus expensive in size (R) are larger machines than ITER.

TABLE I
COMPARISON OF BASIC DESIGN PARAMETERS

Symbol	FNSF	ITER	K-DEMO	E-DEMO
major radius (m)	4.8	6.2	6.8	9
minor radius (m)	1.2	2	2.1	2.25
plasma current (MA)	8	15	12	14
plasma center B_0 (T)	7.5	5.3	7.4	6.8
TF operating current (kA)	62.5	68	65.5	80-85
TF max field (T)	15.5	11.8	16	13.45
TF current density (A/mm^2)	27	17	25	15
TF Amper-turns (MA)	11.25	9.11	15.72	19.8
No. of turns	180	134	240	232
No. of TF coils	16	18	16	16
Half of vertical force (MN)	355	206		
Centering force (MN)	920	403		1220
TF coil inductance (H)		18		51
TF discharge time cons		11-14		23
Fusion power (MW)	450	500	500	500

For the horizontal maintenance of FNSF, large outer board TF legs are required. Straight assembly gaps shall be avoided to alleviate neutron streaming problems. Steady state or long pulsed operations for FNSF are considered for the magnet design.

The next-step fusion reactors require magnet system with a sufficiently large aperture size for plasma fusion reaction. This makes fusion TF magnet highly in-efficient in utilizing the winding pack space because a significant amount of structure support is required to ensure structural integrity of the magnet system for a large sized high field TF magnet system. It is common to have a 2-3 or even higher ratio between the maximum magnetic field on the TF inner leg and the plasma center field as compared to the close to 1-1.1 ratio between maximum field and the central field in typical high field solenoid or dipole magnets with a few cm's bore size. As a result, current density in state-of-the-art fusion TF coils such as in ITER is only 15-17 A/mm^2 as compared to ~50 A/mm^2 winding pack current density in the series-connected hybrid solenoid magnet using also CICC conductors. High field solenoid or accelerator magnets are generally designed to have a high pack factor and so to be highly efficient in using the high field winding pack space with high current density. Figure 2 presents comparison of magnetic field reduction at plasma major radius against radial distance for various fusion devices.

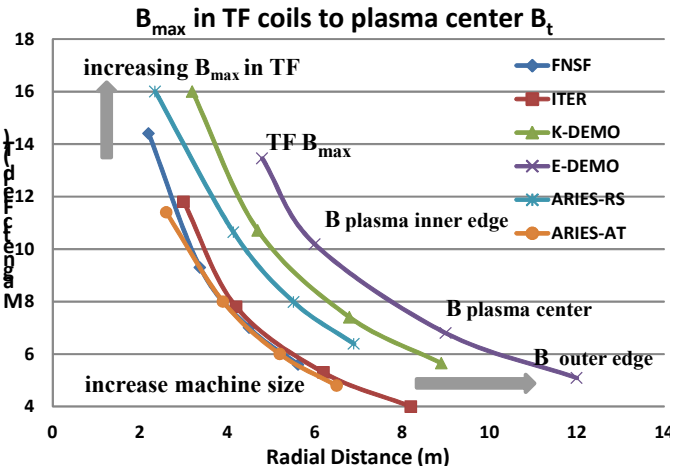

Fig. 2. (a) Toroidal magnetic field as function of radial distance for TF coil winding pack design

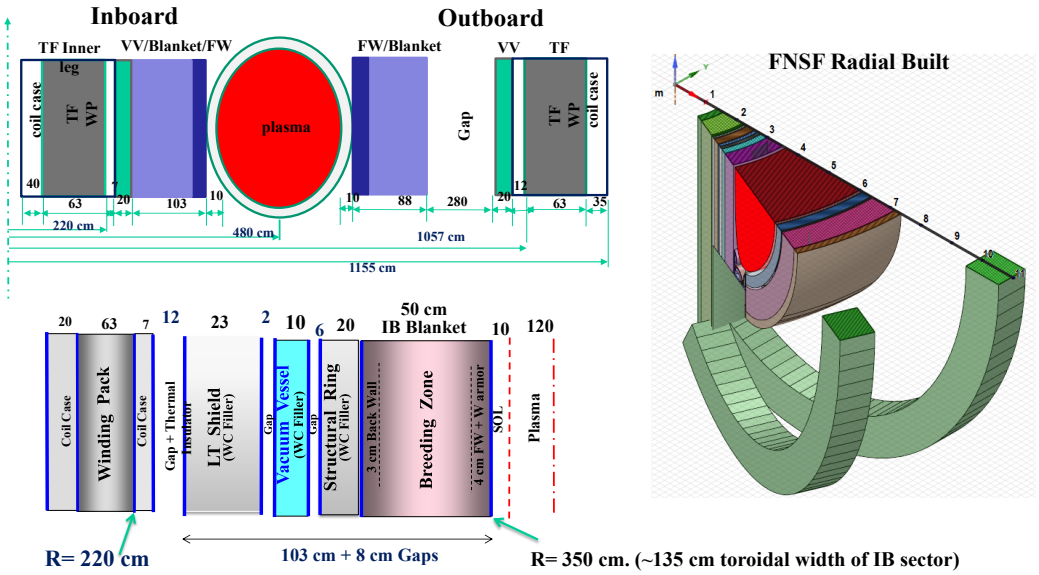

Fig. 3 Inboard and outboard radial built of FNSF (upper left) and details of inboard TF leg radial built (lower left). The plot on the right shows 3-D CAD model of inboard and outboard TF legs in the FNSF radial built.

Figure 3 presents the inboard and outboard radial built for the FNSF. A total inboard sector toroidal width of ~1.35 m is needed for the FNSF TF inner leg due to long pulse and high fluence operation.

Figure 4 presents the TF coil winding pack composition. The TF coil design includes 65% cross-sectional area of the case structure with a thickness of 7-8 cm in facing plasma side, and 35% cross-sectional area of the coil winding pack, which includes 10% superconductor (about 600 Nb_3Sn superconducting strands), about 15-20% copper and 10% insulator. The low activation jacket structural material similar to JK2LB may be selected. Jacket and liquid helium cooling take about 30% of the winding pack area respectively.

High performance Nb_3Sn wires such as the OST RRP wires for FNSF TF coil conductors will be selected for the winding pack design. Figure 6 presents the RRP wire cross section and a jacket thickness of 3-5 mm is needed.

For TF operation, high current cable is needed for coil protection during fast discharges. The 62.5 kA cable-in-conduit conductor with 180 turns will provide the needed Ampere-turns of 11.25 MA for the TF field at plasma center. There is a significantly larger coil centering force as compare to ITER TF coils as shown in the global structural analysis described in Figures 7 and 8.

Fields on PF coils are relatively small and NbTi can be a good LTS option. As the next step fusion machine, the plan for FNSF is steady state non-inductive startup operation.

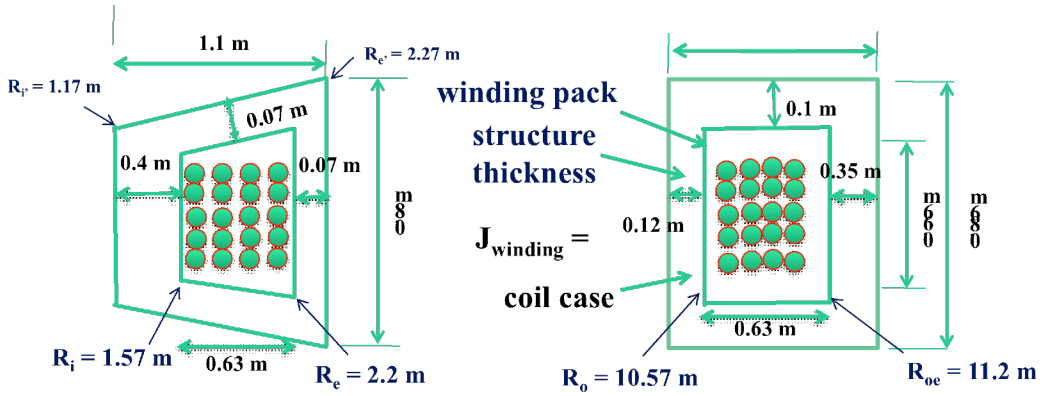

Fig. 4. (a) Dimensional details of TF inner leg winding pack (b) Dimensional details of FNSF TF outer leg and coil structure.

However, a small OH coil is needed for small inductive current drive of the plasma operation. The size of the small OH coil makes the HTS coil design with no-insulation, no cable (direct winding of the HTS tapes) and no liquid helium and combined with conductor grading for improving coil wind efficiency a potential attractive option for the small size, high field FNSF OH coils.

Conductor Radiation Limits

Recent radiation test in LTS and HTS conductors [8-9] indicates that YBCO is no better

TABLE III
CONDUCTOR AND COIL INSULATION

	Conductor	Conductor Insulation	TF Coil Impregnation
ITER	Nb_3Sn	Glass/Polyimide (Kapton)	Blended CE/DGEBF 40/60
ARIES-AT	YBCO	Inorganic MgO	High performance epoxy
FNSF LTS	Ternary Nb_3Sn	Glass/Kapton	Hybrid epoxy
FNSF HTS	REBCO	Ceramic MgO	Epoxy/MgO

Insulations to be used for FNSF and comparison with other fusion machines

than binary Nb3Sn but can be better (bellow 40 K operation) than the ternary Nb_3Sn. REBCO at $3x10^{22}$ n/m2 radiation has over 50% I_c degradation for 64 K operation and at $2x10^{22}$ n/m^2 radiation, it has ~30% I_c degradation for 40 K operation and below 40 K operation is possible at $3x10^{22}$ n/m^2 level of neutron radiation. Table II presents the neutron radiation limits for the conductor and insulation materials. Table III presents the typical conductor and coil insulations used or selected for fusion devices.

TABLE II
MATERIAL RADIATION LIMITS

materials	Fast neutron fluence	unit
Nb_3Sn	$5x10^{22}$	n/m^3
YBCO	$3x10^{22}$	n/m^3
Gd-123 (40 K)		
copper	$2x10^{21}$	n/m^3
epoxy	10^6	Gy
Polyimide/Kapton	10^7	Gy
CE/epoxy	$2x10^8$	Gy
hybrid	$5x10^8$	Gy
Mgo	10^{11}	Gy

YBCO is no better than binary Nb_3Sn but can be better (below 40 K) than ternary Nb_3Sn. Recent test indicates that REBCO at $3x10^{22}$ n/m^2 radiation has > 50% I_c degradation for 64 K operation and at $2x10^{22}$ n/m^2 radiation, it has ~30% I_c degradation for 40 K operation and below 40 K operation is possible at $3x10^{22}$ n/m^2 level of radiation.

LTS Magnets

No additional power consumption except small amount of power for cryogenics is needed for the LTS magnets. Higher current density and higher field can be achieved for the

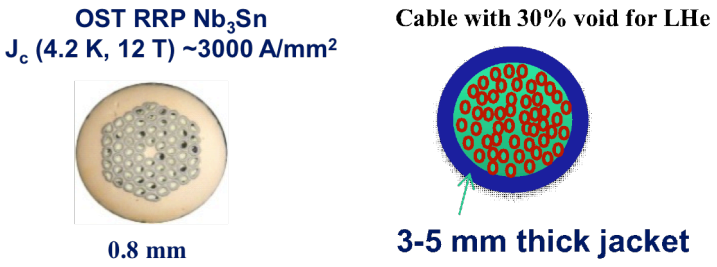

Fig. 5. State-of-the-art cable-in-conduit-conductors for ITER and next step fusion magnets

same size of coils compared to resistive magnets. LTS magnets are better for long time plasma operation as required by FNSF. The construction cost of the LTS magnets, however, is ~30% the total machine cost. In addition, there is limited availability of helium for cooling of the LTS magnets. The cost of helium has risen drastically in the past decade and we may see the disappearance of helium supply completely within the next few decades. Moreover, more space is needed for thermal and radiation shielding of LTS coils. Better ways of integrating advanced insulations are also needed. Figure 6 presents the advanced performance Nb_3Sn wires from OST and the circular cable-in-conduit conductor (CICC) for TF coil winding pack.

SULTAN test of ITER CS Nb_3Sn CICC showed significant degradation with both thermal and magnetic load cycling that is unacceptable for ITER. The cyclic load degradation problem was solved by adjusting the 1st stage cabling pattern to a short twist pitch. It is not fully understood about the mechanism of this performance degradation other than that it is related to filament fracture. SULTAN test of ITER TF CICC conductors also showed degradation after 1000 load cycling. This may be related to the strand properties. Unlike the CS conductor tests, this result of TF CICC performance degradation is directly relevant to the FNSF LTS magnet option since a few thousand load cycles are expected for the FNSF. Recent studies are focused on the correlation of the strand irreversible limits with the wire initial voids/defects induced stress concentration. Figure 7 presents various conductor options for fusion magnets.

Due to the lack of high field pinning capability, the intrinsic limitation of Nb_3Sn magnets is at about 16-17 T for 4.2 K operation. Even if high field pinning capability in wires could be slightly improved, Nb_3Sn would still be intrinsically limited to below 20 T at 1.9 K. In practice, for the FNSF magnets with a peak field on the TF coils higher than that for ITER, design of LTS magnets using high J_c Nb_3Sn wires may be challenging as it will push Nb_3Sn close to its intrinsic field limit. In addition, availability of liquid helium for cooling of the LTS magnets may become very limited and thus increase significantly operating cost for the FNSF LTS magnet option of long pulse plasma operation.

Recent study also indicates that additional heating to ITER TF coils may be an issue. The peak nuclear heating to the ITER TF coils must not exceed 14 kW but the most recent studies showing that this is challenging to meet at the ITER neutron fluence level. In addition, the dose limit to insulation is 10 MGy. The maximum occurs in the front insulation of the coil at inboard mid-plane where the total integrated dose during ITER lifetime is ~3 MGy.

Figure 8 presents the stress distribution under EM loads on FNSF magnets: 1) the top and bottom caps for out-of-plane loads are needed 2) Outer board TF coil superstructure is required which enlarges the structural footprint mostly radially to accommodate horizontal maintenance and toroidal expansion of TF coil structural footprint also helps and should be taken advantage of 3) top and bottom OB structures are required to meet force and stress allowable. With the added radial structure and added structure above and below the horizontal port, the outer leg TF stress is similar to that which was qualified cyclically for ITER (in its inner leg). The FNSF should have less restrictive fatigue requirements. The important conclusion is that RADIAL SERVICING STRESSES OUT. Inner leg torsional shear will need features like ITER. Shear keys in the corner and possibly corner tensioned rings. Inner Leg Stress is still a bit too high and some modest reallocation of metal cross sections may still be needed. Improved yield stainless steels are an option. More steel with less space for conductor may be possible with HTS. If the reactor is truly steady state or very long pulse, Solid Non-CICC Nb_3Sn cable in channel conductor could be an option.

HTS Magnets

High energy margin is obtained for the high operating temperatures. The ideal operation temperature is in the 20-40 K range considering radiation limit, total heating to the coils, availability of helium, etc. Compared to Nb_3Sn, YBCO has relatively low stress and strain limit but YBCO has a relatively low strain sensitivity, low temperature and field dependence to critical current density. HTS such as Bi2212 and YBCO is still a factor of 10-20 times the cost of Nb_3Sn. It is expected the cost gap can be reduced in the next decades for the FNSF. A robust cable design suitable for FNSF magnets is needed based on the TF coil winding structural configuration. Compared to Nb_3Sn, the YBCO has low stress and strain limits, low strain sensitivity and low temperature and field dependence on critical current J_c. A critical need for HTS-based pilot plants is to demonstrate and validate the scalability of HTS coil fabrication technology based on direct winding of coated conductors to the fabrication of large-aperture TF magnets using high current cables. Feasibility studies of TF magnet systems consisting of D-shaped coils show that stress in HTS windings should be manageable, but R&D is needed to develop suitable cooling schemes. Large-aperture TF coils (>1-2m in radial dimension) for next-step HTS fusion magnets will need to be constructed to validate scalability of the HTS coil prototyping and testing using the HTS cable recently developed.

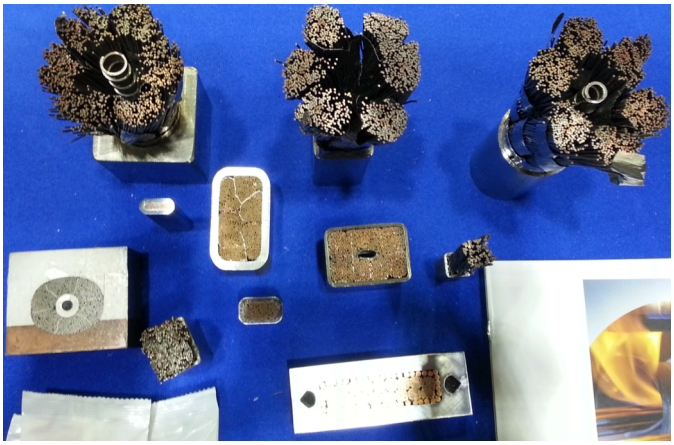

Fig. 6. State-of-the-art cable-in-conduit-conductors for ITER and next step fusion magnets.

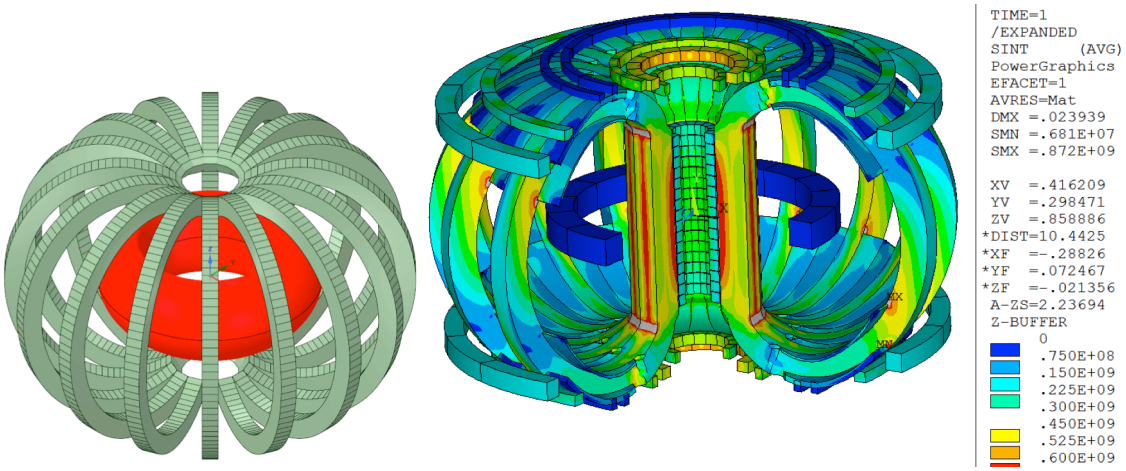

Fig. 7. Stress analysis under EM loads indicate that 1) the top and bottom caps for out-of-plane loads are needed 2) Outer board TF coil superstructure is required which enlarges the structural footprint mostly radially to accommodate horizontal maintenance and toroidal expansion of TF coil structural footprint also helps and should be taken advantage of 3) top and bottom OB structures are required to meet force and stress allowable.

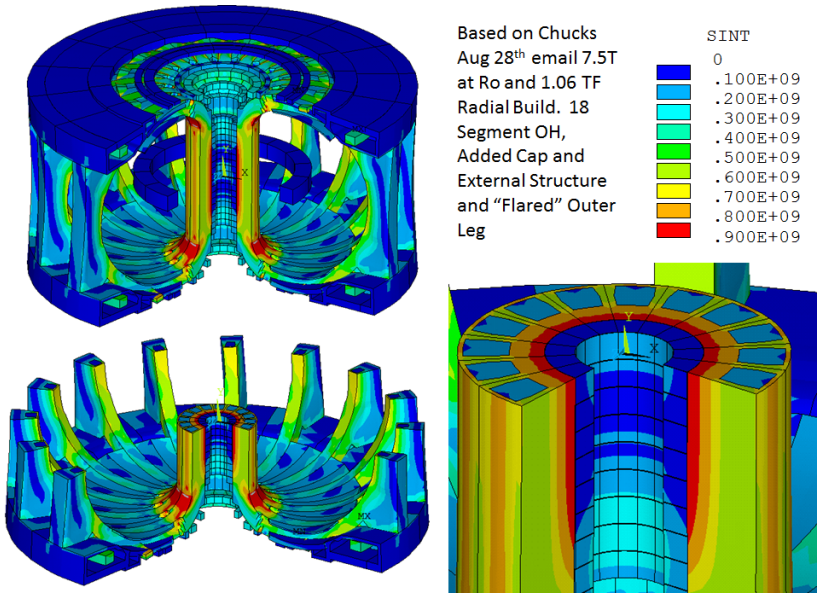

Fig. 8. Inner leg stress distribution under EM loads of normal plasma operation

Conclusions

For next step large scale fusion magnets designed for long pulse plasma or steady state operation after ITER, copper magnets cannot be a long-term option (~10 million dollars per pulse cost of electricity to run Fusion Development Facility for two week long steady state plasma duration). Low temperature superconducting magnets are the present-day state-of-the-art technology option. Initial construction cost can be reduced by conductor grading. Magnet materials with high radiation limits should be selected and tested. ITER experience of CICC performance degradation over significant load cycles is not a critical issue for steady state plasma operation. Global structural analysis indicated that the radial service maintenance used as a basic for plant layout is feasible.

High temperature superconducting magnet is costly but may offer better long term options for small Ohmic heating CS coils for FNSF. Research and development needs for FNSF magnets include wire and cable design option, joint for TF coils and better structural materials. The YBCO irradiation resistance is better than the high J_c ternary NB_3Sn but less tolerant than the binary Nb_3Sn.

References

[1] C. E. Kessel et al, "The Fusion Nuclear Science Facility (FNSF), the Critical Step in the Pathway to Fusion Energy", *Proceedings of Technology of Fusion Energy*, Nov. 9-13, 2014.

[2] R. D. Stambaugh et al, "Fusion Nuclear Science Facility Candidates", *Fusion Sci. Technol.*, 59, Feb., 2011.

[3] K. Kim et al, “Conceptual design study of the K-DEMO magnet system”, *Fusion Eng. Des*., 96-97, 281-285, 2015.
[4] L. Bromberg et al, “ARIES-RS Magnet Systems”, *Fusion Eng. Des*., 38, 159-188, 1997.
[5] F. Dahlgren et al, “ARIES-AR Magnet Systems”, *Fusion Eng. Des*., 80, 139-160, 2006.
[6] J. Clerk Maxwell, *A Treatise on Electricity and Magnetism,* 3rd ed., vol. 2. Oxford, U.K.: Clarendon, 1892, pp. 68–73.
[7] H. W. Weijers, “High Field magnets with HTS conductors”, *IEEE Trans. Appl. Supercond.*, 576-582, Jun. 2010.
[8] H. W. Weber, “private communication”, Jan. 2015.
[9] D. X. Fischer et al, “Effects of faster neutron irradiation on the critical currents in GdBCO coated conductor tapes”, *HTS4Fusion Conductor Workshop*, Sep. 12, 2015.
[10] Y. Zhai, C. Kessel, L. El-guebaly and P. Titus, “Magnet Design Considerations for Fusion Nuclear Science Facility”, *IEEE Transactions on Applied Superconductivity*, in review, 2015.

6-i. Magnet Structural Analysis *(P. Titus and Y. Zhai)*

This report addresses the global structural adequacy of the US-FNSF coil layout as of November 2015. The design point provided as of November has been found to be within present structural design practice, although some modest improvements are needed in the inner leg stress. An important conclusion of this analysis is that the radial servicing logic used as a basis for plant layout is feasible. The concept relies on large TF outer leg inter-coil spaces and a large outer leg radial build to facilitate radial blanket module servicing. The toroidal field at the plasma

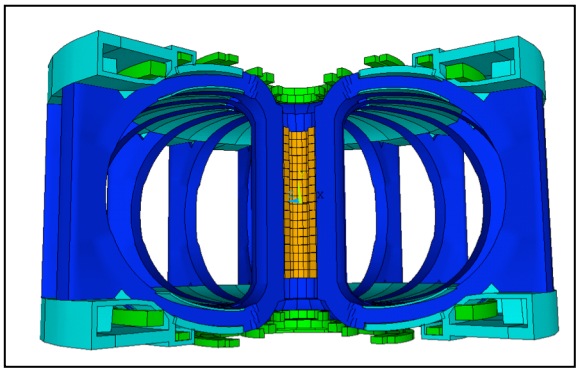

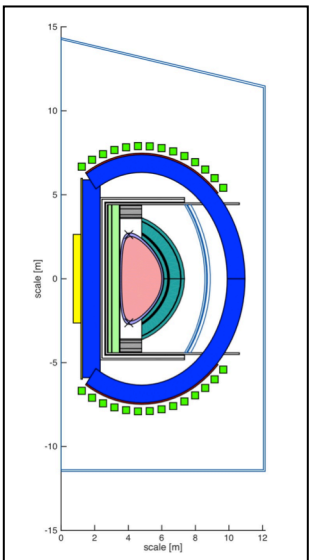

Figure 1 TF Coil Shape from Mark Tillack's System Code

centerline is large, 7.5 T with a peak field of 17.37 Tesla in the inner corners of the TF winding pack. The high fields and large radial build combine to produce a large vertical net load on the upper half of the TF coil system that must be supported by the metal cross sections of the inner leg and outer leg plus additional outer structures. After some iterations with C. Kessel's plasma equilibrium analysis, updated PF coil builds were provided by C. Kessel. This included the addition of another OH segment. The coil profile started with results from Mark Tillack's systems run of the operating point. Ultimately, the TF was "squashed" to allow the PF coils to be closer to the plasma. This is a substantial deviation from the constant tension D shape. Significant inner corner bending stresses result and are discussed and are expected to satisfy static and fatigue criteria.

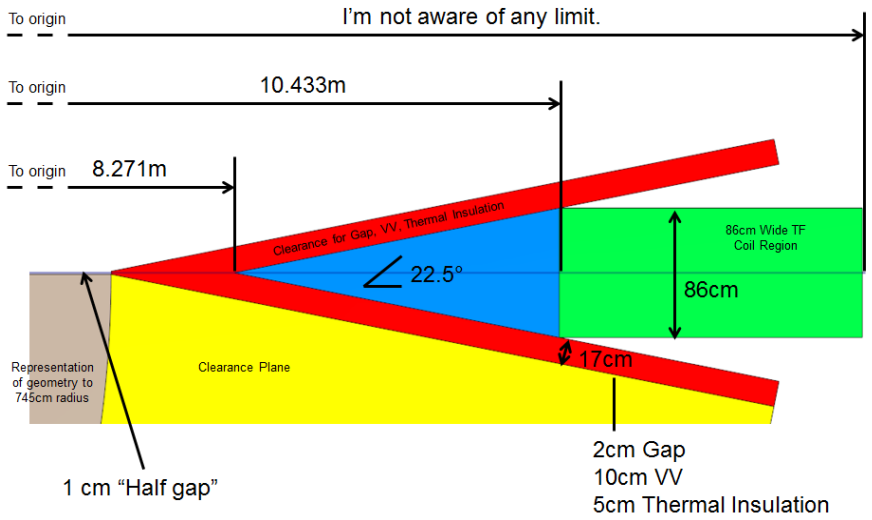

Figure 2 Outer Leg Space Allocation Study

The outer leg position was adjusted to accommodate the dimensional studies by E. Marriot from the University of Wisconsin. These provided the envelope within which the outer leg could be fit, to allow the radial extraction of the core segments.

TF Build

The winding pack cross section is close to that provided by Yuhu Zhai It has been adjusted to facilitate mesh generation. The winding pack is modeled as a central region in the case with an Orthotropic set of moduli. As a default, the orthotropic set is taken from the ITER TF analysis.

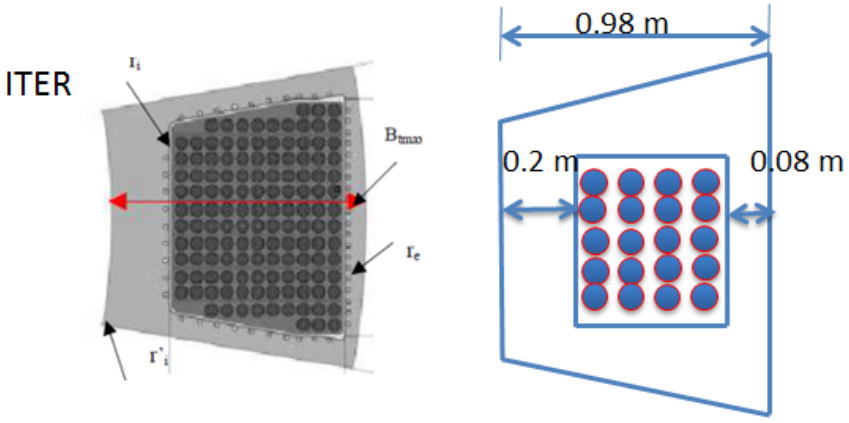

Figure 3 FNSF TF Cross Section Proposed by Yuhu Zhai, Used in the 2015 Analyses.

In Figure 3, the ITER cross section is at left for comparison. The Inner Leg Cross Section used in the analysis is shown in Figure 4 below.

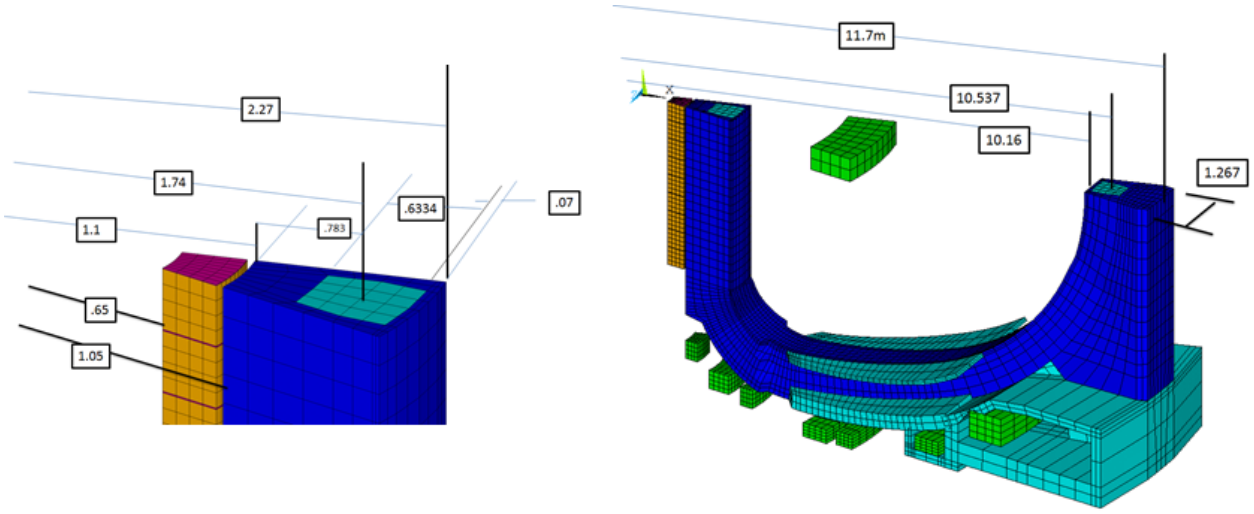

Figure 4 TF Inner Leg Dimensions Used in the Analysis

Winding Pack Properties for the TF Coil Analysis of the US :FNSF

ex,1, 100000000000 $ey,1, 48900000000 $ez,1, 48900000000
gxy,1, 27200000000 $gyz,1, 22700000000 $gxz,1, 6440000000
prxy,1, .24 $pryz,1, .243 $prxz,1, .159

		R0	Bo	Field (T)	TF	Coil MAT	Winding Pack Area, m^2	Winding Pack Current Density, MA/m^2	Primary Membrane Tresca Mpa	
FNSF		4.8	7.5	17.57	16	11.25	0.48	23.4375	800	
ITER		6.2	5.3	10.948	18	9.128	0.5344	17.0808383	705	
HTST	9/15/2014			13.165		2.24	0.0303659	73.7669071		
ST 3 Meter		3	7	16.655	16	6.563	0.17518	37.4643224		
ST 3 Meter		3	7	17.023	10	10.5	0.2534	41.437648		
KDEMO		7	7	16.87	16	15.313	1	15.313	850	
CFETR		5.7	5	9.577	16	8.9065	0.522291	17.0527541	540	
CFETR HTS							1	0		
								#DIV/0!		

Base cable: 40 tapes, 4 mm width, 0.1 mm YBCO Tape Ic (4.2K, 20T) = 170 A

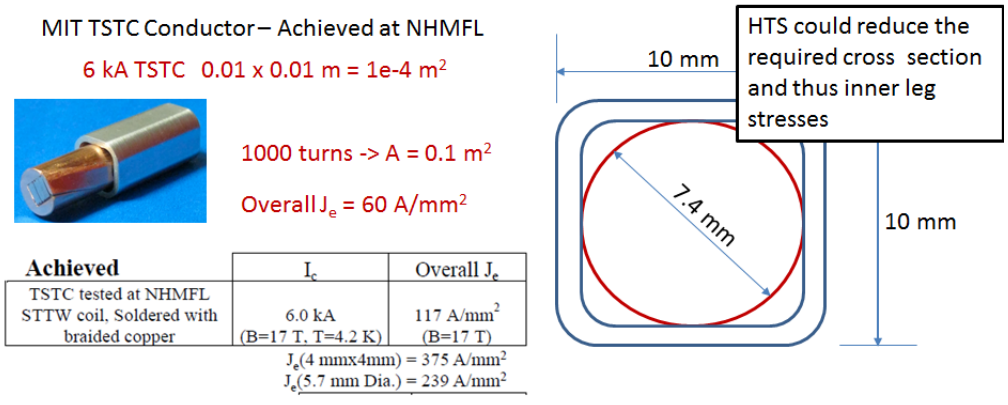

Figure 5 Current Densities for ITER, Representative Pilot Plants and HTS Conductors
Currently, conductors are assumed to contribute little to the structural strength of the winding pack. Nb3Sn conductors are mostly annealed copper and Helium filled voids.

The winding pack properties are taken from the ITER TF "smeared" winding pack orthotropic property set.

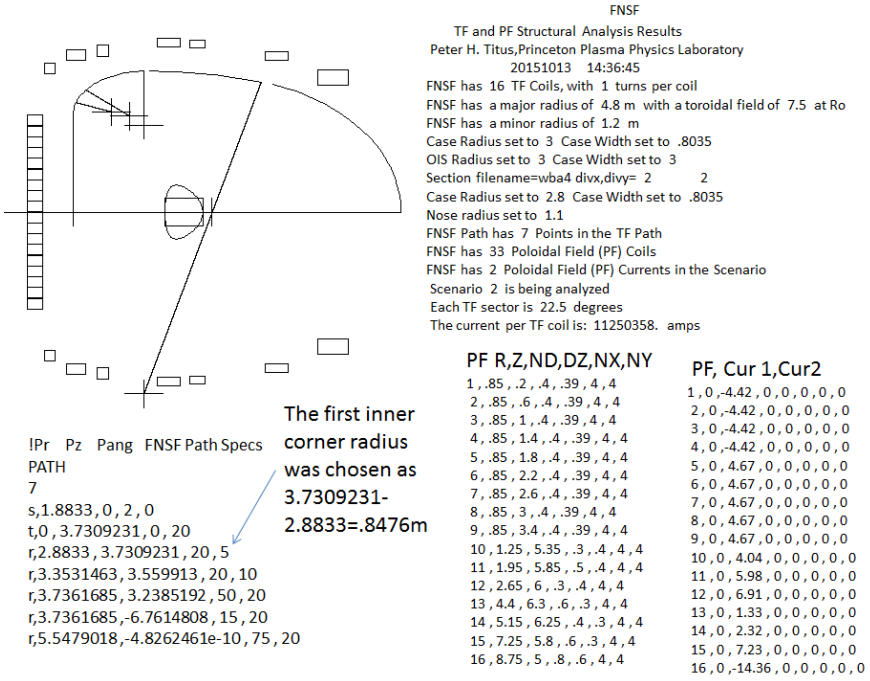

Figure 6 Major Parameters of the Coil Model

Figure 6 shows the major parameters used in the modeling of the FNSF. The path definition in the figure begins with a starting coordinate at the winding pack center, then a translation to create the straight leg, then a series of arc centers and angles. TheTF is assumed to be up-down symmetric.

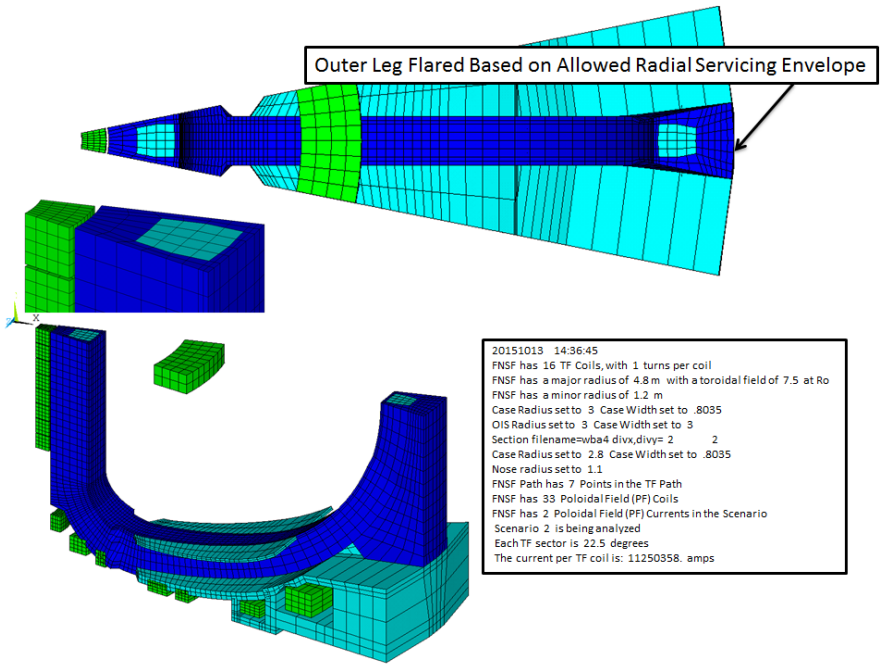

Figure 7 FNSF Analysis Model

Figure 7 shows the "flared" outer leg cross section that uses the available space left by a radial extraction of the core components. The outer leg reinforcement can be increased radially as needed to add to the beam strength of the outer legs.

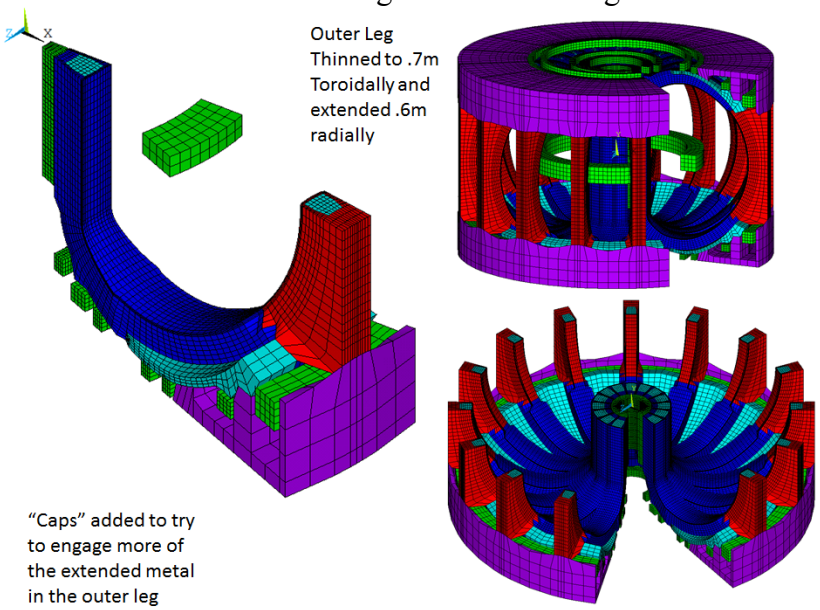

Figure 8 FNSF Analysis Model

The model in figure 8 represents a model in which the outer leg was "thinned to accommodate core component extraction but not "flared. A "cap" was added to help stiffen the ends of the outer leg reinforcement.

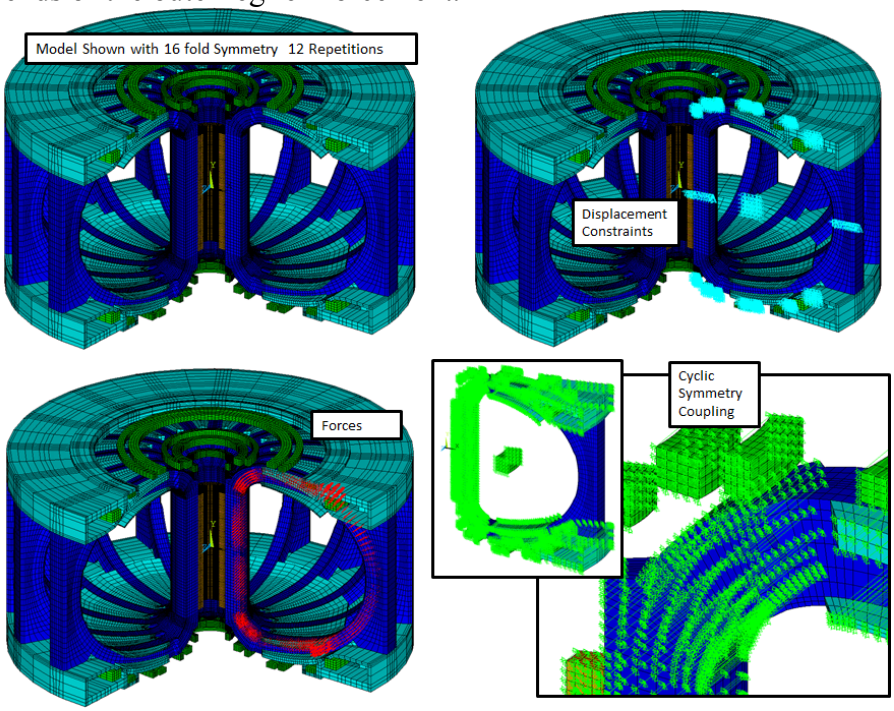

Figure 9 FNSF Analysis Model

Design Input

The geometric data were originally derived from Mark Tillack's systems analysis shown in figure 1. These were replaced with C. Kessel's more detailed plasma equilibrium analysis were used for current and field data. Stress Criteria are from the ITER Magnet Structural Design Criteria, and the NSTX structural design criteria. A pilot plant is expected to operate near steady state rather than experiencing multiple pulses as in an experimental machine such as ITER. This means that the stress requirements are dominated by static stress limits. This relieves many of the constraints on design of local details. Sharper corners are less of a concern. Flaws in materials are not as critical and more practical quality and NDE requirements may be used. This shifts the design problem from design for fatigue to designing to support the extremely large but essentially static magnetic loads.

TF Inner Leg Stress

A reasonable expected yield strength of 316 stainless steel is 1000 MPa at 4 K. The allowable primary membrane stress is then 2/3 of this or 666 MPa. In earlier evolutions of the FNSF, the stress in the inner leg was over 800 MPa but with some later adjustments in build, the stresses have been improved.

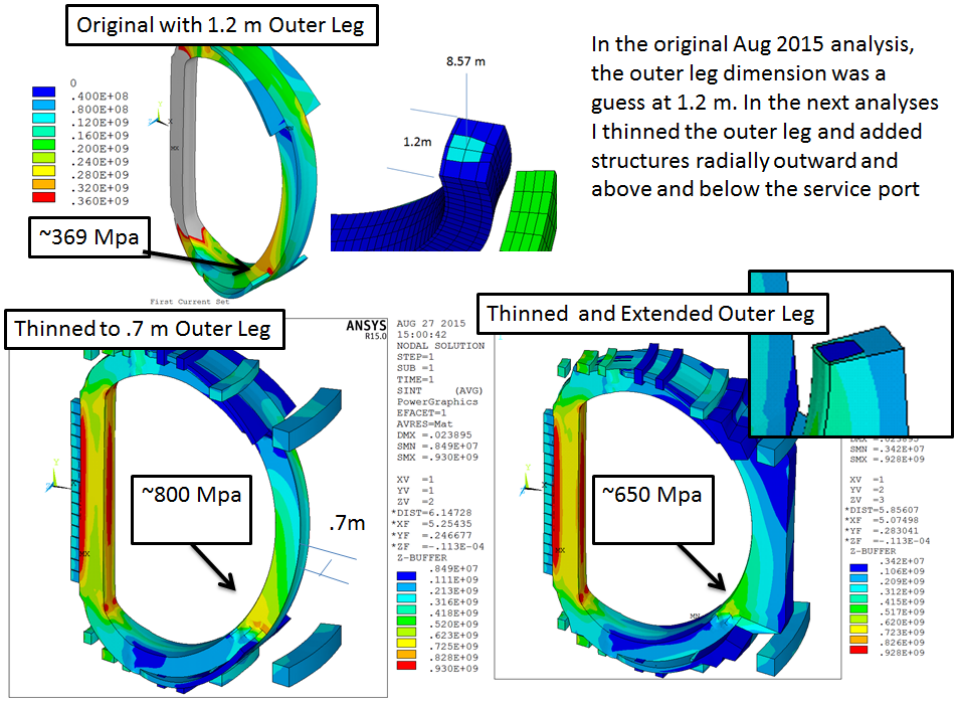

Figure 10 First attempt at computing stresses in the FNSF TF Coil Case

Corrections to the model included an increase in the TF field to 7.5 T, increase in the TF inner leg radial build to 1.06 m, increases in the outer leg radius to facilitate the radial extraction of core components, and a "flare" in the geometry of the outer leg cross

section, taking advantage of the full space envelope available from the needed radial extraction clearance. The stress results are shown in Figure 11.

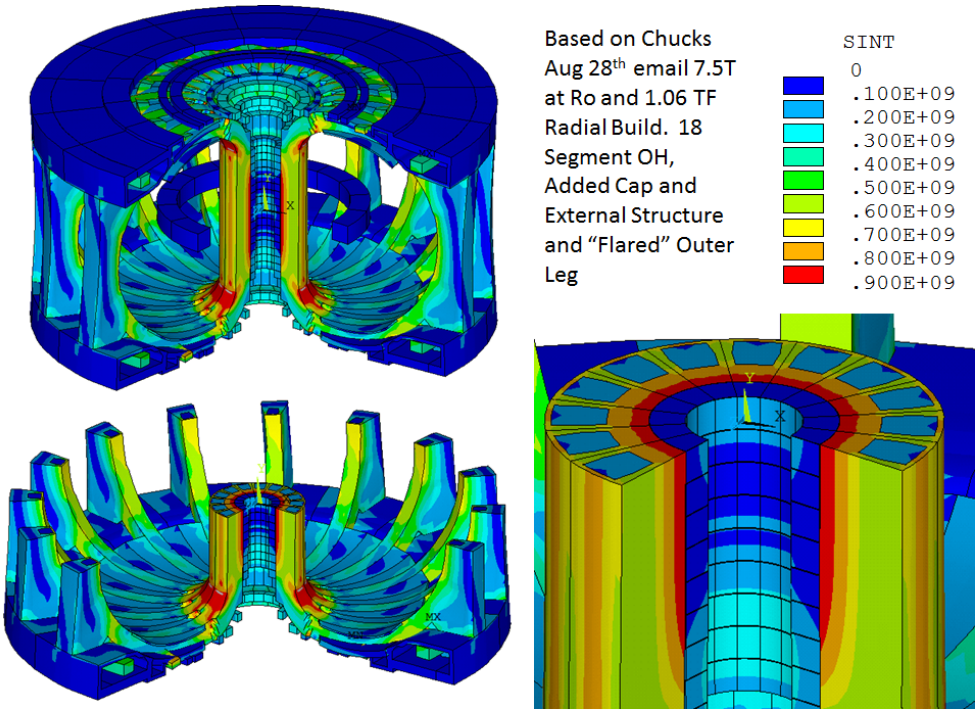

Figure 11 Inner Leg Stress Results

Inner Leg Stress is still a bit too high. The contour boundary mid build of the nose region would represent the primary membrane stress and is about 800 MPa. 666 Mpa is the usual allowable for ITER grade 316 stainless steel. Some modest reallocation of metal cross sections may still be needed. Improved yield stainless steels are an option. Limit analysis has been used to qualify this level of stress by showing a factor of safety of 2.0 against burst over the design loads. This has been explored in the context of the KDEMO reactor. The ITER magnet structural design criteria discusses this method of stress decomposition, i.e. identification of the primary membrane stress from the complex stress field in a finite element analysis. More steel with less space for conductor may be possible with high temperature superconductors(HTS) . REBCO HTS are thin layers of HTS coated HASTELLOY tapes in which the steel tapes make up most of the cross section . If the reactor is truly steady state or very long pulse, Solid Non-CICC Nb3Sn cable in channel conductor could be an option.

HTS Structural Solutions to the Stress Issue

Cable in Conduit(CICC) uses strands that, after reaction, are very weak. High temperature superconductors are being investigated as a means to increase the current density and to add structure to the inner leg. Stacked REPCO tapes are nearly 100% Hastalloy or other stainless steel. If twisted solutions can be avoided by employing slow ramp rates and flux swings, conductors with less void space can be used.

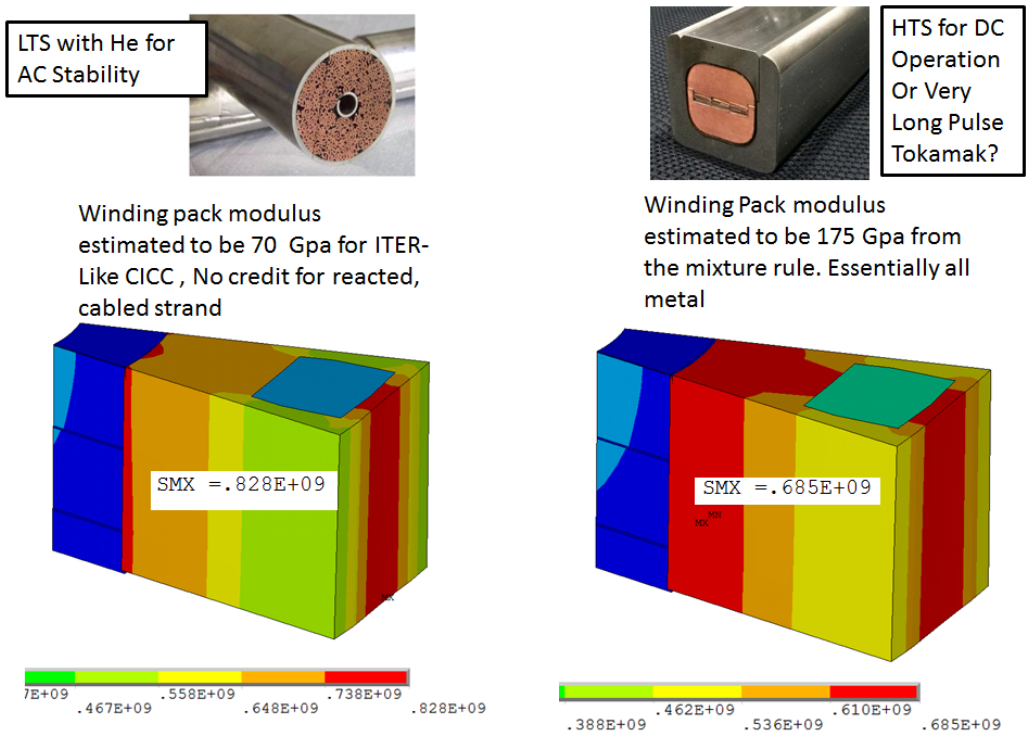

Figure 12 Effects of Metal Fraction Within the Winding Pack

A conductor proposed for a next generation Large Helical Device includes a substantial percentage of copper, which, depending on the state of anneal could contribute to the structure of the winding pack. With a conductor like this, the effective modulus of the winding pack will contribute to the structure more significantly than the present CICC technology. Figure 12 shows 140 MPa improvement in the stress of the case material if a conductor with significant structural capability is used.

TF Corner Stress

The FNSF does not use a constant tension D shape. This is done to allow PF coils to be closer to the plasma. This approach was first used in the ARIES RS studies where small deviations in the D shape provided better plasma shaping and more reasonable PF coil currents, and didn't degrade the TF stress unacceptably. In the present version of the FNSF, the inner corner radius was made relatively small to accommodate the blanket and PF coil geometry. This corresponds to a stress concentration at the corner bend that results from the sharp transition in curvature of the coil from the straight leg to the horizontal leg. This was exaggerated in Mark Tillack's systems code rendition of the coil and a radius was arbitrarily chosen to replace the sharp corner, but the bend radius is still too sharp. Some portion of this will cycle. This is discussed under "Cyclic Life" The primary membrane stress in the nose of the coil is around 800 MPa – larger than the allowable of 666 MPa. Similar stresses have been found in other next generation machines like KDEMO and an upgraded version of CFETR. For KDEMO, it is argued that a better grade of 316 (better than the ITER grade) will have higher yield and tensile stresses. Also limit analysis is performed to show that the structural capacity of the conventional 316 still has ample margin (>a factor of 2 on burst)

Carrying the Machine Torque in the Outer Leg

This is a critical evaluation of the FNSF structure. The Radial servicing logic relies on a larfe opening between the outer legs to extract the core components. In most other next generation machines, this space is taken up by torque structures. Many competing next generation machines use vertical servicing through openings between the horizontal legs of the TF coils. KDEMO is an example. Global machine torques can be carried by outer structures while still allowing radial servicing. In the case of the FNSF, the vertical span of the outer leg must be stiff and strong enough to carry the global torque as beam elements connecting upper and lower structures.

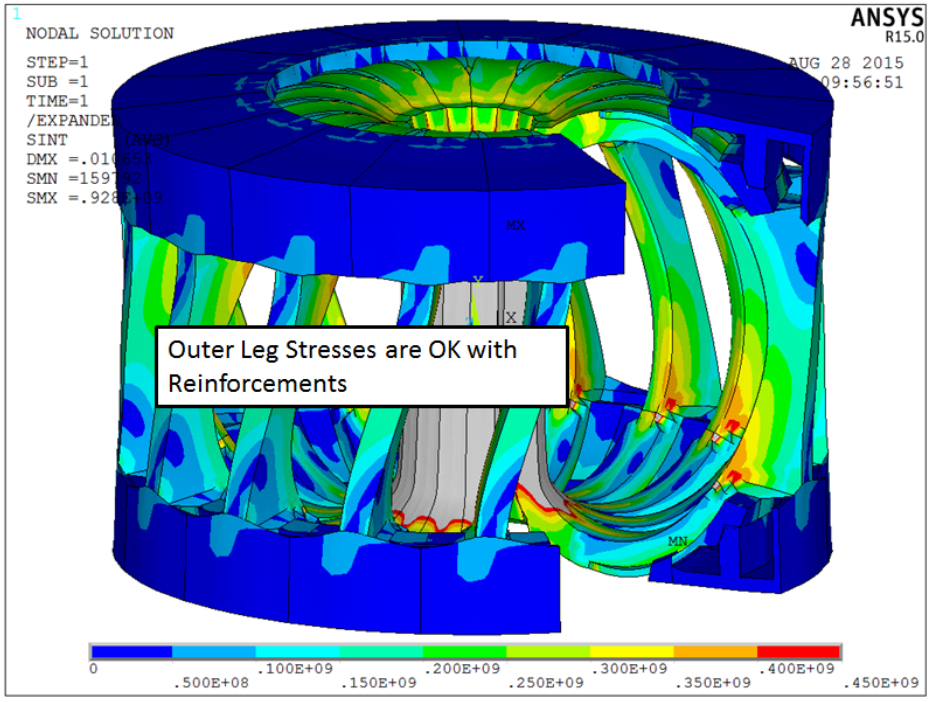

Figure 13 Tresca Stress in the outer legs of the US-FNSF

Carrying the Inner Leg Torsional Shear

Torsion in the inner leg is carried by interconnections between the inner legs that form a large torque cylinder. The inner legs carry the local torques from interactions principally with the OH coil radial fields. For wedged coils, the frictional capacity ideally would be sufficient to support torsional shear. For most tokamaks the radially outward loads from the horizontal legs "de-wedge" the corners, and as with ITER, some additional banding can be used to pull in the corners. Also, as with ITER, keys can lock the coil cases together . For the FNSF wedge pressure at the nose of the TF

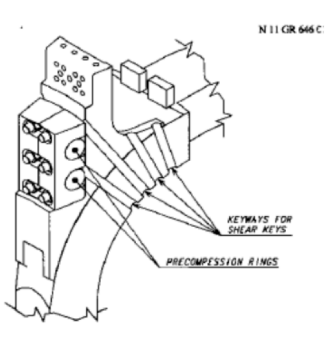

Figure 14 Inner Corner Shear Keys

is ample to take the inner leg torsion with friction

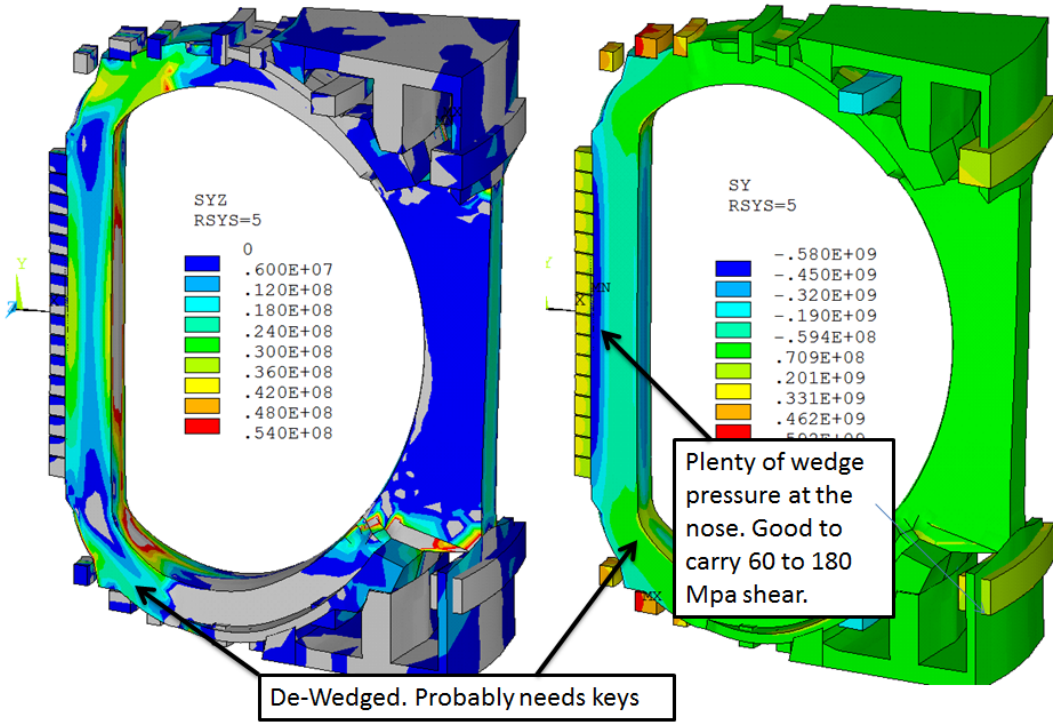

Figure 15 Torsional Shear (Left) Hoop Compression (Right)

Cyclic Life

The Next generation reactors are expected to be long pulse machines, if not steady state. However the Fusion Nuclear Science Facility goes through many upgrades between relatively long operational periods. Some modest cyclic loading will be experienced by the magnet systems.

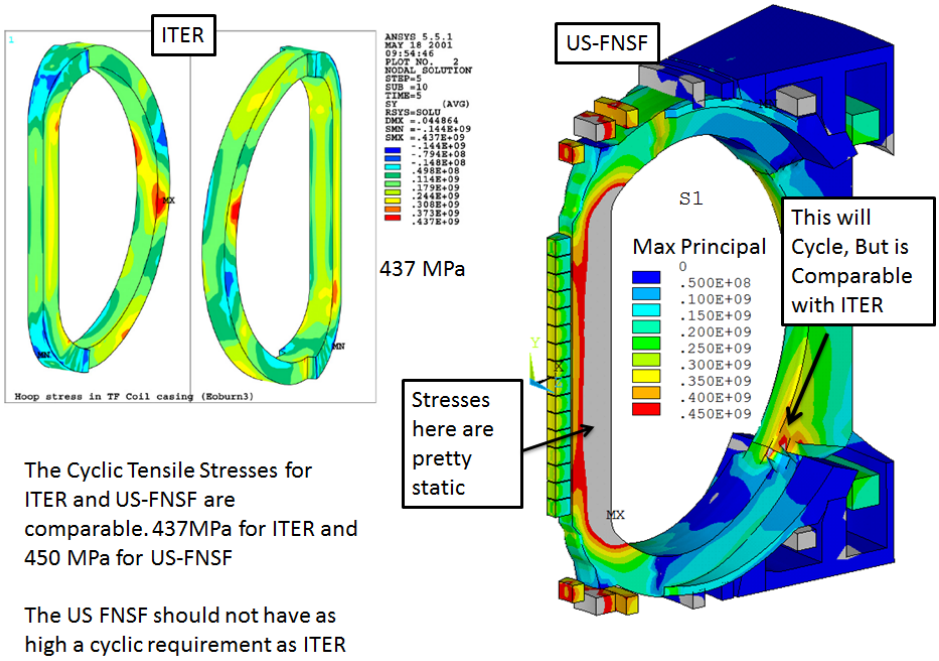

Figure 16 TF Out-of-Plane Cyclic Bending

The out of plane loading that imposes bending on the outboard leg is cyclic, but the FNSF has many fewer design cycles expected for the life of the plant than ITER and other experimental devices. By it's nature to obtain significant fluences, pulses must be long It has been estimated from the present FNSF program, approximately 700 DT shots, and probably another 500 He/H and DD shots would be experienced by the reactor in its design life.

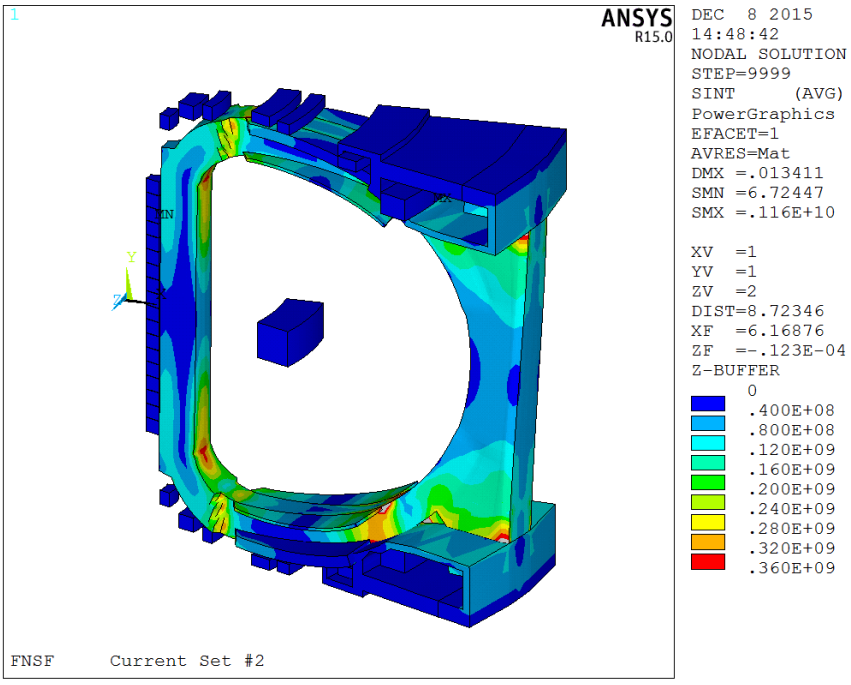

Figure 17 Stress Difference between the TFON and the TFON+PF load case

Figure 17 is a "difference plot" of the TFON+PF load minus the TFON load case. This is a measure of the cyclic stress. Depending on how the OH is "swung" this could be an alternating stress magnitude or a stress range. This is comparable in magnitude with ITER. As expected, the red zones are in the outer leg, but there are also red zones in the inner leg corners. These are predominantly alternating shear stresses from the global twist of the tokamak

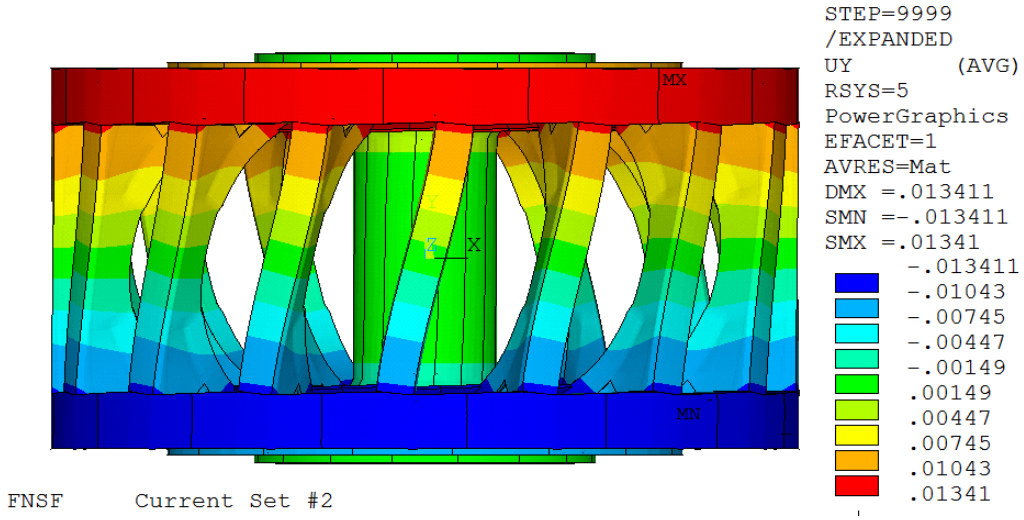

Figure 18 Global Twist of the Machine, Displacement(in meter) Difference between TFON+PF and TFON Only

Figure 18 shows an exaggerated displaced plot of the OOP displacements of the tokamak. The twisting load is mostly supported by outer structures, but the inner leg central column also reacts the twist. The corner stress peaks in Figure 16 are replotted below as shear stresses.

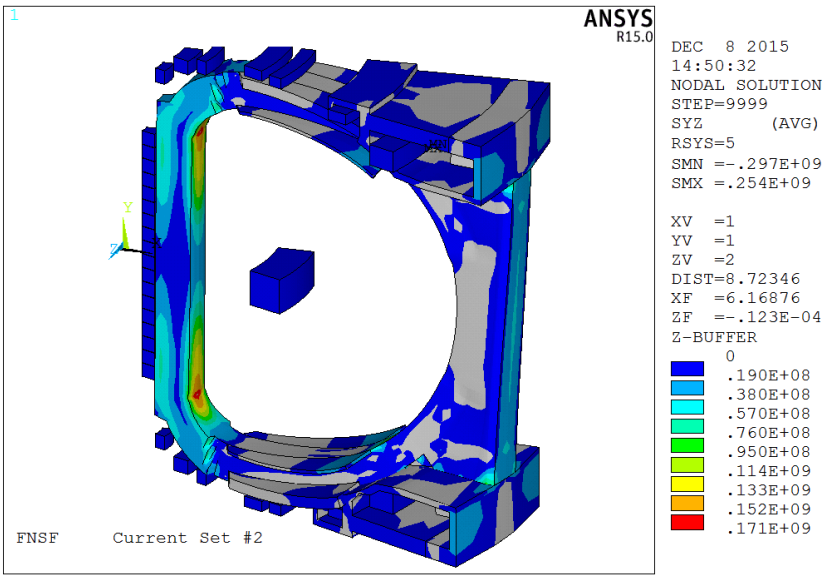

Figure 19 Displacement Difference between TFON+PF and TFON Only –Bending Shear at the Ends of the Inner Legs

TF Fields

This is primarily a structural evaluation but the fields are computed for the Lorentz forces. The local peak field is calculated to be 17.324 T at the inner upper and lower corners. The results are mesh dependent, particulary near the locally sharp radii

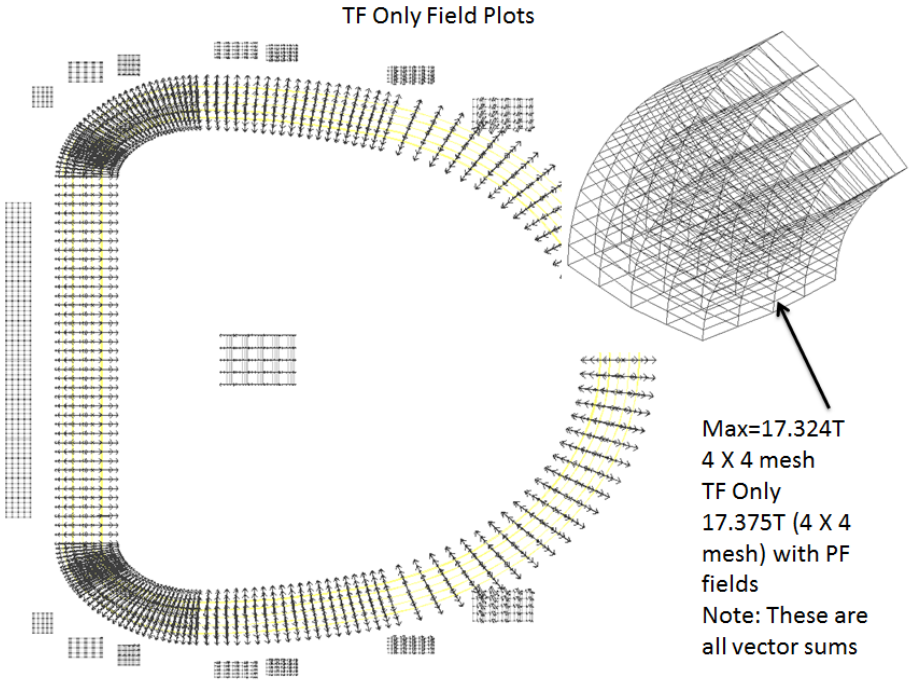

Figure 20 Local Peak TF Field

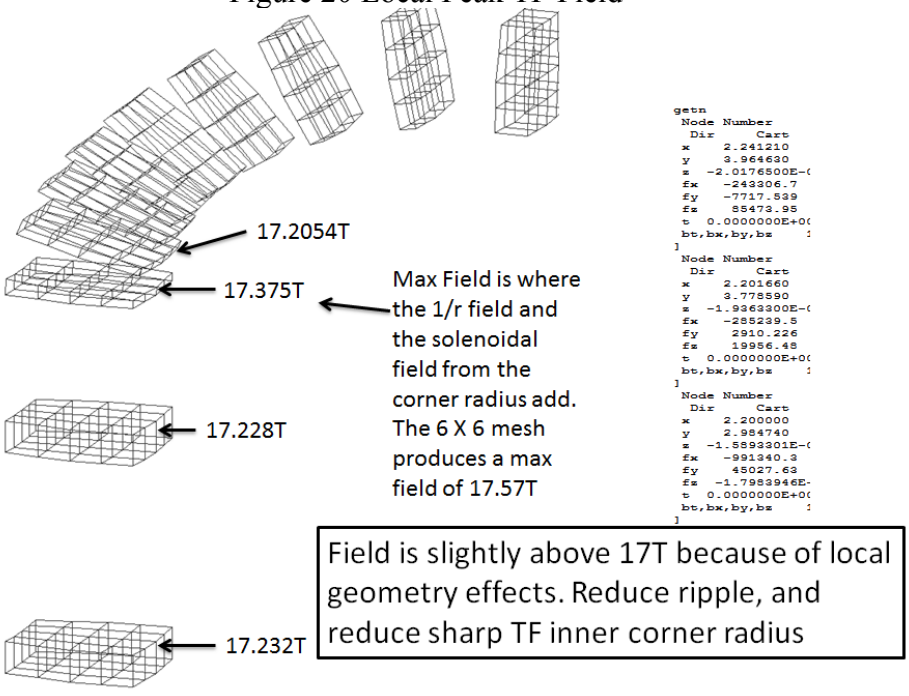

Figure 21 More TF Local Peak Fields

PF Coil Evaluation

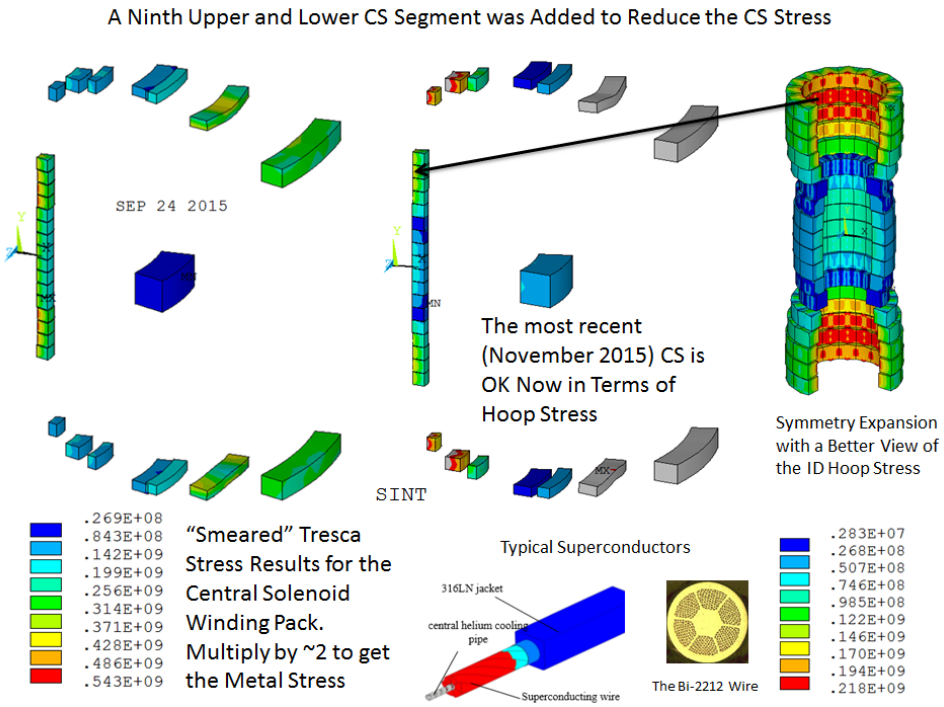

Figure 22 Central Solenoid and PF Stresses

The Central Solenoid (CS) went through a couple of iterations to find an acceptable stress solution. Typical Low Temperature Superconductors (LTS) and HighTemp Superconductors in pulses applications require some jacket for structure and for coolant containment The contoured stresses shown above are "smeared" and a multiplier based on the metal fraction needs to be applied. For the ITER conductor, the multiplier is ~2.0, so the original stress of 543 MPa would translate to 1086 MPa – well above the 450 MPa representative of the jacket stress currently qualified for the ITER CS conductor in fatigue. The PF system was reconfigured and a coil segment added above and below the CS stack.

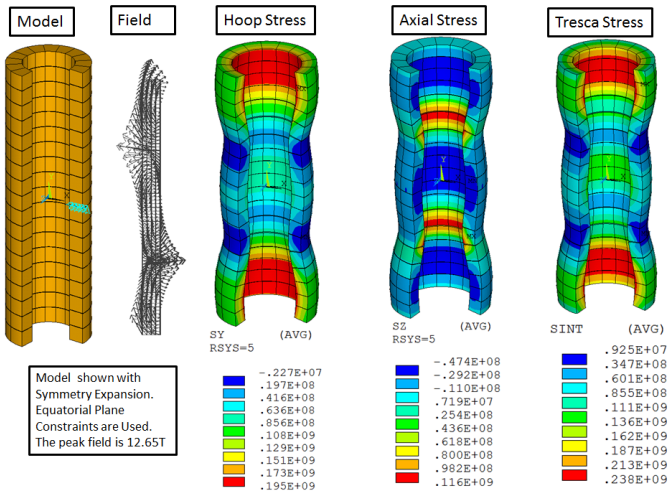

Figure 23 CS Stress Components for the November 2015 Configuration and Currents

The November 2015 iteration of PF coils and currents is adequate. Individual stress components of the Central Solenoid are acceptable as well as the peak field. The vertical tension shown due to the "hour glass" shape of the coil would mean that there would be some separation of the modules at the ID and possibly a need for some central tierod like mechanism.

Conclusion

With the added radial structure and added structure above and below the horizontal port, the outer leg TF stress is similar to that which was qualified cyclically for ITER (in its inner leg). The FNSF should have less restrictive fatigue requirements. The important conclusion is that RADIAL SERVICING STRESSES OUT
Inner leg torsional shear will need features like ITER. Shear keys in the corner and possibly corner tensioned rings.
Inner Leg Stress is still a bit too high Some modest reallocation of metal cross sections may still be needed. Improved yield stainless steels are an option. More steel with less space for conductor may be possible with HTS. If the reactor is truly steady state or very long pulse, Solid Non-CICC Nb3Sn cable in channel conductor could be an option

6-j. Lead-Lithium Thermofluids Analysis *(S. Smolentsev, UCLA)*

The MHD thermofluids studies for the DCLL blanket include: (1) the MHD analysis aimed at evaluation of the pressure drop in the blanket and the pressure distribution along the PbLi flow path, (2) heat transfer analysis to calculate the temperature distribution in the PbLi and in the ferritic walls and FCIs, and (3) mass transfer analysis to address corrosion losses of the RAFM walls in the flowing PbLi. When doing these analyses, one should compare obtained results for the pressure, temperature and the mass loss with the limiting numbers evaluated earlier in the blanket studies in the US and worldwide.
In the BCSS studies (1981) in the US, the maximum MHD pressure drop was limited to 2 MPa. Based on recent blanket studies, it seems to be reasonable to expand this limit to 4 MPa (Malang). The temperature limit at the interface between the RAFM wall and PbLi of 470°C was also suggested in the BCSS studies. The associated mass loss limit (wall thinning) is 20 μm/yr. A more recent criterion for the wall thinning is the maximum thinning of 10% of the wall thickness over the entire blanket operation (Malang). The temperature drop across the SiC FCI should be limited to ~200 K to (for 5-mm FCI) because of the thermal stress limitations.
In 2015, the studies in the MHD thermofluids area for the FNSF DCLL blanket were limited to the MHD analysis for the IB region, where the magnetic field is around 10 T resulting in a high MHD pressure drop. In the reference IB blanket design sketched in Fig. 1, PbLi enters the blanket at the bottom through the inlet manifold and is distributed into 5 poloidal front rectangular ducts where it flows upwards. At the top it makes a 180° turn and flows downwards through the 5 rear ducts. At the bottom, PbLi leaves the module through the outlet manifold.

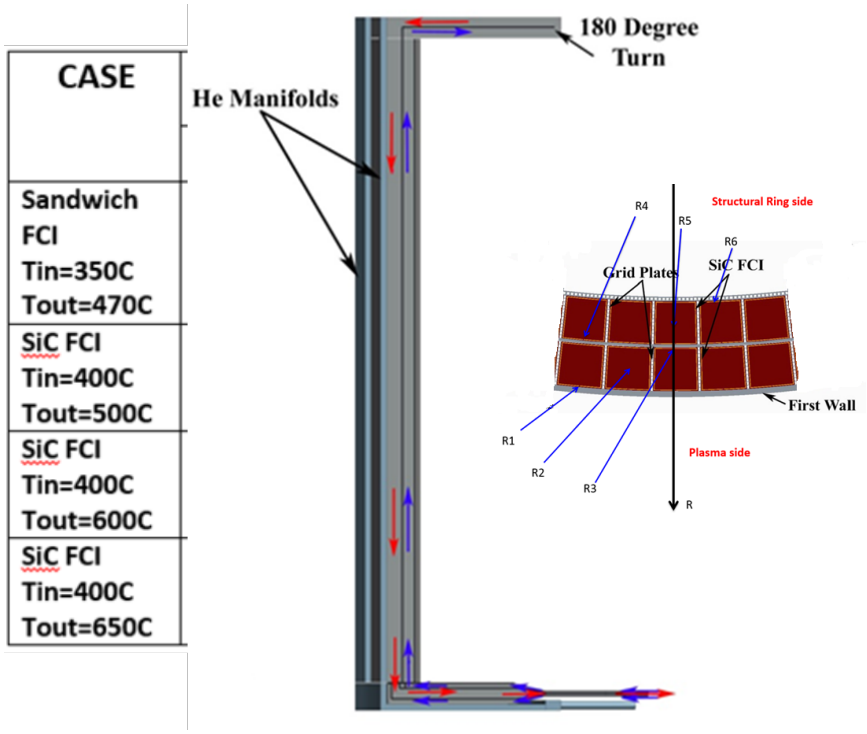

Figure 1. PbLi flow path in the DCLL IB blanket.

Both the LT blanket option with the sandwich (steel-alumina-steel) FCI and HT DCLL blanket were considered as also shown in Fig. 1.

In the analysis, the following data and assumptions were employed:

- Each IB blanket module has 5 front and 5 back rectangular ducts. Pbli flows upwards in the front ducts facing the plasma and downwards in the back ducts.
- Each poloidal duct has the toroidal width of 250 mm (228 mm PbLi bulk flow + 2x5=10 mm FCI + 2x2=4 mm PbLi gap + 2x4=8 mm RAFM wall = 250 mm) and the radial depth of 215 mm (193 mm PbLi bulk flow + 2x5=10 mm FCI + 2x2=4 mm PbLi gap + 2x4=8 mm RAFM wall = 215 mm).
- The thickness of the RAFM wall is 4 mm.
- The poloidal length from top to bottom (along the flow path) is 10 m.
- The FCI is 5 mm thick.
- A sandwich FCI has 3 mm steel (gap side)+1.5 mm (alumina) +0.5 mm (bulk flow side).
- The averaged NWL over the IB region is 1.4 MW/m2 (peak value) times 0.7=0.98 MW/m2.
- The magnetic field in the IB region is 10 T.
- There are two co-axial access pipes. “Cold” PbLi flows in through the concentric gap, while the “hot” PbLi flows out through the inner pipe. The inner and outer pipes both have an FCI.
- For simplicity, in the MHD analysis, instead of the co-axial pipes, two separate pipes (D=10 cm) are considered.
- The length of the access pipes is 6.5 m.

The following blanket components have been identified, for which calculations of the MHD pressure drop ware performed using either empirical correlations and analytical solutions or numerical computations:

- Poloidal flow in a rectangular duct with FCI (numerical code),
- Flow in the insulating inlet/outlet manifold (correlation),
- Flow in access pipes with FCI in a uniform B-field (analytical solution),
- Flow in access pipes with FCI in a fringing B-field (correlation),
- 180 degree turn at the top of the module in the plane perpendicular to B-field (numerical code).

At this moment, three possible approaches to the manifold are under consideration. In option A, the flow starts with a single pipe, followed by an expansion region, followed by a set of parallel ducts. Option B involves branching of pipes from one to two, to four, and then to eight. Each branch point could be made symmetric. This would lead to symmetric flows. Option C is based on single feeding pipes for each blanket module. This results in a set of feeding pipes running through the vacuum vessel. In this way, the manifold is moved outside the magnetic field, resulting possibly in a lower pressure drop. In this analysis for the manifold, we limit our investigations of the MHD pressure drop to option A (classical manifold).
The results of the MHD computations are summarized in Table I for all LT and HT DCLL blanket options.

Using these results, the following conclusions have been made.

- The LT DCLL with sandwich FCI has an unacceptably high MHD pressure drop of ~ 6 MPa. There can be several ways to reduce this pressure drop, such as: (1) to make the steel layer of the sandwich FCI thinner and (2) to design a low pressure drop manifold.
- The two HT DCLL designs (Delta P of 2 and 1.5 MPa) are both acceptable from the point of view of the MHD pressure drop.
- The one that has Delta P of ~4 MPa may be also acceptable but verifying stress calculations are needed.
- The manifold (option A) is the main contributor into the total MHD pressure drop. This means that it has to be designed carefully and also analyzed properly. In this first analysis, an approximate correlation was used, which may not be accurate enough. It might be reasonable to look at options B (branching) and C (single feeding pipe).
- Hydrostatic pressure is not included and the pressure losses in the ancillary system are not included either. In stress calculations, these pressure losses should be calculated and added to the MHD pressure drop to evaluate the pressure distribution in the PbLi.
- This MHD analysis alone is not sufficient to select a proper DCLL design. More analysis needed, including heat transfer and corrosion.

Table I. Summary of computations of the MHD pressure drop for DCLL blanket in the FNSF.

CASE	DELTA P, MPa				
	Poloidal duct	Inlet/outlet manifold	Inlet/outlet pipe	Pipe through fringing B-field	TOTAL
Sandwich FCI Tin=350C Tout=470C	2.67	2x0.98=1.96	2x0.1=0.2	2x0.57=1.14	**5.97**
SiC FCI Tin=400C Tout=500C	0.194	2x1.18=2.36	2x0.04=0.08	2x0.67=1.34	**3.97**
SiC FCI Tin=400C Tout=600C	0.097	2x0.59=1.18	2x0.02=0.04	2x0.35=0.70	**2.02**
SiC FCI Tin=400C Tout=650C	0.078	2x0.44=0.88	2x0.01=0.02	2x0.28=0.56	**1.54**

6-k. Thermomechanical Analysis of PFCs and Electromagnetic Effects of Disruptions

(James Blanchard and Carl Martin, Univ of Wisconsin)

Thermomechanical Analyses

We have been carrying out a series of analyses of the plasma facing components in the FNSF in order to address a variety of thermomechanical issues, including allowable heat loads, design optimization, and component lifetime. Loading includes coolant pressure, volumetric heating, steady surface heating, and transient heating due to both ELMS (anticipated) and disruptions (unanticipated). The analysis includes heat transfer, mechanical effects (stress, strain, and displacement), thermal creep, and fracture. Failure criteria considered include melting, excessive stress or strain as defined by existing design codes, creep rupture, mechanisms considered through a design by analysis approach (such as ratcheting), and fracture (using integral approaches). All analysis is carried out using ANSYS, a commercial finite element code.

For steady loading, we model an ARIES-style plate divertor using ARIES-level heat loads from a recent paper (Kessel, et al, "The evaluation of the heat loading from steady, transient and off-normal conditions in ARIES power plants," Fusion Sci Technol, 64, 440, 2013). The design is pictured below:

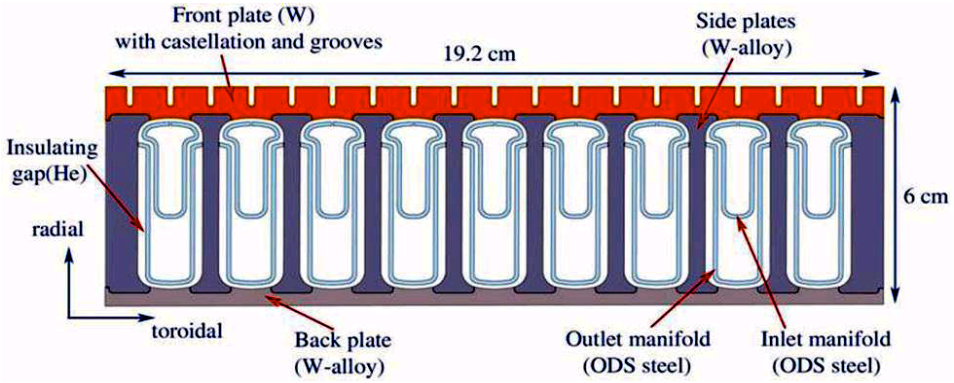

The key loads are a coolant pressure of 10 MPa and a surface heating of 11 MW/m^2. The peak temperature in the structure is found to be 1961 C (for a bulk coolant temperature of 600 C). Fracture analysis indicates that stress-intensity factors for reasonable sized cracks are on the order of known fracture toughness values for tungsten at the temperatures of interest. This indicates that knowledge of the toughness of future alloys or tungsten preparations will be critical for component validation. Creep rupture was also shown to be a potential failure mechanism for these designs and designs updated for the FNSF will have to account for it.

The first wall considered here is also ARIES-style, with a steel structure that may have a surface coating of tungsten. The steady loads here include a coolant pressure of 8 MPa and a surface heating of 0.28 MW/m^2. In this case, the peak temperature is 480 C for a bulk coolant temperature of 436 C. Stresses in this structure are quite low relative to the yield stress expected for fusion-grade, low activation steels. Fracture was not considered due to the high ductility of these alloys.

ELM loads considered in the divertor and first wall featured steady heat loads of 9.5 and 0.28 MW/m^2, respectively, with superimposed pulses of at least 1,100 and 23 MW/m^2 peak heat fluxes for 1.3 ms due to an ELM. The ELM frequency was considered parametrically. All default cases for these conditions produced melting in the divertor. The combinations of steady and pulsed heat fluxes that will just melt are shown below.

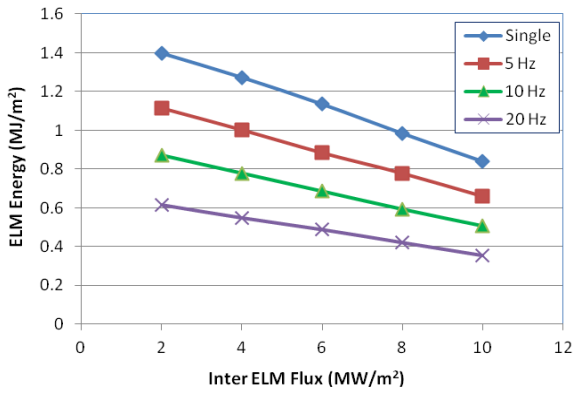

The ELM loading on the first wall did not produce melting. Hence, it appears that the first wall of an ARIES class device can withstand ELMS without melting. Further work is required to assess the fatigue behavior of these components.

The transient heat fluxes on the divertor and first wall resulting from a disruption are estimated to be at least 6,000 and 220 MW/m^2, respectively. Pulse durations are assumed to be 8 ms for disruptions. Melting will occur in the divertor under such conditions. Melting of a bare first wall will occur, but can be prevented with a tungsten coating, as shown below.

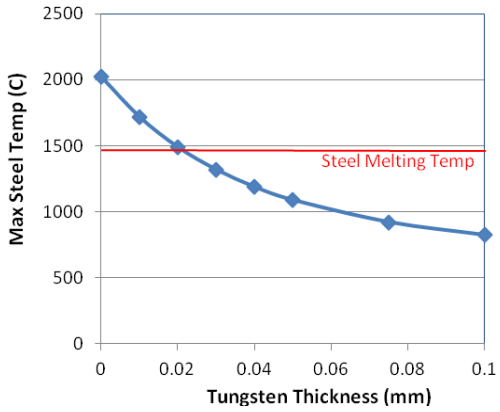

Electromagnetic Effects of Disruptions

For these simulations, the plasma current was assumed to decay linearly over a 30 ms time period. The components modeled are shown below.

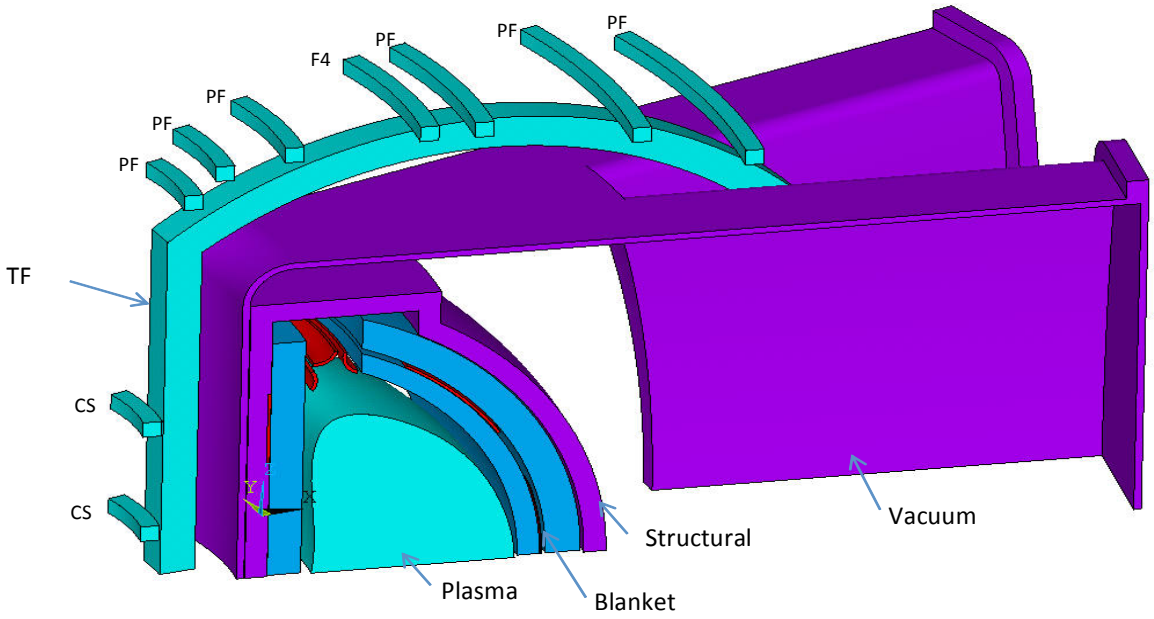

The model predicts all currents induced in these structures, along with the associated forces. Equivalent pressures on these components, resulting from a static plasma quench, are as follows:

- Inboard of structural ring: 2.6 MPa
- Inboard of vacuum vessel: 0.67 MPa

Resulting stresses in the vacuum vessel peak at approximately 35 MPa. Loading of the divertor results from eddy currents, so there are overturning moments, along with local pressures and net forces. Efforts to characterize these divertor loads are under way.

Future Work

1. All component geometries and loads will be updated to be consistent with our current FNSF design.
2. All thermomechanical and disruption calculations will be repeated with these new geometries and loads.
3. Ferromagnetic loads on all ferritic steel components will be assessed.
4. Disruption simulations will be updated to consider VDEs.

Publications (FNSF and Related Manuscripts)

1. JP Blanchard and CJ Martin, “Thermomechanical Analysis of Tungsten Plasma-Facing Components Under Transient Loading,” submitted to IEEE for SOFE Proceedings.
2. HH Toudeshki, CJ Martin, F Najmabadi, and JP Blanchard, “ARIES ACT-1 Vacuum Vessel Design and Disruption Analysis,” Fus Sci Tech, 68, 2015, 535.
3. JP Blanchard and CJ Martin, “Thermomechanical Analysis for an All-Tungsten ARIES Divertor,” Fus Sci Tech, 67, 2015, 158.

6-l. Examination of Activities in FNSF Operation Phases *(K. Young and C. Kessel, PPPL)*

The activities during the operational phases of the FNSF are being examined in order to provide better constraints on time frames required for plasma operation functions and maintenance functions. Below are a sample of tables used to assess Phase 2 (DD plasma operations), Phase 2-3 transition, and Phase 3 (DT plasma operations). Plasma shot allocations are used to determine credibility reaching goals and to track the neutron fluence (dpa). In particular, developing the very long plasma pulse lengths in Phase 3 is being considered, by laying out the shot sequences to reach this goal. The overall program time frames can be compressed if this could be achieved.

Table 1: Activity during Phase 2 operation (DD nuclear operation: (> $1x10^{26}$ 2.4 MeV neutrons, plenty 14 MeV neutrons)

Activity during Phase 2	**Approx. # of shots**	**Time (weeks)**
Bring operational capability in D-D to performance with H/He scenarios	50	5
Develop operating scenario leading to long-pulse capability (< 10^5s)	100	23
Develop plasma operational scenarios with different heating systems for long pulse (< $3x10^5$s). Optimize heating.	80	25
Evaluate divertor operational techniques		Con
Fully evaluate diagnostic operation		Con
Develop plasma control scenarios	30	15
Evaluate disruptions/disruption mitigation technique(s)	50	10
Evaluation of first-wall and divertor monitoring system		Con
Operation of tritium-handling system		Con
Check-out of dust monitoring equipment		Con
Check-out operation of initial blankets		Con
Short vacuum opening/change-out for handling dust/material samples etc.		12
Demonstration of relevant shielding and safety monitoring (Regulatory)		Con
Total Time Allocated (weeks, including maintenance periods)		90

Assume 8 hour pulse established in He/H phase

12 hour pulse, 20 shots
16 hour pulse, 20 shots
20 hour pulse, 20 shots
24 hour pulse, 20 shots
28 hour pulse, 20 shots

_____
2000 hrs 100 shots
83.3 days (vs 23 weeks or 161 days, OK)

34 hour pulse, 10 shots
44 hour pulse, 10 shots
54 hour pulse, 10 shots
64 hour pulse, 10 shots
74 hour pulse, 10 shots
84 hour pulse, 10 shots (~3.5 day long pulse)

_____
3540 hrs 60 shots
147.5 days (vs 25 weeks or 175 days, OK)

assume we want to reach 10 days long pulses
5 day pulse, 10 shots
10 day pulse, 10 shots

_____
150 days 20 shots
21.4 additional weeks

Table 2: Activity during D-D change-out period

Activity during vacuum opening during D-D phase
All in-vessel work by remote handling/inspection
Inspection of all in-vessel services/ replace as needed
Handle dust and material samples for external evaluation
Possibly change a divertor segment, test blanket module or diagnostic port plug
Maintain/replace diagnostic components
Evaluate test blanket module
Maintain heating/CD systems
Routine maintenance/upgrading of all external systems
Allocated time: ~ 12 weeks

Table 3: Activity during Phase 2 – Phase 3 Preparation Phase (shutdown pre-DT operation)

Activity during phase 2 – phase 3 Preparation Phase
Most in-vessel work by remote handling/inspection
Post-run calibration of diagnostics
Examination of all interior surfaces/replace if necessary
Full check-out of remote inspection system
Ex-vessel analyses of in-vessel surfaces and dust
Remove/replace divertors
Maintain all electrical, pumping systems, etc.
Check-out all (non-diagnostic) monitoring equipment

Replace diagnostics as necessary
Full check-out/analysis of gas-handling/fueling systems
Enhancement of in-situ blanket systems
Partially reduce heating/CD systems; refurbish as needed
Reduce some of diagnostic set
Enhance blanket modules to fill available locations; replace blanket sectors/ TBMs with DT appropriate systems
Finalize fueling, disruption-mitigation etc. hardware
Ensure total tritium compatibility of all systems
Implementation of full relevant shielding
Full in-vessel calibration of diagnostics
Obtain regulatory approval for D-T operation
Allocated time: 52 weeks

Table 4: Activity during Phase 3 (early DT operation)

Activity during Phase 3	**Approx. # of shots**	**Time (weeks)**
Bring tokamak operations to full capability of phase 2	30	3
Initial operational testing with long-pulse DD and trace T	15	2
Operate short-pulse full D-T	30	5
Developing scenarios for reaching and controlling at N_W = 1.5 MW/m^2	50	20
Operation to extend pulse lengths at N_W = 1.5 MW/m^2 (>1x10^6 s)	30	50
Demonstration of operation without disruptions and/or continuation through disruption with amelioration system	20	10
Vacuum opening for engineering change-outs (at ~ 2 dpa)		12
Extend operation to wall-loading ~ 7 dpa	20	30
Monitoring of 1st wall and divertors		Con.
Determination of necessary heating/CD systems for final control		Con.
Testing to determine set of diagnostics necessary for control and protection		Con.
Demonstration of tritium system regeneration		Con.
Demonstration of blanket performance		Con.
Demonstration of all safety systems		Con.
Total Time Allocated (weeks, including maintenance periods)		122

Begin with small tritium fraction added to DD discharges
1 day pulse, 20 shots
5 days pulse, 10 shots
10 days pulse, 3 shots

_____
100 days 33 shots

14.3 weeks

full DT with Nw(peak) = 1.5 MW/m2
1 hour pulse, 20 shots
5 hour pulse, 20 shots
10 hour pulse, 20 shots
24 hour pulse, 20 shots

_____
33.3 days 80 shots
4.8 weeks (1.37 peak dpa)

full DT with Nw(peak) = 1.5 MW/m2 to full 10 day pulse length
2 day pulse, 20 shots
5 day pulse, 10 shots
10 day pulse, 5 shots

_____
140 days 35 shots
20 weeks (5.75 peak dpa)

→ reached total of 7.12 dpa

6-m. Preliminary Ideal MHD Analysis of FNSF Plasmas *(C. Kessel, PPPL)*

The plasma physics strategy for the FNSF is to guarantee that the facility can reach its mission with the lower beta operating regime, but be capable of taking advantage of operating above the no-wall beta limit at least to some level. This is chosen to address the need for robust plasmas as the pulse duration reaches days to weeks. Meanwhile, this also allows the increase of the neutron wall loading, bootstrap current fraction, operating space, and higher fusion gain, if higher beta's can be reached. In order to take advantage of higher beta operation requires, feedback control of error fields and/or RWM fields, plasma rotation, and or kinetic stabilization via fast particle populations. Ideal MHD analysis is performed using the JSOLVER flux coordinate equilibrium code, the BALMSC high-n ballooning stability code, and PEST1 low-n kink stability code. This is used to identify the no-wall beta limit, and what the impact of a conducting wall could have on this beta limit.

Since the plasma has approximately 50% bootstrap current, the remaining plasma current must be driven by external current drive sources, such as neutral beams (NB), lower hybrid (LH), ion cyclotron fast wave (ICRF), ion cyclotron high harmonic fast wave (HHFW), or electron cyclotron (EC). As a preliminary step, the current profiles that are typical of these sources are mocked up in the JSOLVER code, and added to the self-consistent bootstrap current. The pressure profile is prescribed as a compound parabolic. The beta limit can be found by varying the pressure and adjusting the external current drive so that the total plasma current is fixed to the FNSF operating point value. Shown in Fig. 1 is β_N versus li(1), with the results of the ARIES-ACT2 plasma study in red (no wall beta limit) and green (with wall beta limit), and the FNSF cases. The three cases assume current driven from 1) NB and IC, 2) NB, IC, and LH, and 3) IC, LH and HHFW, which provide peaked, medium, and broad current profiles, respectively. If no wall is assumed the maximum normalized beta is 2.55, 2.47, and 2.6, respectively. If a conducting wall is assumed at the back of the breeding zone in the blanket, then the beta limit rises to the X's (2.8, 2.65, and 2.9, respectively), and if it is placed between the first and second breeding zones, they rise significantly to the pound signs, which range from3.2 to > 3.6.

More generic scans of arbitrary current profiles indicated that those with current concentrated in the plasma center would yield high beta limits even without a wall. These would require considerable on-axis current drive, but were calculated self-consistently with bootstrap current. These and other profiles will be examined, along with those from the time-dependent simulations.

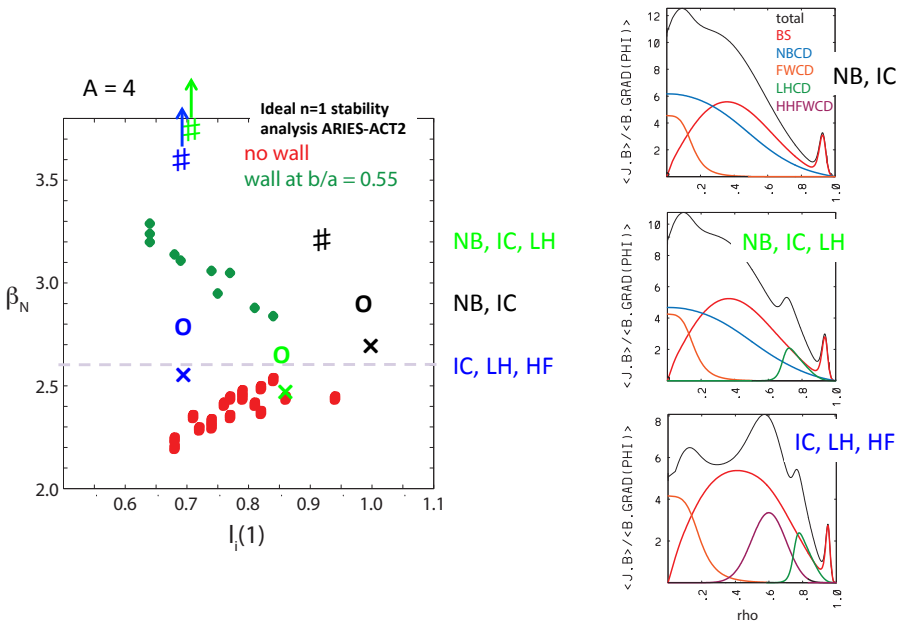

Figure 1. The normalized plasma beta as a function of the plasma internal self-inductance, showing the no-wall and with wall beta limits. The green and red symbols are from the ARIES-ACT2 study, while the X, O, and # are for the FNSF. The parallel current profile and its components are shown at the right.

6-n. Plasma Scrape-Off Layer and Divertor Simulations *(M.E. Rensink and T.D. Rognlien, LLNL)*

1. Divertor plasma solutions and material heat loads

The UEDGE simulations of the SOL and divertor plasma are based on a 2-D mesh created from an MHD equilibrium configuration that is consistent with the FNSF Systems Code point model design for FNSF-2015. Two types of divertor configurations are considered: one has the divertor plates orthogonal to the poloidal magnetic flux surfaces and the second has strongly tilted divertor plates as in the ITER design. Strongly radiating, detached plasmas are found for both cases: a fully detached plasma for the orthogonal divertor plate configuration and a partially detached plasma for the tilted divertor plate configuration. The radiating impurity in these simulations is neon, but any of the noble gases could be used. The fully detached plasma yields lower peak heat flux in steady state than the tilted-plate plasma, so it is an attractive solution, but there are important issues concerning plasma startup and transient heats for the orthogonal plate case. These two types of plasma solutions correspond to those discussed for the larger ACT-1 design [Ref. Rensink, Rognlien, FST **67** (2015) 125], while the results reported here are for the different parameters and size of FNSF-2015.

The ion density at the core boundary 2.4 cm inside the magnetic separatrix at the midplane is 1.0×10^{20} m^{-3}, and the total power into the SOL for the lower half of the double-null configuration is 88 MW. The heat flux width in the SOL at the entrance to the divertor leg is mainly controlled by input parameters (particle and thermal diffusivities) that model anomalous radial transport. These diffusivities are chosen to fit results from present experimental devices and in our FNSF simulations they yield a heat flux width of about 3 millimeters when mapped to the outboard midplane, similar to that expected in ITER.

1a. Fully detached plasma solution

Full plasma detachment means the electron temperature is less than 1 eV over the entire divertor plate. In general, we find that to obtain full plasma detachment, the plates cannot be strongly tilted, so we take the orthogonal plate case as representative of this type of solution. The figure shows contours of the electron temperature in the divertor region, with red indicating temperatures over 100 eV and blue temperatures less than 1 eV. The neon impurity concentration relative to the local hydrogenic ion density is 0.25%. Particle control is achieved via the pumping of neutrals on the surface of the private flux (PF) dome. All other surfaces are 100% recycling. Over 90% of power into the SOL is radiated in the divertor region near the X-point. The peak heat flux on the outer divertor plate is 1.5 MW/m^2, mainly due to impurity and hydrogen line-radiation.

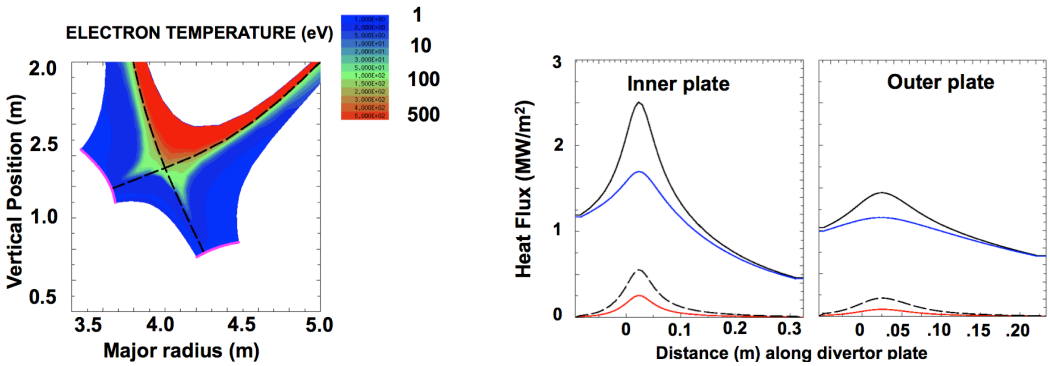

Fig. 1. Electron temperature in divertor region for orthogonal-plate configuration (left) and heat flux profiles on across the divertor plates. Colors correspond to: solid black - total; blue - hydrogen and neon radiation; dashed - plate recombination; and red - plasma

1b. Partially detached plasma solution

Partially detached ITER-like plasma solutions are found for strongly tilted divertor plate configurations. Here the electron temperature is below 1 eV in the PF region and at the strike point on the divertor plates, but is higher in the outer SOL region where the tilted plate and resultant plasma profiles directs recycled neutral particles preferentially toward the strike point. In this case an acceptable solution is found with 0.4% neon impurity concentration and gas puffing into the outer divertor leg to enhance the partial detachment there. The peak heat flux on both divertor plates in this case is about 10 MW/m^2, mainly due to plasma particle heat conduction and convection. The peak heat flux can be adjusted modestly by changing the tilt angle of the plates.

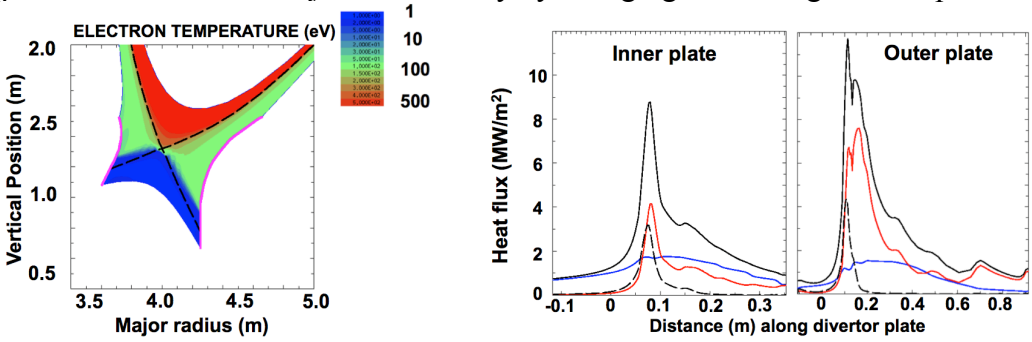

Fig. 2. Electron temperature in divertor region for tilted-plate configuration (left) and heat flux profiles on the divertor plates. Colors correspond to: solid black - total; blue - hydrogen and neon radiation; dashed - plate recombination; and red - plasma kinetic energy.

1c. Impact of divertor leg length

Divertor leg length is important for at least two reasons: (1) long legs take up valuable space in the divertor region which makes the device larger and more expensive and (2) short legs place the ionization front for fully detached plasmas close to the X-point which may degrade core plasma confinement. Plasma simulations for three divertor sizes (leg lengths) indicate that fully detached plasmas can be achieved (Fig. 3).

Peak heat fluxes on the divertor plates are in the 1-3 MW/m^2 range and are mainly due to radiation from the nearby ionization front.

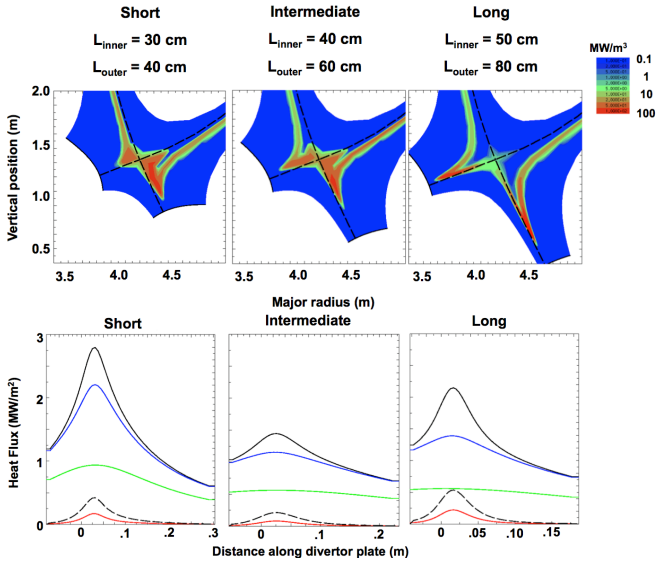

Fig. 3. Electron temperature in the lower divertor for 3 lengths of the inner and outer distance between the X-point and the plate (upper plot). Corresponding heat flux profiles on the outer plate (lower). Colors correspond to: solid black - total; blue - hydrogen and neon radiation; green - neon-only radiation; dashed - plate recombination; and red - plasma kinetic energy.

1d. Impact of impurity concentration

A sequence of simulations in which the impurity concentration is systematically increased shows the expected increase in radiation as demonstrated in Figure 4 and a corresponding decrease in the peak heat flux on the divertor plates. However it also reveals some abrupt changes between attached and detached plasmas. We find that for some range of concentrations there are two possible solutions, one strongly radiating (in red) in which both inboard and outboard divertor plasmas are fully detached and one moderately radiating (in blue) in which the outboard divertor plasma remains attached. These two solutions have identical input parameters, but are accessed via different initial conditions as indicated by the arrows in the Figure below. Similar results were seen in our previous ACT-1 study of divertor plasmas. This behavior can significantly complicate parameter scans and might also indicate possible stability problems for detached plasma states as observed in some existing experimental devices.

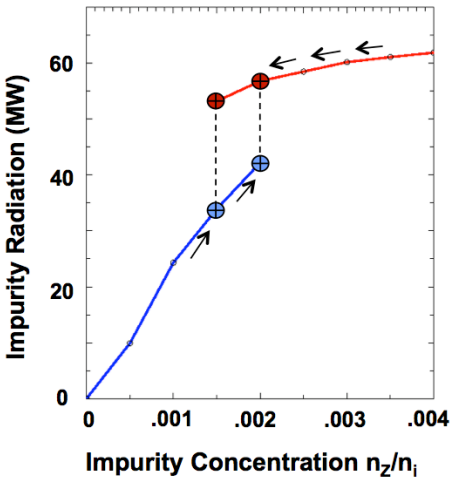

Fig. 4 Neon radiation for various concentrations for orthogonal plate case; input power to SOL is 88 MW. Blue and red lines show two solutions for some concentrations.

2. Related Model Validation

The divertor plasma conditions that give an acceptable heat flux to the divertor plates and side walls shown in Sec. 1 correspond to highly radiating plasmas with very

low electron temperatures (~1 eV) in the region where the magnetic separatrix intersects the divertor-plate. There is presently a strong experimental effort in the national experimental confinement program to obtain and analyze such divertor plasmas. Most recently, the DIII-D tokamak has obtained detailed measurements of the divertor plasma under detached conditions using the divertor Thomson scattering (DTS) diagnostic to accurately measure electron density and temperature [A. McLean et al., JNM **463** (2015) 533; also A. McLean et al., invited presentation VI2.00001, APS-DPP Annual Meeting, Savannah, GA, Nov. 16-20, 2015.].

This experimental data has provided a very important means for validating the basic features of solutions presented in Sec. 1, especially for the case with orthogonal divertor plates. The DIII-D divertor has regions of comparatively low tilted plates on the lower divertor where the DTS measurements are made. A variety of cases have been studied with a focus on cross-field drift effects for another project, the existence of comparable stable detached divertor plasma in both experiment and simulations gives us confidence that our similar solution for FNSF-2015 are realistic. An example of the comparison is shown in the Fig. 5. It should be noted that these DIII-D UEDGE simulations sometimes find different steady-state solutions when starting from different initial conditions as discussed in Sec. 1d.

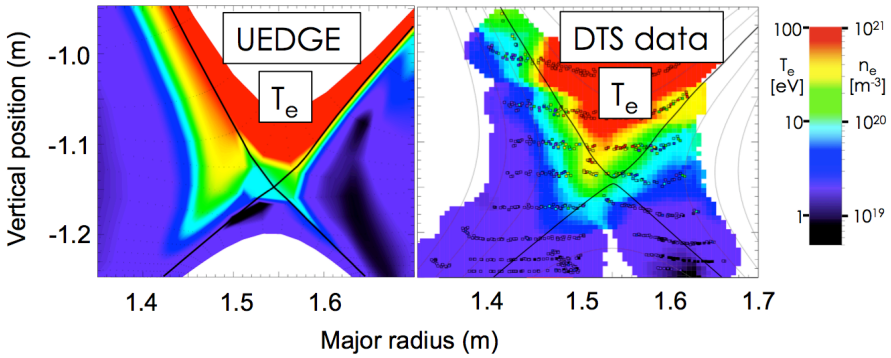

Fig. 5. A comparison of electron temperature in the lower divertor of DIII-D for a detached plasma as simulated by UEDGE and measured by divertor Thomson scattering [A. McLean et al. APS-DPP 2015 invited paper].

3. Improvements to neutral modeling

In previous divertor plasma simulations for ACT-1, a fluid neutral model of only atoms was used with the role of molecules being represented by an electron energy loss for their dissociation into atoms. Comparisons with DEGAS 2 Monte Carlo simulations show that the fluid model reasonably represents the ionization source of atoms into ions, but the gas pressure in the private flux region (related to pumping) was much too high in the atom-only fluid model.

This year we have begun to use and develop a fluid model of molecules as well as atoms. For an ITER-like case, we find that this model produces an ionization source close to our previous atom-only model (and DEGAS 2), and in addition, it now produces a much lower neutral pressure in the private flux region, even for a simple characterization of a constant molecular temperature. The remaining task is to add a temperature equation for the molecules (DEGAS 2 indicates that this temperature can vary in the range of 0.025 eV to 1 eV or more). Once completed, this model will allow us to characterize pumping requirements using an efficient fluid model calibrated with DEGAS 2.

6-o. Engineering Layout and Critical Topics *(S. Malang, consultant)*

Subjects of my contributions are in the areas of DCLL breeding blankets, He-cooled divertor target plates, and system integration including maintenance of power core components.

Particular issues addressed in some publications, internal memos, conference calls, and numerous e-mails are:

A) Basic lay-out of the FNSF power core based on DCLL breeding blankets and He-cooled divertor target plates with Tungsten used as structural material and sacrificial tiles

B) Arrangement of the PbLi flow manifolds connecting the external coolant loop with the breeding blanket segments

C) Compatibility between PbLi and ferritic steel under operational conditions

D) Candidate Tungsten alloys suitable as structural material in the He-cooled divertor target plates

<u>To A) Basic lay-out of the FNSF power core</u>

In this memo, the key principle of the layout of an FNSF with DCLL blankets and He-cooled divertor target plates at top and bottom region will be described. The basic concept is characterized by the following features:

a) Helium cooled VV operating at ~ 400 C.
b) Power core components supported by a Structural Ring separated toroidal into 16 sectors but continuous in poloidal direction.
c) Structural ring rests on the VV in the bottom region only and can expand freely in all direction relatively to the VV.
d) For each power core sector, the IB blanket segment, the two outboard blanket segments, and the upper and lower divertor target plates are attached to the structural ring.
e) Either some or all the power core components can be separated from the SR for a replacement in the hot cell. Replacement of the SR as well as the re-use of the old one should be possible in the hot cell.
f) The coolant access pipes to all the power core elements are attached to the structural ring in the bottom region only since this is the mechanical fix point with the VV.
g) Concentric tubes are used for all the coolant access pipes. To facilitate the design of such access tubes, the temperature of inner and outer tube should be maintained at nearly identical values in order to void differential thermal expansion.

- *Breeding blankets*: With the anticipated coolant conditions, (He inlet/outlet temperature 350 C/450 C, PbLi inlet/outlet temperature 450 C/650 C), there will be the "cold" inlet PbLi flow in the annulus and the "hot" exit PbLi flow in the inner tube with a thermal insulator inside the inner tube. In the region of the magnetic field, this thermal insulator has to act as electrical insulator too to minimize MHD impact. Here an additional electrical insulator at the inner surface of the outer tube is required for MHD reasons.
For the He coolant the flow arrangement will be the opposite. Here the "hot" exit flow will be in the annulus and the "cold" inlet flow in the inner tube, separated with a thermal insulator inside the inner tube. This means all the tube will operate at ~450 C, allowing the use of RAFM steels.

- *Divertor target plates*: In order to achieve an operational temperature of the tungsten structure of at least 800 C to avoid irradiation embrittlement, the He inlet/exit temperatures will be around 700 C/800 C. Here the "cold' inlet flow will be in the annulus, the "hot" exit flow in the inner tube with a thermal insulator inside this tube. This means both tubes will be operated at ~ 700 C, possible with advanced ODS steels.

To B) Arrangement of the PbLi flow manifolds connecting the external coolant loop with the breeding blanket segments

For the overall layout of the FNSF power core it is important, to select the most promising method for connecting the external PbLi loops with the LM ducts inside the blanket segments. The following three candidate LM manifolding systems have been evaluated:

a) Start with a single pipe, followed by an expansion region, followed by a set of parallel ducts.
b) Branching of pipes from one to two to four to eight. Each branch point could be made symmetric. This would lead to symmetric flows.
c) Single feeding pipe for each poloidal duct in the blanket module. Move the manifold outside the magnetic field. This results in a set of feeding pipes running through the vacuum vessel.

Historically, the method a) has been used in nearly all power plant studies with DCLL breeding blankets as well as for the US ITER DCLL TBM. Here, a single concentric pipe is attached to each blanket segment, and inside the segment there is an expansion zone in which the LM flow direction is changed from radial to toroidal. All the poloidal ducts in the segment are connected to this expansion zone, requiring a change in flow direction from toroidal to poloidal.
The big question mark with all the changes in flow direction relatively to the direction of the magnetic field is the impact of 3D-MHD issues on pressure drops and flow rate distribution. Unfortunately, MHD models and codes are not yet developed to the point to allow a sufficiently precise evaluation of the resulting pressure drop and especially the uniformity of the flow rates in all the parallel LM ducts in the blanket segment. There are promising approximation and some

experimental results for the transition from one into three poloidal ducts. However, it remains to be seen if this manifolding system will be feasible in a real power plant blanket.

This uncertainty in the real flow behavior with the manifolding system a) was the reason, why in ARIES ACT a different system had been selected as described above under c). Here, nearly all regions with potentially critical 3D MHD issues are shifted to the outside of the VV where the magnetic field strength is much lower, avoiding in this way any uncertainty about flow uniformity in the parallel poloidal ducts. Such a system can be analyzed with available MHD codes, but the price to be paid for this advantage is the need for "a forest of coolant access pipes" penetrating the VV. For example, a power core sector composed of IB-, OB1-,and OB2-blanket segments is characterized by > 30 poloidal LM ducts inside these blankets, requiring the same number of concentric coolant access pipes penetrating the VV and connecting the external LM loops to the blanket segments.

A compromise between *method a)* and *c)* has been proposed in ARIES ACT and is described above as *method b*).
Here, only one concentric coolant access pipe is required for each sector (as in *method a)*. This access pipe is brunched symmetrically from one to four to eight parallel ducts, resulting into equal flow rates for every duct.

Conclusions on the issue of PbLi manifolding concepts:
Main emphasis should be placed on developing MHD-models and codes capable of evaluating the feasibility of manifold *method a)* for the DCLL FNSF blanket segments.
This would facilitate design, manufacturing, and maintenance of the breeding blankets.

For the (unlikely) case that the issues of MHD pressure drop and LM flow rate uniformity will with this method cause not solvable problems, method c) should be kept as alternative method. For a real plant, method c) is considered as too complicated in terms of fabrication and assembly, even if this method has the smallest requirement on the development of suitable MHD codes.

<u>To C) Compatibility between PbLi and ferritic steel under operational conditions</u>

There was a suggestion to use as structural material in PbLi breeder blankets a steel with a few percent Aluminum concentration. The intention is to have the Aluminum content in such a steel reacting with the flowing PbLi to form a protective Alumina coating. However, the performance of such a layer in direct contact with the PbLi under realistic operational conditions (irradiation, cyclic stresses in the steel structure, high purity PbLi) is very questionable.
The question is, if it would it be really necessary to look for a more corrosion resistant steel to be used in DCLL blankets in FNSF?

Do we really have a corrosion problem with our present RAFM steel in the DCLL blanket? The answer to this question depends on the anticipated operational conditions and especially on the criterion used to determine the corrosion limit. For a long time I rose the question if the criterion selected 1983 in the US-BCSS (< 20 micron-m/year) is relevant for the operation of DCLL blankets. This criterion had been based on the risk of plugging small cross sections in the primary loop (valves, HX tubes, cold traps) as observed in Na loops for fast breeder reactors. It leads in general to a maximum temperature of ~ 470 C at the steel/PbLi interface. All the evaluations I am aware of showed that even this criterion will be met in a DCLL blanket operating with the following temperatures:
- PbLi inlet/outlet 450 C/650 C
- He inlet/outlet 350 C/450 C
The most difficult issue is the analysis of corrosion in the small gaps between steel wall and the SiC-FCI's. There are computer codes available to analyse the corrosion rates at all these location with including the material transport under realistic MHD conditions.

However, I suggested since a long time to use a different criterion for determining the allowable corrosion rates in a DCLL blanket.
Why do we not limit the maximum corrosion in the DCLL blanket during the entire operation time to 10 % of the wall thickness at any location inside the blanket?
I am convinced that this criterion will be met with our present RAFM steel, and that there is no danger of plugging a flow area in the blanket or the primary loop.

To D) Candidate Tungsten alloys suitable as structural material in the He-cooled divertor target plates

The He-cooled divertor target made of a tungsten alloy is a very promising concept for fusion power plants. Such a concept had been proposed by FzK in 2002, and a number of improvements have been made in the ARIES studies (see for example [1] and [2]).
In order to increase the allowable heat flux to values > 10 MW/m**2, the original target plate had been modified to a modular finger concept where small fingers with a diameter of ~ 20 mm are brazed into a ~ 8 mm thick front plate made of a W-alloy (for example WL10). In order to provide a double containment of the high pressure Helium, a cylindrical ring inside the thimble had been suggested in the frame of the ARIES study (see figure attached with typical dimensions).
A key issue of the feasibility of a divertor concept based on Tungsten is to operate the W-structure between 800 C (to avoid irradiation embrittlement) and ~ 1300 C (to avoid re-crystallization). This temperature range is not possible with the original KIT concept because there the thimbles are connected to steel with a lower allowable temperature.
Another important issue is to select a suitable W-alloy for the fabrication of the small thimbles. These thimbles are fabricated by deforming a flat sheet with a

thickness of ~ 1mm into a cup with an outer diameter of ~ 20 mm and a total height of ~ 10 mm. Which W-alloy can be used for such thimbles?
More than 10 years ago we had suggested to check the feasibility of using VM – Tungsten for the fabrication of such thimbles. This material is an alloy with > 99.95 W doped with small amounts (in ppm) of aluminium- and potassium-silicate. It is used since a long time as small wires (diameter up to 1 mm) in light bulbs. It is also obtainable as sheets with a thickness up to 2 mm. Important is the high deformation required for achieving excellent mechanical properties ("as thinner as better"). Unfortunately, this proposal has never been seriously considered by the material community. The only test I am aware of is a sharpy impact test performed by Michael Rieth (KIT). His conclusion was that VM-W tends even more to delamination than other W-alloys. However, I am convinced that delamination is relevant only for bending loads, causing shear stress in the specimen, and not for the thimbles which are basically pressure vessels with mainly tensile stresses.
To overcome this situation, I would like to suggest to include VM-W as a promising candidate material into the material program. The tensile strength and strain of probes fabricated from a 1 mm thick sheet obtained by rolling in different direction should be determined in the temperature region between 800 C and 1300 C in un-irradiated conditions and after irradiation.

[1] TOFE 19 (2008) : "High Performance Divertor Target Plate for a Power Plant: A combination of Plate and Finger Concept", X.R. Wang[a], S. Malang[b], M.S. Tillack[a] and the ARIES Team
[2] FNSF Project Meeting Feb. 2015: "Helium Cooled Divertor Design Concepts", M.S. Tillack, J.P.Blanchard

PPPL PRINCETON PLASMA PHYSICS LABORATORY

Princeton Plasma Physics Laboratory
Office of Reports and Publications

Managed by
Princeton University

under contract with the
U.S. Department of Energy
(DE-AC02-09CH11466)

P.O. Box 451, Princeton, NJ 08543
Phone: 609-243-2245
Fax: 609-243-2751

E-mail: publications@pppl.gov

Website: http://www.pppl.gov